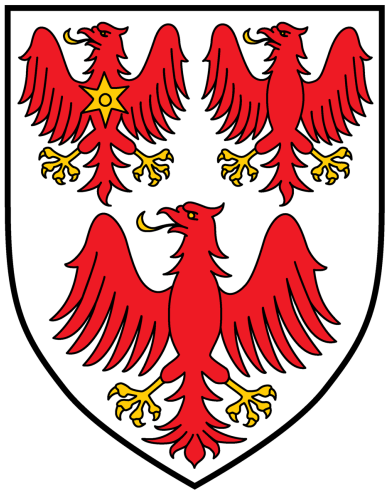
From N-Heterocyclic Imine to N-Heterocyclic Boryloxy Derived Main Group Species





Ying Kai Loh

The Queen's College

Thesis submitted for the Degree of Doctor of Philosophy

November 2019

Acknowledgements

I would like to thank Prof. Simon Aldridge for giving me the opportunity to join his group and giving me the space (both lab space and space to develop my ideas) to explore main group chemistry. Also, the unwavering guidance and support throughout the three years, always patient for discussions down to the most minute of details. Most importantly, always providing a much-needed positive spin on things in times of doubt, which bolsters my morale and confidence to strive on.

I would like to thank Lu Ying for his contribution to the synthetic work on the dioxysilylene, which completes the series of group 14 heavier dioxycarbene analogues (Chapter 3). I thank my Part II student Kieran Porteous for assisting on the oxoborane project (Chapter 4). I thank Dr. Maria Ángeles Fuentes for being an indispensable crystallographer (responsible for thirteen of the fourteen published structures; Chapeters 2, 3, 4), and constantly pushing me for new structures. I thank Dr. Jamie Hicks for assisting me with crystallography (Chapter 4), and for the countless chemistry discussions and fruitful insights shared. I thank Dr. Dinh Cao Huan Do for DFT contributions (Chapter 3, 4), and for helping me settle in at Oxford. I thank Dr. Petra Vasko for contributing her vital expertise on DFT (Chapter 2). I also thank all Aldridge group members for accommodating me in the lab.

I would like to thank the Agency for Science, Technology and Research (A*STAR) for the National Science Scholarship (NSS, PhD). I thank my parents for the continual support and trips made to visit me over the past three years. Last but not least, I thank my girlfriend Yang Yu Peh for her artwork highlighting the N-heterocyclic boryloxy ligand (Chapter 3), which graces the cover of Angewandte Chemie. Also, for always believing in me and motivating me to be constantly at the top of my game.

Abbreviations

Dipp = 2,6-$^{i}Pr_2C_6H_3$

Mes = 2,4,6-$Me_3C_6H_2$

Xy = 2,6-$Me_2C_6H_3$

Ad = 1-Adamantyl

p-Tol = 4-MeC_6H_4

IDipp = $(HCDippN)_2C$

IDippN = $[(HCDippN)_2CN]^-$

IDippNH = $(HCDippN)_2CNH$

Nacnac = $HC(MeCMesN)_2$

Cp* = $[C_5Me_5]^-$

TMS = $SiMe_3$

Tf = CF_3SO_2

OTf = CF_3SO_3

HOTf = CF_3SO_3H

Tf_2O = $(CF_3SO_2)_2O$

OTs = $(p\text{-Tol})SO_3$

DMAP = 4-$(Me_2N)C_5H_4N$

DFT = Density functional theory

NPA = Natural population analysis

HOMO = Highest occupied molecular orbital

LUMO = Lowest occupied molecular orbital

SOMO = Singly occupied molecular orbital

Abstract

In this thesis titled *"From N-Heterocyclic Imine to N-Heterocyclic Boryloxy Derived Main Group Species"*, we present in a series of four chapters, an overarching theme regarding the transformation of the well-known N-heterocyclic imine (NHI) ligand to its isoelectronic N-heterocyclic boryloxy (NHBO) counterpart, and their employment to tame unprecedented main group species.

Chapter One

Chapter one represents an introduction to ligands based around the N-heterocyclic carbenes (NHCs) framework. Carbenes were once considered as laboratory curiosities. Since the introduction of the 'bottleable' NHCs, they have been elevated to compounds of immense practical importance. While the NHCs have been widely regarded as privileged ligands, their strong nucleophilicity and huge steric profile can be transferred via the carbene centre to an appended *p* block element. This allows the design of new NHC derived ligands such as the N-heterocyclic imines (NHIs) and N-heterocyclic olefins (NHOs). The use of NHIs and NHOs to stabilize unprecedented main group species are described. Furthermore, such a concept can be extended to the N-heterocyclic boryl (NHB) anions, which are isoelectronic group 13 carbene analogues. NHB derived systems, such as the N-heterocyclic borylamino (NHBA) ligands can be designed, and their applications towards group 14 systems are documented.

Chapter Two

Carbonyl cations are among the most commonly invoked reactive intermediates in organic synthesis. While Olah pioneered superacids to provide a "stable ion" environment for their study *in situ*, isolated examples are rare. Here, we disclose successive protonation of an NHI derived carbonyl compound $(IDippN)_2CO$, to the monocation $[(IDippN)(IDippNH)CO]^+$, and the doubly protonated dication $[(IDippNH)_2CO]^{2+}$. $[(IDippN)(IDippNH)CO]^+$ represents a rare example of an N-protonated carbonyl cation and $[(IDippNH)_2CO]^{2+}$ the first example of a superelectrophilic carbonyl dication. All three compounds have been characterized by X-ray crystallography and IR spectroscopy, revealing stepwise strengthening of the C=O bond on protonation. The unique stability of these systems is attributed to the enhanced basicity and steric profile provided by the NHI substituents. In addition, we report the related singly NHI-stabilized cation $[IDippNCO]^+$. Crystallographic and DFT analyses provide insight into the interaction between the carbonyl fragment and the NHI, which reveals that the $[CNCO]^+$ unit (isoelectronic to CCCO) can be described as an acylium ion masked as a cumulene. We further describe complete oxide (O^{2-}) ion abstraction of $(IDippN)_2CO$ to generate the first linear carbodication, $[(IDippN)C(NIDipp)]^{2+}$, containing a cumulative $[CNCNC]^{2+}$ unit, and thus could be described as a carbodication masked as a cumulene, based on crystallographic and DFT analyses.

Chapter Three

We introduce a new type of strongly donating N-heterocyclic boryloxy (NHBO) ligand, $[(HCDippN)_2BO]^-$, which is isoelectronic with the well-known NHI ligand. This 1,3,2-diazaborole functionalized oxy ligand can be employed to stabilize the first acyclic

two-coordinate dioxysilylene and its Ge, Sn and Pb congeners, thereby presenting the first complete series of heavier group 14 dioxycarbene analogues. All four compounds have been characterized by X-ray crystallography and DFT, enabling analysis of periodic trends: the potential for the $[(HCDippN)_2BO]^-$ ligand to subtly vary its electronic donor capabilities is illustrated via snapshots revealing gradual evolution of arene π coordination on going from Si to Pb.

Chapter Four

We disclose the synthesis and structural characterization of the first acid-free anionic oxoborane, [K(2.2.2-crypt)][$(HCDippN)_2BO$], which is isoelectronic with classical carbonyl compounds. The oxoborane can readily be accessed from its borinic acid by a simple deprotonation/sequestration sequence. Crystallographic and DFT analyses support the presence of a polarized terminal B=O double bond. Subsequent π bond metathesis converts the B=O bond to a heavier B=S containing system, affording the first anionic thioxoborane [K(2.2.2-crypt)][$(HCDippN)_2BS$], isoelectronic with thiocarbonyls. Facile B=O bond cleavage can also be achieved to access B–H and B–Cl bonds, and via a remarkable oxide (O^{2-}) ion abstraction to generate a borenium cation $[(HCDippN)_2B(NC_5H_5)][OTf]$. By extension, the oxoborane can act as an oxide transfer agent to organic substrates, a synthetic role traditionally associated with transition metal compounds. Hence we show that B−O linkages, which are often considered to be thermodynamic sinks, can be activated under mild conditions towards bond cleavage and transfer, by exploiting the higher reactivity inherent in the B=O double bond.

Chapter 1

From N-Heterocyclic Carbene to N-Heterocyclic Boryl Derived Ligands and their Applications in Main Group Chemistry

CONTENTS

Introduction 1

Carbenes 1

NHC Derived Ligands 3

N-Heterocyclic Imine Ligands 4

NHI Stabilization of Multiply Bonded Main Group Species 6

NHI Stabilization of Low Valent Main Group Species 7

NHI Stabilization of Main Group Radical Species 9

N-Heterocyclic Olefin Ligands 10

N-Heterocyclic Boryl Anions 12

N-Heterocyclic Borylamino Ligands 14

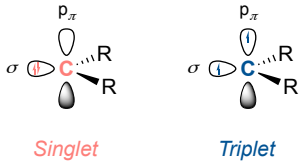
Summary and Outlook 16

References 17

Introduction

Carbenes

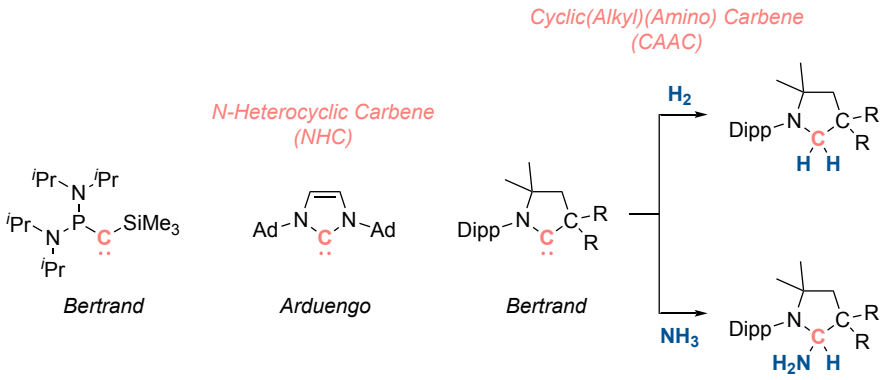
Carbenes are fascinating chemical species featuring a central two-coordinate carbon atom with only six valence electrons, thereby violating the Octet Rule.[1] Thus, they have long been regarded as highly elusive species, being postulated as fleeting intermediates in important chemical transformations. The substituents attached to the central carbon atom dictate the ground state electronic configuration. Thus, carbenes can adopt either a singlet state – with a doubly filled σ orbital and a vacant *p*π orbital, or a triplet state – with both the σ and *p*π orbitals singly filled (Scheme 1).[1a] While the parent carbene (H_2C), possesses a triplet diradical ground state which makes it highly reactive, singlet carbenes are thought to be intrinsically more stable due to their closed shell nature.



Scheme 1. Electronic configurations of carbenes.

A major breakthrough in the quest for isolable carbenes came in 1988 when Bertrand and co-workers successfully isolated the first room temperature stable singlet carbene (Scheme 2).[2a] Shortly afterwards in 1991, Arduengo and co-workers reported the first example of a 'bottleable' N-heterocyclic carbene, commonly abbreviated as an NHC.[2b] The successful taming of the first carbenes can be attributed to two major factors, namely electronic perturbation and steric protection.[1a] Firstly, they exploit heteroatom substituents which electronically disfavour the triplet state and promote the adoption of a singlet ground

state. For Bertrand's case, the phosphino(silyl)carbene benefits from complementary action of the phosphino group to raise the energy of the *p*π orbital on the carbene centre by π donation and silyl group to stabilize the σ lone pair orbital by hyperconjugative effects. Arduengo's NHC features diamino substituents which also destabilize the *p*π orbital by π donation while simultaneously acting as electronegative substituents to lower the energy of the σ lone pair orbital. Furthermore, the NHC also enjoys enhanced stability from its cyclic 6π aromatic framework. Secondly, steric factors also play a vital role. The large steric profile around the carbene centres in both cases offers kinetic protection and inhibits potential dimerization pathways. Based on this two-pronged approach, a plethora of stable singlet carbenes with varying singlet-triplet gaps and steric profiles has been accessed in recent years.[1c] A large number of these can be regarded as derivatives of Arduengo's original NHC scaffold, reflecting its high degree of modularity and ease of synthesis.



Scheme 2. Phosphino(silyl)carbene, NHC and CAAC systems; single site small molecule activation by a CAAC.

In 2006, Bertrand and co-workers introduced a variant on the NHC theme by modifying the heterocycle to formally replace one of the flanking nitrogen atoms by an alkyl group. The resulting systems are known as cyclic(alkyl)(amino)carbenes or CAACs (Scheme

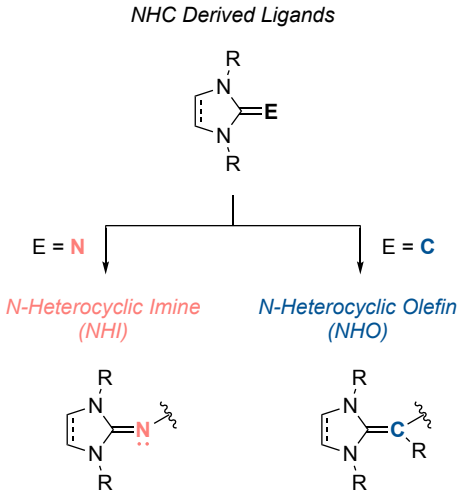
2).[1e,2c-d] The reduced π donation in tandem with enhanced σ donation from the alkyl substituent leads to a more ambiphilic carbene with a smaller singlet-triplet gap. The influence of these changes on reactivity are profound, and CAACs can accomplish the single site activation of the thermodynamically strong bonds in small molecules such as H_2 and NH_3, showing that carbenes can mimic the activity of transition metals.

Since their inception, NHCs have been elevated from mere laboratory curiosities to compounds of immense practical significance in a number of avenues of chemistry. They are primarily employed as ligands in a range of applications such as i) stabilization of hitherto unknown main group species, ii) in transition metal-based catalysts, iii) in metallopharmaceuticals and iv) in functional materials.[1f-g] Aside from acting as ligands, they find applications as i) organocatalysts, ii) activators of thermodynamically strong bonds in small molecules, and iii) as platforms to support organic radicals.[1f]

NHC Derived Ligands

One of the more interesting applications of the NHC ligand class derives from their versatility not only to act as ligands themselves, but to transfer their electronic and steric properties to an attached (C-bound) exocyclic moiety, and thereby act as platforms for new ligand design.[3] A variety of *p* block elements (E) can be installed onto the carbene centre to furnish a range of ligands derived from the original NHC (Scheme 3). In main group coordination chemistry, the spotlight has been centred on N-heterocyclic imine (NHI)[4] and closely related N-heterocyclic olefin (NHO) ligands.[5] These NHC derived ligands typically harness the strong σ donor properties of the NHC to generate strong E centred donors. Furthermore, they also benefit from the availability of an extensive library of NHCs with

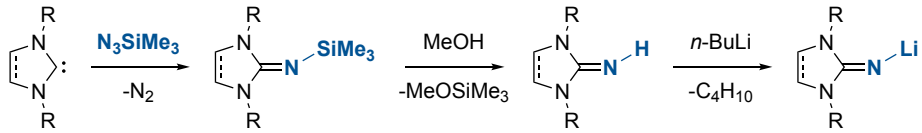
properties that are well established, allowing fine tuning of both steric and electronic properties to afford tailor-made ligands.



Scheme 3. NHC derived ligands (e.g. NHIs and NHOs).

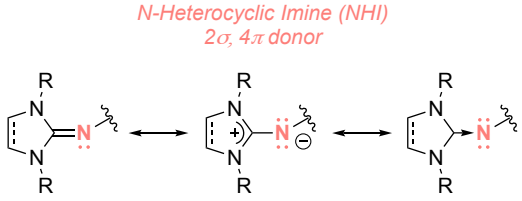
N-Heterocyclic Imine Ligands

The N-heterocyclic imine (NHI) functionality was initially introduced by Kuhn and co-workers in 1995.[4] However, it only attracted significant interest some ten years later when the group of Tamm established a general synthetic protocol (Scheme 4).[4b] Starting from the parent NHC, a Staudinger-like reaction with N_3SiMe_3 installs the imine functionality on the carbene centre to form the NHI. Methanolysis gives the "protio" ligand, IDippNH, which can be lithiated to afford IDippNLi which is a convenient precursor to the NHI ligand. This procedure offers convenient access to a wide range of NHIs. In addition, constructing the NHI directly from the corresponding NHC is a highly intuitive approach for the purpose of tuning its steric and electronic properties.



Scheme 4. General synthetic protocol to access NHI ligands.

The electronic properties of NHI ligands can be described on the basis of three contributing canonical forms (Scheme 5).[4] Due to the effective delocalization of positive-charge within the NHC framework, the highly polarized ylidic form ($C^{\delta+}$—$N^{\delta-}$) is thought to be dominant, and NHIs are thus generally regarded as strong 2σ, 4π donor ligands.

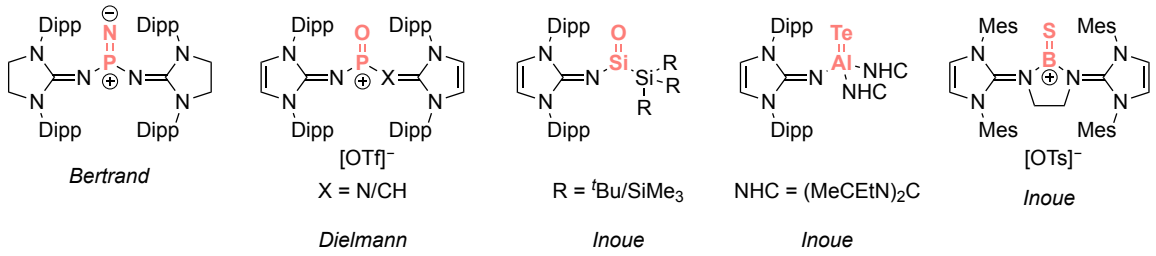


Scheme 5. Canonical forms of NHIs.

Perhaps the most spectacular applications of NHIs in recent years, however, have come when their strong donor capabilities have been exploited to tame highly electron-deficient *p* block element species.[4a] While a recent comprehensive review by Inoue in 2016 documents the rapidly expanding body of work utilizing NHIs in main group systems,[4a] a surge of activity in the intervening three years has led to the synthesis of a range of landmark new systems. As such, what is presented here is a brief survey focusing on the latest most exciting results from the literature, complemented by selected examples from Inoue's review.

NHI Stabilization of Multiply Bonded Main Group Species

In 2012, Bertrand and co-workers reported the landmark synthesis of the long-sought-after phosphinonitrene, a nitrogen analogue of a carbene (Scheme 6).[6a-e] Previous attempts which employed simpler amino ligands led to the isolation of the corresponding head-to-tail dimer (i.e. a cyclodiphosphazene).[6b] Hence, the stability of this once elusive species has largely been attributed to the more basic nature and larger steric profile provided by the flanking NHI ligands. The efficacy of the NHI family to tame unprecedented main group species is further evidenced by the more recent isolation of an oxophosphonium ion by the Dielmann group, which is isoelectronic with the phosphinonitrene.[6f] This cation (containing a P=O double bond) is even more fiercely electrophilic, and judicious employment of the NHI eliminates the need for external Lewis base stabilization.



Scheme 6. Examples of NHI stabilization of multiply bonded main group species.

Aside from phosphorus, the NHI has also demonstrated its versatility in tackling more electropositive elements to its left in the Periodic Table. Thus for example, the Inoue group accomplished a major milestone in silicon chemistry by fulfilling "Kipping's dream" of an isolable acyclic silanone containing a Si=O double bond (Scheme 6).[6g] Key to this landmark achievement is the strong π donation from the single NHI substituent attached to the electron-deficient silicon centre. Furthermore, Inoue and co-workers have also described an

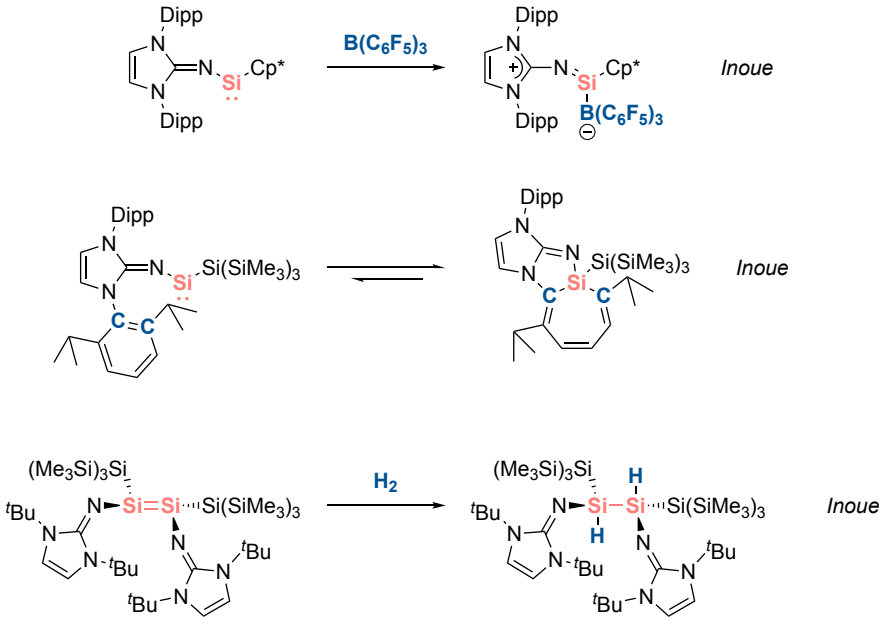
aluminium telluride bearing an Al=Te double bond, supported by a combination of NHI and NHCs.[6h] This example nicely illustrates the significance of the imidazolium framework (present in both NHC and NHI families) to counter the electron-deficiency of *p*-block elements engaged in a multiple bond with a terminally bound atom.

Recent work has shown that NHIs can not only be employed as monodentate ligands, but can also be transformed into bidentate donors linked by an ethylene tether through the imino nitrogen atoms. The group of Inoue elegantly employed this bis(NHI) chelate to quench the electron-deficiency of a cationic thioxoborane, containing an exocyclic B=S double bond (Scheme 6).[7i]

NHI Stabilization of Low Valent Main Group Species

The versatility of the NHI ligand stems from its ability to augment its donor capacity by varying between imine form (2σ, 2π donor) and ylidic form (2σ, 4π donor). As such, to accommodate more electron rich main group species, it can readily adopt the less donating imine form. A good example to illustrate this phenomenon comes from a report by the Inoue group in 2012 of an acyclic iminosilylene (Scheme 7, top).[7a] The NHI bound Si(II) centre features a short imine C=N double bond distance of 1.280(6) Å and long Si–N single bond (1.691(5) Å). However, upon coordination of the Lewis basic Si(II) centre to the strong Lewis acid $B(C_6F_5)_3$, the imine C–N distance stretches to 1.302(4) Å (i.e. more consistent with the ylidic form), whereas the Si–N distance shrinks to 1.605(3) Å, signaling the formation of a Si=N double bond. This example neatly illustrates the potential for the NHI to conserve its electron density in the imine form and yet to be able to shuttle electron density to quench the electron deficiency at the Si centre via transitioning to the ylidic form.

More recently, Inoue and co-workers reported that switching the substituent on the iminosilylene from Cp* to $Si(SiMe_3)_3$ results in unprecedented reactivity patterns (Scheme 7, centre).[7b] This acyclic imino(silyl)silylene reversibly inserts into an aromatic C=C double bond in an intramolecular fashion to form a silepin, thereby establishing an equilibrium between the silylene and the silepin. This astounding reactivity might be attributed to the strong σ, π donor ability of the NHI, coupled with the strong σ donor properties of the hypersilyl group, rendering a small singlet-triplet gap of 103.9 kJ mol^{-1}. While Si(II)-to-Si(IV) oxidative addition is well documented, this work opens the door to Si(IV)-to-Si(II) reductive elimination processes that have been a long standing challenge in developing catalysis at a silicon centre.



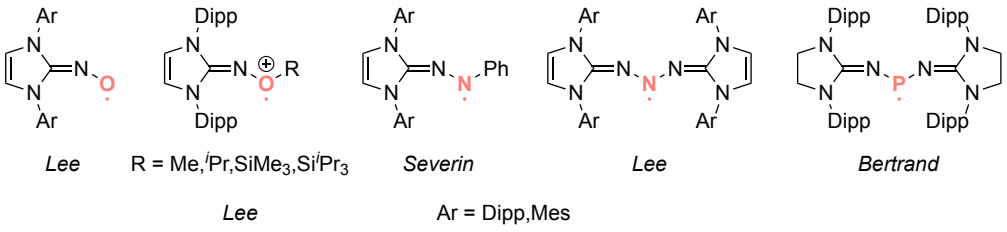
Scheme 7. Examples of NHI stabilization of low valent main group species.

In further work targeting an isolable imino(silyl)silylene, Inoue and co-workers attempted to replace the aromatic Dipp groups on the NHI with ^{t}Bu groups to prevent intramolecular insertion (Scheme 7, bottom).[7c-d] However, the reduced steric profile led to the

dimerization of the target imino(silyl)silylene to form a highly *trans*-bent and twisted disilene with an exceptionally long Si=Si double bond. These geometric features are consistent with a description featuring a donor-acceptor interaction between the two silylene units. This unique bonding motif, enforced by the steric congestion brought by the NHI and hypersilyl groups, primes the Si=Si double bond to accomplish the activation of H_2, an unprecedented mode of reactivity for disilenes.

NHI Stabilization of Main Group Radical Species

Open shell radicals are highly reactive species which often achieve enhanced stability through spin delocalization. In this respect, the NHI framework offers an extended π system to potentially tame such main group radical species. In 2015, Lee and co-workers documented air and moisture stable nitroxyl radicals, which can be viewed as O-centred radicals stabilized by an NHI substituent (Scheme 8).[8a] Examination of the SOMO revealed delocalization of the spin density across the entire π network, thereby emphasizing the critical influence of the NHI moiety on its stability. This nitroxyl radical could be further alkylated to afford oxime ether radical cations, which can also be described as NHI-stabilized OR radical cations.[8b]

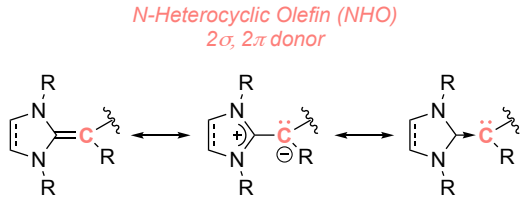


Scheme 8. Examples of NHI stabilization of main group radical species.

Aside from oxygen, the Severin group showed in 2016 that the NHI framework can also be employed to tackle N-centred aminyl radicals (Scheme 8).[8c] In the following year, Lee and co-workers reported another form of aminyl system, isolating triazenyl radicals featuring three adjacent nitrogen atoms.[8d] These radicals attain their stability by spin delocalization across the planarized π systems of the two communicating NHI units. The Bertrand group further demonstrated that the isoelectronic heavier phosphinyl radicals can also be accessed with two NHI ligands.[8e] Most notably, in stark contrast to its lighter congeners, spin density resides principally on the phosphorus centre.

N-Heterocyclic Olefin Ligands

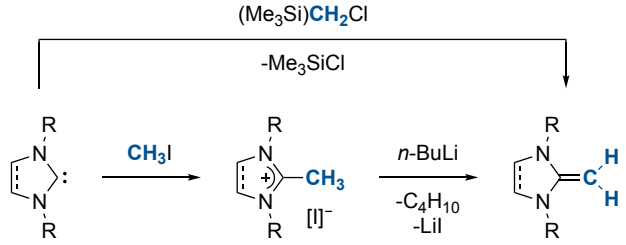
Another ligand class which is derived from the NHC framework are N-heterocyclic olefins (NHOs), which formally constitute a class of anionic vinyl ligand.[5] The NHO's properties can also be represented by a combination of canonical forms, with the highly polarized ylidic form ($C^{\delta+}-C^{\delta-}$) thought to be dominant, making them strong 2σ, 2π donors (Scheme 9).



Scheme 9. Canonical forms of the NHO.

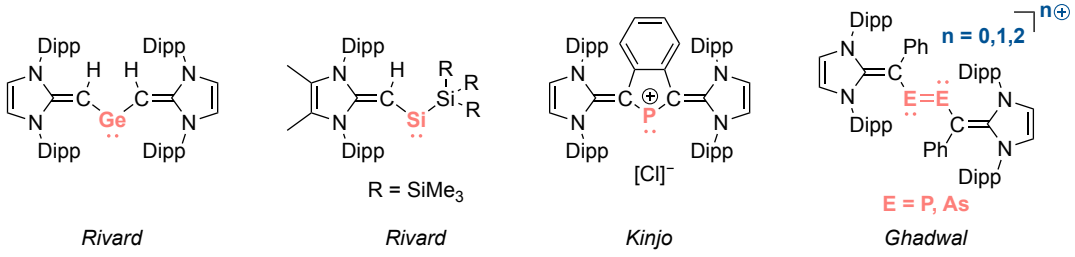
In a similar vein to the NHI ligand family, NHOs can also be directly accessed from the parent NHC. The olefin functionality can be installed onto the carbene centre by treatment with MeI, followed by deprotonation with *n*-BuLi (Scheme 10).[5] An alternative

approach utilizes $(Me_3Si)CH_2Cl$ which takes advantage of Me_3SiCl elimination to transfer the CH_2 unit to the NHC.



Scheme 10. General synthetic protocol to access NHO ligands.

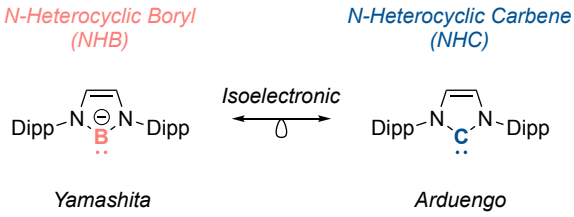
In 2017, the Rivard group employed the NHO family to stabilize a divinyl germylene (Scheme 11).[9a] More recently, they extended the series to include an acyclic vinyl(silyl)silylene.[9b] Kinjo and co-workers utilized the NHO in a bidentate fashion to stabilize a cyclic bis(NHO)phosphenium ion.[9c] The strong donor properties of the NHO ligands render the phosphorus centre nucleophilic despite its inherently cationic nature – as shown by complexation to CuCl. Ghadwal and co-workers employed NHOs as substituents for dipnictenes (E = P, As).[9d-e] These systems feature planar, hexatriene-type (C=C−E=E−C=C) π conjugation, therefore allowing access to stable radical cations and dications of diphosphenes and diarsenes.[9f-g]



Scheme 11. Examples of NHO stabilization for vinyl-substituted main group species.

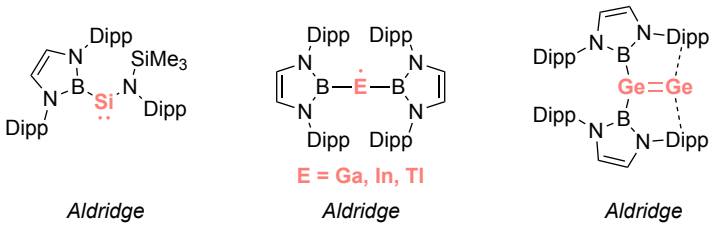
N-Heterocyclic Boryl Anions

Employing the classical NHCs as platforms, systematic variation of the appended *p* block element on the carbene centre can offer direct access to a range of new NHC derived ligands, which inherit electronic and steric properties from their parent NHCs. Another approach which offers the opportunity to fundamentally alter ligand properties is to seek alternatives to the NHCs. A potential candidate presented itself in 2006, when Yamashita and co-workers reported the breakthrough discovery of an isolable boryllithium species containing an anionic boryl $[(HCDippN)_2B]^-$ fragment (Scheme 12).[10a-b] This boryl anion is isoelectronic with classical NHCs, and can be regarded as an anionic group 13 carbene analogue, thus it can be termed an N-heterocyclic boryl (NHB) ligand.[11] It shares similar traits with NHCs, such as its singlet ground state, with a lone pair of electrons in a σ orbital and a formally vacant *p*π orbital, thus making it somewhat ambiphilic as well. However, it is predominantly more nucleophilic than electrophilic, a feature in common with the NHCs, presumably due to the contribution of the 6π aromatic form induced by the diazabutadiene ligand scaffold. Its reactivity as a boron nucleophile, as opposed to the inherent electrophilicity associated with classical tricoordinate boron compounds has thus been thoroughly explored by Yamashita and co-workers, pairing it with a series of organic electrophiles to perform umpolung borylation reactions.[10b] Furthermore, they have also probed the NHB's propensity to act as a ligand, by analogy with NHCs. The NHB's ability to strongly push electron density through the electropositive boron centre, coupled with its anionic character renders it a stronger σ donor than NHCs, as has been well documented in transition metal chemistry.[10c]



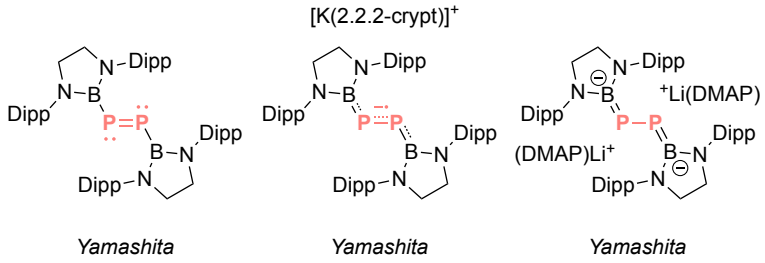
Scheme 12. N-Heterocyclic boryl (NHB) and its isoelectronic analogy with the classical N-heterocyclic carbene (NHC).

In the field of main group chemistry, in 2012, our group exploited the NHB as a ligand to tame the first acyclic two-coordinate silylene (Scheme 13).[10d] Strong σ donation from the ligand considerably narrows the singlet-triplet gap, enabling the first single site H_2 activation at a Si(II) centre. A few years later, the group further probed the NHB's behavior towards elusive main group centred radicals.[10e] The stabilization of Ga(II), In(II) and Tl(II) radicals could be attributed to the strong B−E_{13} bonding and the steric screening imparted by the imposing steric profile of the NHB, inhibiting potential decomposition pathways of the otherwise highly reactive radicals. More recently, we reported the discovery of a germavinylidene, R_2GeGe featuring a terminal Ge=Ge double bond.[10f] This species is a structural isomer of the more commonly encountered digermyne form, RGeGeR. This unprecedented species owes its stability to the NHBs, holding the Ge=Ge fragment together by the complementary action of the strong σ donating boron to the three-coordinate germanium centre and the arene π interactions from the flanking Dipp groups to the terminal germanium atom.



Scheme 13. Examples of NHB stabilization of unprecedented main group species.

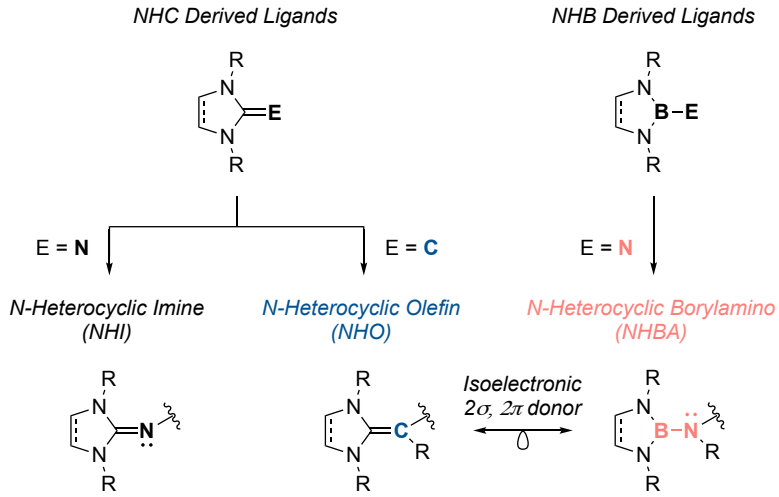
More recently, the Yamashita group employed the NHB to generate a uniquely perturbed diphosphene that is amenable towards successive single electron reduction (Scheme 14).[10g-i] The central P=P double bond of the diphosphene stretches upon reduction (due to occupation of the P=P π* orbital) from 2.0655(17) Å (diphosphene) to 2.1453(19) Å (radical anion) to 2.2761(11) Å (dianion). The supporting NHB ligands play a key role in allowing π delocalization of the radical and the anionic charges. This chemistry mimics the successive one electron oxidation of NHC-stabilized diphosphorus species reported by the groups of Robinson[12a] and Bertrand,[12b] thereby reinforcing the analogy between NHB and NHC donor families.



Scheme 14. Examples of NHB stabilization of a diphosphene, its radical anion and dianion.

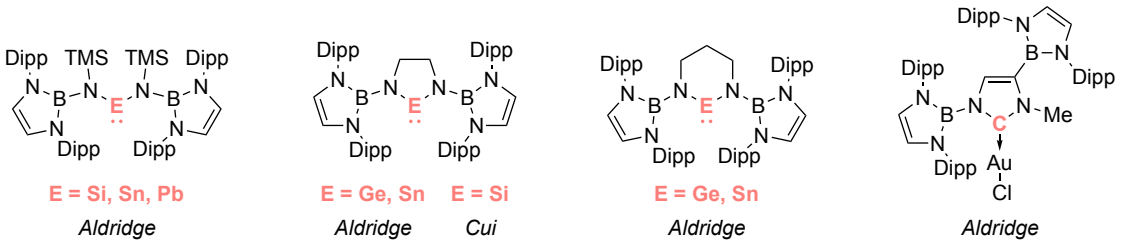
N-Heterocyclic Borylamino Ligands

The NHB ligand, being isoelectronic and isostructural with classical NHCs, presents itself as an ideal alternative platform from the NHC for new ligand design. The stronger σ donating abilities of NHBs and huge steric profile could be transferred to the installed exocyclic moiety, in a similar fashion to NHCs, to forge strongly donating and sterically imposing NHB derived ligands. Our group has incorporated this design element to introduce the N-heterocyclic borylamino (NHBA)[13a] ligand (Scheme 15), which is isoelectronic with N-heterocyclic olefin (NHO)[5] – under the family of NHC derived ligands.



Scheme 15. N-Heterocyclic borylamino (NHBA) ligands isoelectronic with N-heterocyclic olefin (NHO).

In 2016, our group documented the efficacy of the NHBA ligand to stabilize the first acyclic bis(amino)silylene and its heavier (Sn, Pb) congeners (Scheme 16).[13a] A few years later, we incorporated the NHBA in a bidentate fashion by tying up the nitrogen atoms with an ethylene or propylene linker to furnish cyclic bis(NHBA)-germylenes and stannylenes.[13b] Most recently, Cui and co-workers reported a stable silylene by employing this cyclic bis(NHBA) ligand.[13c] Attempts to synthesize a cyclic bis(NHBA)carbene were met with limited success, frustrated by a facile N-to-C shift of the NHB unit upon generation of the transient carbene.[13d] However, a modified carbene featuring N-bound NHB and a methyl groups can be trapped by complexation with transition metals [Au(I) and Rh(I)] and adduct formation with elemental selenium, thereby facilitating structural elucidation of this elusive carbene.



Scheme 16. Examples of NHBA stabilization in the synthesis of carbene and its heavier congeners.

Summary and Outlook

A brief survey of the literature on NHI-stabilized main group species reveals the significance and impact the NHI ligand family has had on the field of main group chemistry. Notably, a raft of exciting results has been witnessed in the last three years, showing the rapidly growing interest in the NHI ligand. The versatility of the NHI framework to tailor its donor ability to accommodate highly electron-deficient main group centred multiple bonds, low valent species and even open shell radicals has been clearly demonstrated.

Conspicuously absent from these reports are carbon-based species. Carbon is the quintessential element of life and thus forms the basis of organic chemistry. Hence, in chapter two, we harness the strong donor nature of the NHI to attain structural authentication of hitherto unknown organic electrophiles, including the first superelectrophile, by successive protonation of an NHI derived carbonyl compound.[14]

In chapter three, we exploit the isoelectronic analogy with the NHI to introduce a new class of strongly donating N-heterocyclic boryloxy (NHBO) ligand – under the family of NHB derived ligands.[15] We further disclose its application towards *p* block group 14 elements by accessing the first acyclic dioxysilylene and its heavier congeners to complete the series of heavier dioxycarbene analogues.

In chapter four, we show that the robust nature of the NHBO framework can be further employed to stabilize the first acid-free anionic oxoborane containing a terminal B=O double bond.[16] We further exploit its isoelectronic analogy with carbonyl compounds to induce classical carbonyl-like reactivity, and also to act as an oxide ion (O^{2-}) transfer agent to organic fragments – new modes of reactivity which is unprecedented with respect to classical B–O containing compounds.

References

(1) For recent reviews on carbenes: (a) Bourissou, D.; Guerret, O.; Gabbaï, F. P.; Bourissou, D.; Bertrand, G. Stable noncyclic singlet carbenes. *Chem. Rev.* **2009**, *109*, 3333-3384. (b) Vignolle, J.; Cattoën, X.; Bourissou, D. Stable carbenes. *Chem. Rev.* **2000**, *100*, 39-91. (c) Melaimi, M.; Soleilhavoup, M.; Bertrand, G. Stable cyclic carbenes and related species beyond diaminocarbenes. *Angew. Chem., Int. Ed.* **2010**, *49*, 8810-8849. (d) Martin, D.; Melaimi, M.; Soleilhavoup, M.; Bertrand, G. A brief survey of our contribution to stable carbene chemistry. *Organometallics* **2011**, *30*, 5304-5313. (e) Martin, D.; Melaimi, M.; Soleilhavoup, M.; Bertrand, G. Stable singlet carbenes as mimics for transition metal centers. *Chem. Sci.* **2011**, *2*, 389-399. (f) Hopkinson, M. N.; Richter, C.; Schedler, M.; Glorius, F. An overview of N-heterocyclic carbenes. *Nature* **2014**, *510*, 485-496. (g) Smith, C. A.; Narouz, M. R.; Lummis, P. A.; Singh, I.; Nazemi, A.; Li, C.; Crudden, C. M. N-Heterocyclic carbenes in materials chemistry. *Chem. Rev.* **2019**, *119*, 4986-5056.

(2) For carbenes: (a) Igau, A.; Grützmacher, H.; Baceiredo, A.; Bertrand, G. α,α'-bis-carbenoid triply bonded species: synthesis of a stable λ^3-phosphinocarbene–λ^3-phosphaacetylene. *J. Am. Chem. Soc.* **1988**, *110*, 6463-6466. (b) Arduengo, A. J. III; Harlow, R. L.; Kline, M. *J. Am. Chem. Soc.* **1991**, *113*, 361-363. (c) Lavallo, V.; Canac, Y.; Präsang, C.; Donnadieu, B.; Bertrand, G. Stable (cyclic)(alkyl)aminocarbenes as rigid or flexible, bulky, electron-rich ligands for transition-metal catalysts: a quaternary carbon atom makes a difference. *Angew. Chem., Int. Ed.* **2005**, *44*, 5705-5709. (d) Frey, G. D.; Lavallo, V.; Donnadieu, B.; Schoeller, W. W.; Bertrand, G. Facile splitting of hydrogen and ammonia by nucleophilic activation at a single carbon center. *Science* **2007**, *316*, 439-441.

(3) For carbene derived ligands: Doddi, A.; Peters, M.; Tamm, M. N-Heterocyclic carbene adducts of main group elements and their use as ligands in transition metal chemistry. *Chem. Rev.* **2019**, *119*, 6994-7112.

(4) For recent reviews on NHI: (a) Ochiai, T.; Franz, D.; Inoue, S. Applications of N-heterocyclic imines in main group chemistry. *Chem. Soc. Rev.* **2016**, *45*, 6327-6344. (b) Wu, X.; Tamm, M. Transition metal complexes supported by highly basic imidazolin-2-iminato and imidazolin-2-imine N-donor

ligands. *Coord. Chem. Rev.* **2014**, *260*, 116-138. (c) Trambitas, A. G.; Panda, T. K.; Tamm, M. Rare earth metal complexes supported by ancillary imidazolin-2-iminato ligands. *Z. Anorg. Allg. Chem.* **2010**, *636*, 2156-2171.

(5) For recent reviews on NHO: For recent review of NHO: Roy, M. M. D.; Rivard, E. Pushing chemical boundaries with *N*-heterocyclic olefins (NHOs): from catalysis to main group element chemistry. *Acc. Chem. Res.* **2017**, *50*, 2017-2025.

(6) For NHI-stabilized multiply bonded main group species: (a) Dielmann, F.; Back, O.; Henry-Ellinger, M.; Jerabek, P.; Frenking, G.; Bertrand, G. A crystalline singlet phosphinonitrene: a nitrogen atom–transfer agent. *Science* **2012**, *337*, 1526-1528. (b) Schulz, A.; Villinger, A. Stabilized transient R_2PN species. *Angew. Chem., Int. Ed.* **2013**, *52*, 3068-3070. (c) Dielmann, F.; Moore, C. E.; Rheingold, A. L.; Bertrand, G. Crystalline, Lewis base-free, cationic phosphoranimines (iminophosphonium salts). *J. Am. Chem. Soc.* **2013**, *135*, 14071-14073. (d) Dielmann, F.; Andrada, D. M.; Frenking, G.; Bertrand, G. Isolation of bridging and terminal coinage metal-nitrene complexes. *J. Am. Chem. Soc.* **2014**, *136*, 3800-3802. (e) Dielmann, F.; Bertrand, G. Reactivity of a stable phosphinonitrene towards small molecules. *Chem. Eur. J.* **2015**, *21*, 191-198. (f) Wünsche, M. A.; Witteler, T.; Dielmann, F. Lewis base free oxophosphonium ions: tunable, trigonal-planar Lewis acids. *Angew. Chem., Int. Ed.* **2018**, *57*, 7234-7239. (g) Wendel, D.; Reiter, D.; Porzelt, A.; Altmann, J.; Inoue, S.; Rieger, B. Silicon and oxygen's bond of affection: an acyclic three-coordinate silanone and its transformation to an iminosiloxysilylene. *J. Am. Chem. Soc.* **2017**, *139*, 17193-17198. (h) Franz, D.; Szilvási, T.; Irran, E.; Inoue, S. A monotopic aluminum telluride with an Al=Te double bond stabilized by *N*-heterocyclic carbenes. *Nat. Commun.* **2015**, *6*, 10037. (i) Franz, D.; Irran, E.; Inoue, S. Isolation of a three-coordinate boron cation with a boron−sulfur double bond. *Angew. Chem., Int. Ed.* **2014**, *53*, 14264-14268.

(7) For NHI-stabilized low valent main group species: (a) Inoue, S.; Leszczyńska, K. An acyclic imino-substituted silylene: synthesis, isolation and its facile conversion into a zwitterionic silaimine. *Angew. Chem., Int. Ed.* **2012**, *51*, 8589-8593. (b) Wendel, T. D.; Porzelt, A.; Herz, F. A. D.; Sarkar, D.; Jandl, C.; Inoue, S.; Rieger, B. From Si(II) to Si(IV) and back: reversible intramolecular carbon−carbon bond activation by an acyclic iminosilylene. *J. Am. Chem. Soc.* **2017**, *139*, 8134-8137. (c) Wendel, D.; Szilvási, T.; Henschel, D.; Altmann, P. J.; Jandl, C.; Inoue, S.; Rieger, B. Twist of a silicon−silicon

double bond: selective *anti*-addition of hydrogen to an iminodisilene. *J. Am. Chem. Soc.* **2017**, *139*, 9156-9159. (d) Wendel, D.; Szilvási, T.; Henschel, D.; Altmann, P. J.; Jandl, C.; Inoue, S.; Rieger, B. Precise activation of ammonia and carbon dioxide by an iminodisilene. *Angew. Chem., Int. Ed.* **2018**, *57*, 14575-14579.

(8) For NHI-stabilized main group radicals: (a) Park, J.; Song, H.; Kim, Y.; Eun, B.; Kim, Y.; Bae, D. Y.; Park, S.; Rhee, Y. M.; Kim, W. J.; Kim, K.; Lee, E. *N*-Heterocyclic carbene nitric oxide radicals. *J. Am. Chem. Soc.* **2015**, *137*, 4642-4645. (b) Kim, Y.; Kim, K.; Lee, E. Oxime ether radical cations stabilized by N-heterocyclic carbenes. *Angew. Chem., Int. Ed.* **2018**, *57*, 262-265. (c) Eymann, L. Y. M.; Tskhovrebov, A. G.; Sienkiewicz, A.; Bila, J. L.; Živković, I.; RØnnow, H. M.; Wodrich, M. D.; Vannay, L.; Corminboeuf, C.; Pattison, P.; Solari, E.; Scopelliti, R.; Severin, K. Neutral aminyl radicals derived from azoimidazolium dyes. *J. Am. Chem. Soc.* **2016**, *138*, 15126-15129. (d) Back, J.; Park, J.; Kim, Y.; Kang, H.; Kim, Y.; Park, M. J.; Kim, K.; Lee, E. Triazenyl radicals stabilized by *N*-Heterocyclic carbenes. *J. Am. Chem. Soc.* **2017**, *139*, 15300-15303. (e) Oliver, B.; Donnadieu, B.; Hopffgarten, M. v.; Klein, S.; Tonner, R.; Frenking, G.; Bertrand, G. *N*-Heterocyclic carbenes *versus* transition metals for stabilizing phosphinyl radicals. *Chem. Sci.* **2011**, *2*, 858-861.

(9) For NHO-stabilized main group species: (a) Hering-Junghans, C.; Andreiuk, P.; Ferguson, M. J.; McDonald, R.; Rivard, E. Using N-heterocyclic vinyl ligands to access stable divinylgermylenes and a germylium cation. *Angew. Chem., Int. Ed.* **2017**, *56*, 6272-6275. (b) Roy, M. M. D.; Ferguson, M. J.; McDonald, R.; Zhou, Y.; Rivard, E. A vinyl silylsilylene and its activation of strong homo- and heteroatomic bonds. *Chem. Sci.* **2019**, *10*, 6476-6481. (c) Chong, C. C.; Rao, B.; Ganguly, R.; Li, Y.; Kinjo, R. Bis(N-heterocyclic olefin) derivative: an efficient precursor for isophosphindolylium species. *Inorg. Chem.* **2017**, *56*, 8608-8614. (d) Rottschäfer, D.; Sharma, M. K.; Neumann, B.; Stammler, H.; Andrada D. M.; Ghadwal, R. S. A modular access to divinyldiphosphenes with a strikingly small HOMO-LUMO energy gap. *Chem. Eur. J.* **2019**, *25*, 8127-8134. (e) Sharma, M. K.; Blomeyer, S.; Neumann, B.; Stammler, H.; Ghadwal, R. S. Crystalline divinyldiarsenes and cleavage of the As=As bond. *Chem. Eur. J.* **2019**, *25*, 8249-8253. (f) Sharma, M. K.; Rottschäfer, D.; Blomeyer, S.; Neumann, B.; Stammler, H.; van Gastel, M.; Hinz A.; Ghadwal, R. S. Diphosphene radical cations and dications with a π-conjugated $C_2P_2C_2$-framework. *Chem. Commun.* **2019**, *55*, 10408-10411. (g) Sharma, M. K.; Blomeyer, S.; Neumann, B.; Stammler, H.; van Gastel, M.; Hinz, A.; Ghadwal, R. S.

Crystalline divinyldiarsenes radical cations and dications. *Angew. Chem., Int. Ed.* (doi.org/10.1002/anie.201909144).

(10) For NHB: (a) Segawa, Y.; Yamashita, M.; Nozaki, K. Boryllithium: isolation, characterization, and reactivity as a boryl anion. *Science* **2006**, *314*, 113-115. (b) Segawa, Y.; Suzuki, Y.; Yamashita, M.; Nozaki, K. Chemistry of boryllithium: synthesis, structure, and reactivity. *J. Am. Chem. Soc.* **2008**, *130*, 16069-16079. (c) Segawa, Y.; Yamashita, M.; Nozaki, K. Syntheses of PBP pincer iridium complexes: a supporting boryl ligand. *J. Am. Chem. Soc.* **2009**, *131*, 9201-9203. (d) Protchenko, A. V.; Birjkumar, K. H.; Dange, D.; Schwarz, A. D.; Vidovic, D.; Jones, C.; Kaltsoyannis, N.; Mountford, P.; Aldridge, S. A stable two-coordinate acyclic silylene. *J. Am. Chem. Soc.* **2012**, *134*, 6500-6503. (e) Protchenko, A. V.; Dange, D.; Harmer, J. R.; Tang, C. Y.; Schwarz, A. D.; Kelly, M. J.; Phillips, N.; Tirfoin, R.; Birjkumar, K. H.; Jones, C.; Kaltsoyannis, N.; Mountford, P.; Aldridge, S. Stable GaX_2, InX_2 and TlX_2 radicals. *Nat. Chem.* **2014**, *6*, 315-319. (f) Rit, A.; Campos, J.; Niu, H.; Aldridge, S. A stable heavier group 14 analogue of vinylidene. *Nat. Chem.* **2016**, *8*, 1022-1026. (g) Asami, S.; Okamoto, M.; Suzuki, K.; Yamashita, M. A boryl-substituted diphosphene: synthesis, structure, and reaction with *n*-butyllithium to form a stabilized adduct by pπ-pπ interaction. *Angew. Chem., Int. Ed.* **2016**, *55*, 12827-12831. (h) Asami, S.; Ishida, S.; Iwamoto, T.; Suzuki, K.; Yamashita, M. Isolation and characterization of radical anions derived from a boryl-substituted diphosphene. *Angew. Chem., Int. Ed.* **2017**, *56*, 1658-1662. (i) Asami, S.; Suzuki, K.; Yamashita, M. Two-electron reduction of diboryldiphosphene: formation of intramolecular charge-transfer complex of dianionic $B^-=P-P=B^-$ species. *Chem. Lett.* **2017**, *46*, 686-689.

(11) For recent reviews on NHB: (a) Weber, L. Modern 1,3,2-diazaborole chemistry - metamorphosis from electrophilic to nucleophilic boron. *Eur. J. Inorg. Chem.* **2012**, *21*, 5595-5609. (b) Weber, L. 1,3,2-diazaborolyl anions - from lab curiosities to versatile reagents in synthesis. *Eur. J. Inorg. Chem.* **2017**, *21*, 3461-3488.

(12) For NHC-stabilized P_2: (a) Wang, Y.; Xie, Y.; Wei, P.; King, R. B.; Schaefer III, H. F.; Schleyer, P. v. R.; Robinson, G. H. Carbene-stabilized diphosphorus. *J. Am. Chem. Soc.* **2008**, *130*, 14970-14971. (b) Back, O.; Donnadieu, B.; Parameswaran, P.; Frenking, G.; Bertrand, G. Isolation of crystalline carbene-stabilized P_2-radical cations and P_2-dication. *Nature Chem.* **2010**, *2*, 369-373.

(13) For NHBA-stabilized main group species: (a) Hadlington, T.; Abdalla, J. A. B.; Tirfoin, R.; Aldridge, S.; Jones, C. Stabilization of a two-coordinate, acyclic diaminosilylene (ADASi): completion of the series of isolable diaminotetrylenes, :E(NR_2)$_2$ (E = group 14 element). *Chem. Commun.* **2016**, *52*, 1717-1720. (b) Kristinsdóttir, L.; Oldroyd, N. L.; Grabiner, R.; Knights, A. W.; Heilmann, A.; Protchenko, A. V.; Niu, H.; Kolychev, E. L.; Campos, J.; Hicks, J.; Christensen, K. E.; Aldridge, S. Synthetic, structural and reaction chemistry of N-heterocyclic germylene and stannylene compounds featuring *N*-boryl substituents. *Dalton Trans.* **2019**, *48*, 11951-11960. (c) Zhu, L.; Zhang, J.; Cui, C. Intramolecular cyclopropanation of alkali-metal-substituted silylene with the aryl substituent of an N-heterocyclic framework. *Inorg. Chem.* **2019**, *58*, 12007-12010. (d) Kristinsdóttir, L.; Vasko, P.; Niu, H.; Kolychev, E. L.; Campos, J.; Fuentes, M. A.; Hicks, J.; Thompson, A. L.; Aldridge, S. Borylated N-heterocyclic carbenes: rearrangement and chemical trapping. *Chem. Eur. J.* **2019**, *25*, 2556-2568.

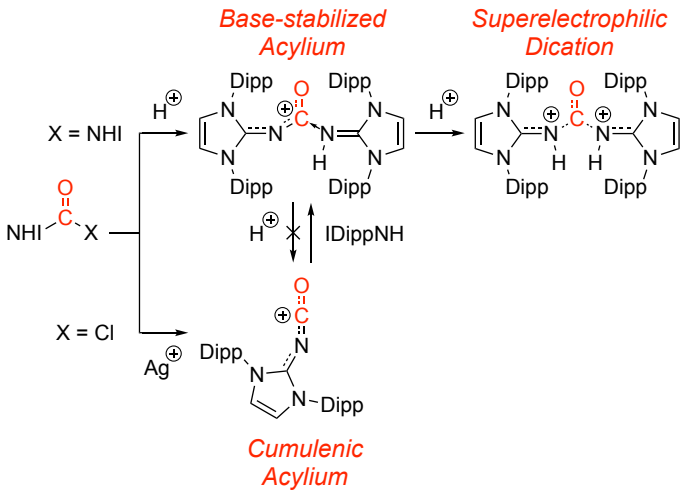
(14) For chapter 2: Loh, Y. K.; Fuentes, M. A.; Vasko, P.; Aldridge, S. Succsessive protonation of an N-heterocyclic imine derived carbonyl: Superelectrophilic dication versus masked acylium ion. *Angew. Chem., Int. Ed.* **2018**, *57*, 16559-16563.

(15) For chapter 3: Loh, Y. K.; Ying, L.; Fuentes, M. A.; Do, D. C. H.; Aldridge, S. An N-heterocyclic boryloxy ligand isoelectronic with N-heterocyclic imines: access to an acyclic dioxysilylene and its heavier congeners. *Angew. Chem., Int. Ed.* **2019**, *58*, 4847-4851.

(16) For chapter 4: Loh, Y. K.; Porteous, K.; Fuentes, M. A.; Do, D. C. H.; Hicks, J.; Aldridge, S. An acid-free anionic oxoborane isoelectronic with carbonyl: facile access and transfer of a terminal B=O double bond. *J. Am. Chem. Soc.* **2019**, *141*, 8073-8077.

Chapter 2

Successive Protonation of an N-Heterocyclic Imine Derived Carbonyl: Superelectrophilic Dication Versus Masked Acylium Ion



Loh, Y. K.; Fuentes, M. A.; Vasko, P.; Aldridge, S.

Angew. Chem., Int. Ed. **2018**, *57*, 16559-16563.

CONTENTS

Introduction 1

Organic Electrophiles 1

N-Heterocyclic Imine Ligands 2

Results and Discussion 4

Synthesis of a bis(NHI)Carbonyl Compound 4

Protonation in Acidic Media 5

Protonation in Superacidic Media 7

An Alternative Route to an Acylium Ion 8

Analysis of C−O Stretching Frequencies 11

DFT Analysis 12

Conclusions 13

Outlook 14

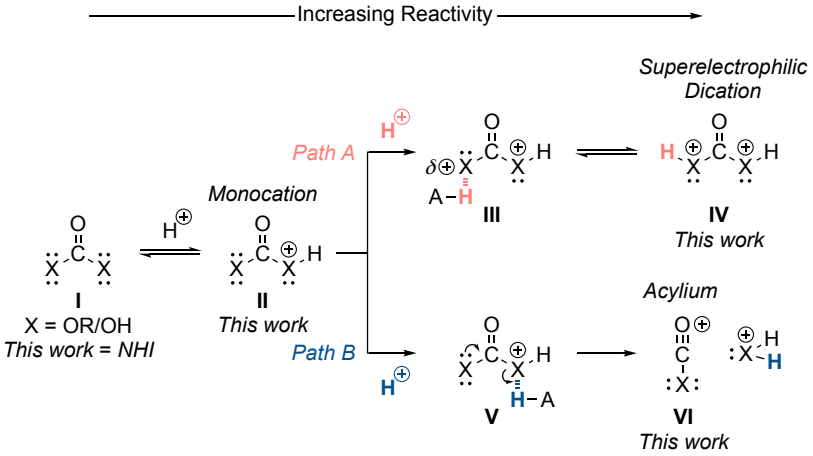
Experimental 17

References 31

Introduction

Organic Electrophiles

The carbonyl (C=O) group is ubiquitous in organic chemistry as exemplified by its presence in aldehydes, ketones, esters, carboxylic acids, amides, ureas etc. As such, it represents a fundamental building block and a classical electrophile in organic transformations. In acidic media, reactivity of the carbonyl species can be enhanced.[1] While it is widely recognized that initial protonation of carbonyl compound **I** (Scheme 1) introduces a positive charge that enhances electrophilicity, the proposed reactive intermediate (singly protonated carbonyl cation **II**) has only been observed in-situ and rarely isolated or structurally characterized.[2] During the 1970s, Olah proposed the seminal concept of superelectrophilic activation.[3] In the presence of a superacid (Path A, Scheme 1), monoprotonated cation **II** forms an equilibrium between proto-solvated monocation **III** and in limiting cases, doubly protonated carbonyl dication (superelectrophile) **IV**. These species



Scheme 1. Protonation of carbonyl derivative **I** in superacidic media to form monocation **II**, superelectrophilic dication **IV** and acylium ion **VI**.

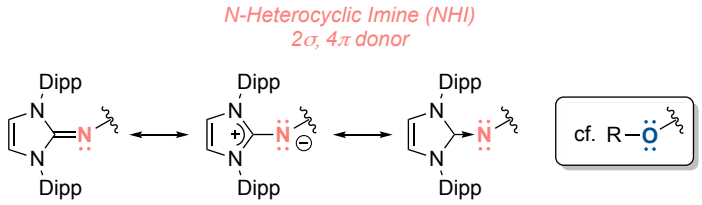
are significantly more activated than their parent electrophiles **II**, and are proposed to be the de facto reactive intermediates in the activation of the π bonds of arenes, alkenes, and in some cases the σ bonds of alkanes.[4a-c] While the employment of superacidic media provide a "stable ion" environment to create and study these superelectrophilic species, their isolation and structural authentication still remains elusive.[4c-e]

Alternatively, in a superacidic media (Path B, Scheme 1), proto-solvation might occur on the $[-XH]^+$ substituent instead, promoting the extrusion of $[XH_2]^+$ to generate a free acylium ion $[XCO]^+$ **VI**.[3a-d] Despite the central role of such species in Friedel-Crafts acylation,[5] they are typically generated in situ, and only a handful have been structurally characterized. In 1968, Boer reported the first X-ray structure of the acetylium $(MeCO)^+$,[6a] revealing its linear geometry and extremely short CΞO triple bond distance of 1.11 Å (cf. 1.13 Å for carbon monoxide).[7] While the groups of Weiss[6b] and Kochi[6c] subsequently studied the structures of acylium ions $[ArCO]^+$ featuring pendant aryl groups, heteroatom-functionalized acylium ions $[XCO]^+$ **VI** are extremely rare.[6d,e] We rationalized that the interest in heteroatom analogues is not merely a laboratory curiosity (i.e. for probing the interaction between the heteroatom substituent and the CO fragment), but might potentially pave the way to direct access of heteroatom-functionalized carbonyl compounds via the Friedel-Crafts reaction.

N-Heterocyclic Imine Ligands

The N-heterocyclic imine (NHI) is a class of formally anionic iminato ligands derived from the classical N-heterocyclic carbene or NHC (Scheme 2; Chapter 1).[8] Harnessing the strongly electron-releasing abilities of the NHC scaffold, the exocyclic C=N double bond is highly polarized in an ylidic fashion ($C^{\delta+}-N^{\delta-}$), making the NHI an electron-rich 2σ, 4π

donating iminato ligand. While this attribute has been successfully exploited to stabilize low-coordinate, highly electron-deficient main group species,[8a] some of which contain a multiple bond,[9] applications towards the synthesis of unprecedented carbon-based species remain under-explored. Motivated by this, and the isolobal analogy of NHI (−N=NHC) with conventional O-based (−OR, −OH) substituents in Olah's seminal studies, we proposed to employ the NHI moiety as a strongly basic surrogate to tame and permit structural authentication of hitherto unprecedented mono- and dicationic organic electrophiles (Scheme 1). With this in mind we targeted the synthesis of a bis(NHI)carbonyl compound as the starting point of our investigation.

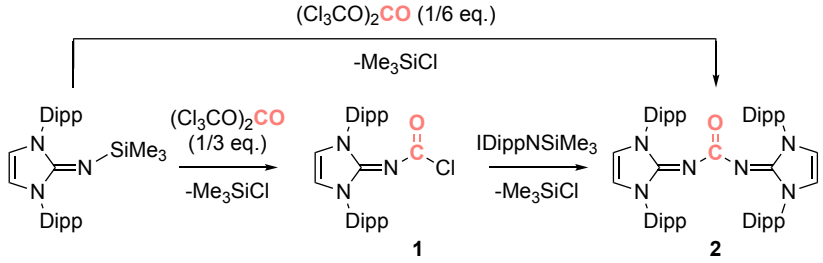


Scheme 2. Canonical forms of the NHI ligand which is isolobal with conventional O-based substituents.

Results and Discussion

Synthesis of a bis(NHI)Carbonyl Compound

To install the NHI unit onto the carbonyl group, we treated IDippNSiMe$_3$ with (Cl$_3$CO)$_2$CO (1/3 equiv.), liberating Me$_3$SiCl to afford acyl chloride **1** in 61% yield (Scheme 3). The $^{13}C\{^1H\}$ NMR resonance corresponding to the acyl carbon of **1** can be found at 149.4 ppm, which is in the typical range of N-substituted acyl chlorides. Next, to attach the second NHI unit, we subjected acyl chloride **1** to another equivalent of IDippNSiMe$_3$. Subsequent Me$_3$SiCl elimination afforded the desired bis(NHI)carbonyl compound **2**. Alternatively, carbonyl **2** can also be accessed directly from the one-pot reaction of IDippSiMe$_3$ with (Cl$_3$CO)$_2$CO (1/6 equiv.) at room temperature in good yield (76%), illustrating the facile nature of the C−N coupling, despite the huge steric profile of the NHI substituents.



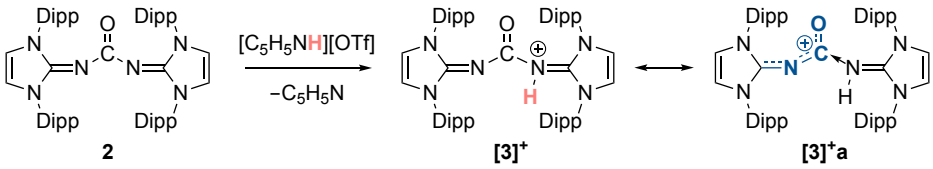
Scheme 3. Sequential and one-pot installation of NHI substituents onto a carbonyl group to afford **1** and **2**.

Concentrating a solution of carbonyl **2** in toluene at 0 °C yielded single crystals suitable for X-ray diffraction analysis (Figure 1, left). Immediately apparent in the solid-state structure is the shielding of the central carbonyl fragment by the large steric profile of the flanking NHIs. The central carbon, C1, adopts a trigonal planar geometry, and the C1−O1 bond distance of 1.230(13) Å is within the range expected for the C=O double bonds of

carbonyl compounds (1.21-1.24 Å) and close to that of acetone (1.22 Å).[7] The disparate N−C(O) and N−C(N) distances (means: 1.385 and 1.297 Å), coupled with the wide torsion angles between the NHI rings and the central C=O fragment (mean: 39.9°) indicate limited π delocalization from the NHIs to the carbonyl function. This presumably accounts for the similarity in the C=O bond distance to that measured for acetone, which does not contain π donating substituents.

Protonation in Acidic Media

With neutral carbonyl **2** in hand, we set off to pursue the corresponding mono- and dications via protonation. Treatment of **2** with one equivalent of $[C_5H_5NH][OTf]$ resulted in desymmetrization of the two NHI fragments, as evidenced by ^{1}H and $^{13}C\{^{1}H\}$ NMR spectroscopy, hinting at protonation of a single NHI unit rather than terminal O-protonation of the central carbonyl fragment (Scheme 4). Notably, the fate of the proton is also revealed in the ^{1}H NMR spectrum, appearing as a singlet at 6.05 ppm. In addition, the $^{13}C\{^{1}H\}$ NMR shift corresponding to the carbonyl C appears to be shifted upfield to 148.9 ppm.



Scheme 4. Mono-protonation of **2** to yield **[3]⁺** (alternative canonical form **[3]⁺a**).

Single crystals suitable for X-ray diffraction analysis were obtained by layering a solution of the product in 1,2-difluorobenzene with *n*-hexane. The solid-state structure unambiguously confirms the single N-protonation event to yield a carbonyl monocation **[3]⁺** with $[OTf]^-$ as the counteranion (Figure 1, right). Interestingly, **[3]⁺** represents a rare example

of protonation at the α-nitrogen of the carbonyl functionality. In the case of amides, O-protonation tends to be thermodynamically more favourable (by ~7 p*K*a units).[2d] The few reported examples of N-protonation are those of 'twisted' amides, whereby confinement of the amide nitrogen in a bicyclic system disrupts π communication, thereby augmenting its basicity and priming it for N-protonation instead.[2] As such, this underscores the idea of strong basicity and interrupted π conjugation between the NHI and the C=O fragment in bis(NHI)carbonyl compound **2**.

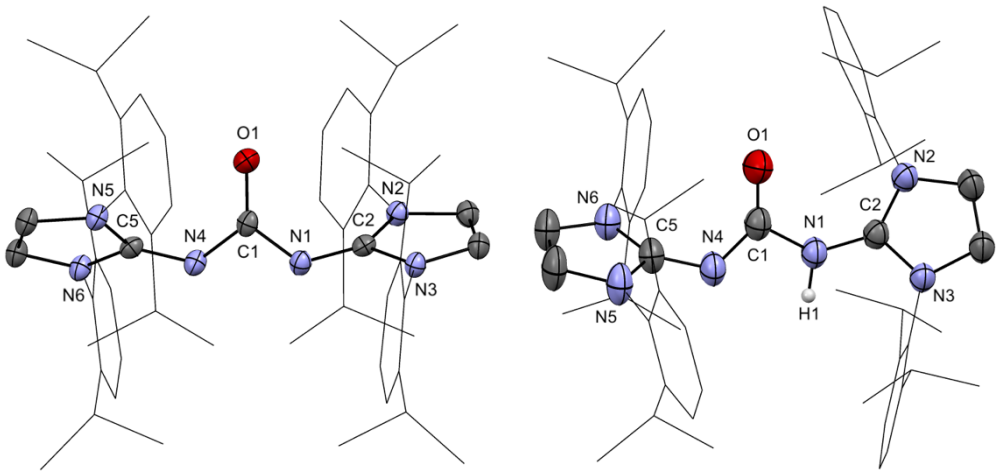


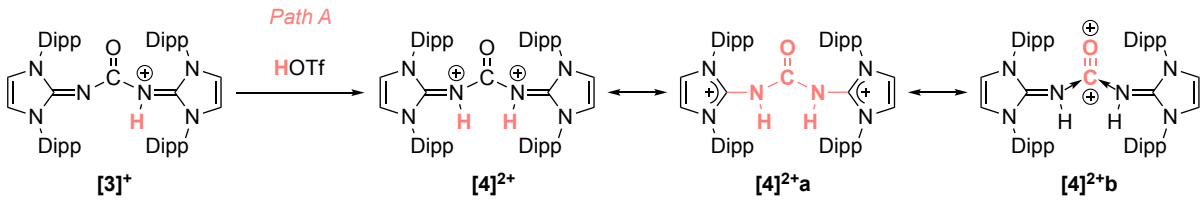
Figure 1. Solid-state structures of **2** (left) and **[3]**$^{+}$ (right). For clarity, [OTf]$^{-}$ and hydrogen atoms except H1 are omitted, Dipp groups are simplified as wireframes. Thermal ellipsoids set at 50% probability. Selected bond lengths (Å) and angles (°): **2**: C1−O1 1.230(13), C1−N1 1.386(13), C1−N4 1.384(14), N1−C2 1.298(13), N4−C5 1.296(13). **[3]**$^{+}$: C1−O1 1.216(2), C1−N1 1.429(2), C1−N4 1.326(2), N1−C2 1.352(2), N4−C5 1.336(2), O1−C1−N4 131.9(16).

Protonation results in notable structural distinctions between the two NHI units (Figure 1, right). Firstly, for the non-protonated NHI, the N−C(O) bond distance shortens significantly [from 1.385 Å (mean for **2**) to 1.326(2) Å], while the N−C(N) distance lengthens considerably [from 1.297 Å (mean for **2**) to 1.336(2) Å]. On the other hand, for the protonated NHI, the N−C(O) distance elongates remarkably [from 1.385 Å (mean for **2**) to

1.429(2) Å]. Taking these structural parameters into account, it appears that the non-protonated NHI is partially displacing the protonated NHI from the central carbonyl group by π donation, to an extent that the N−C(O) bonds are now ~0.10 Å different in length. The extrusion is further assisted by carbonyl O-to-C π donation, reflected in the shrinking of the C1−O1 distance [from 1.230(13) Å (for **2**) to 1.216(2) Å] and the widening of the O1−C1−N4 angle by ~9° to 131.9(16)°. Viewed from another perspective, **[3]**$^{+}$ can be considered a Lewis base adduct of an acylium ion **[3]**$^{+}$**a** (Scheme 4).

Protonation in Superacidic Media

With this in mind, we subjected monoprotonated carbonyl **[3]**$^{+}$ to the superacid HOTf. We were curious to ascertain whether superelectrophilic solvation would proceed via Path A, forming a doubly protonated carbonyl dication or Path B, to complete the liberation of the protonated NHI as a leaving group and generate a Lewis base free acylium ion (Scheme 1). Treatment of **[3]**$^{+}$ with excess HOTf in dichloromethane led quantitatively to a single symmetrical product based on its ^{1}H and ^{13}C{^{1}H} NMR spectra (Scheme 5). In the ^{1}H NMR spectrum, the signal of the NH proton in monoprotonated **[3]**$^{+}$ is replaced by a new resonance integrating to 2H at 10.19 ppm; the downfield shift by >4 ppm, hints at the formation of a pair of significantly more acidic protons.



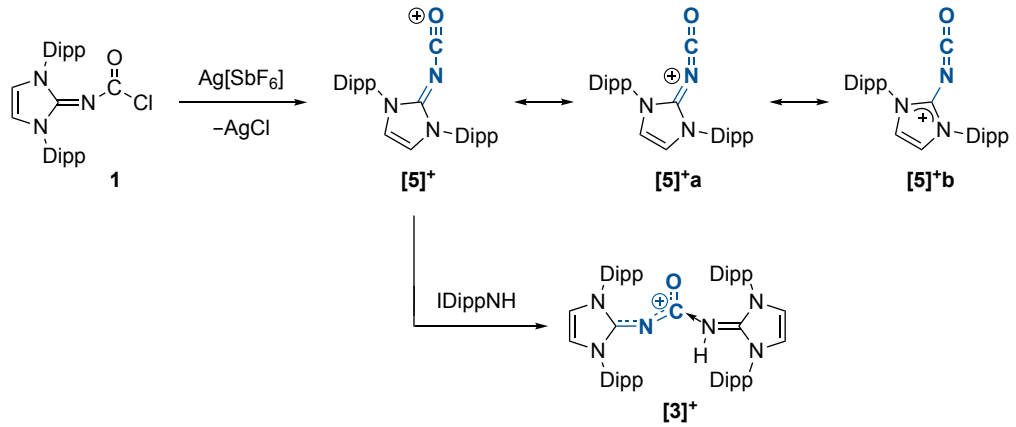
Scheme 5. Protonation of **[3]**$^{+}$ to give superelectrophile **[4]**$^{2+}$ via Path A (alternative canonical forms **[4]**$^{2+}$**a** and **[4]**$^{2+}$**b**).

Single crystals suitable for X-ray diffraction analysis were obtained by layering a solution of the product in dichloromethane with *n*-hexane. The solid-state structure unambiguously reveals a symmetrical doubly protonated species **[4]$^{2+}$**, with two [OTf]$^{-}$ as counteranions (Figure 2, left). To the best of our knowledge, **[4]$^{2+}$** represents the first structurally characterized superelectrophilic (i.e. doubly protonated) carbonyl dication. It is apparent from both NMR data and crystallographically (N−Hs located on the difference Fourier map), that the second protonation event also occurs on the exocyclic nitrogen of the NHI rather than the carbonyl oxygen, reflecting the more basic nature of the NHI functionality. Structurally, the C1−O1 bond distance is shortened to 1.204(2) Å (cf. **[3]$^{+}$**: 1.216(2) Å). On closer inspection, the similar N−C(O) and N−C(N) bond distances (means: 1.390 Å and 1.374 Å, respectively), together with the reduced torsion angle (mean: 20.6°) between the NHIs and the central C=O fragment indicate extensive delocalization of the positive charges across the entire molecule. Therefore, **[4]$^{2+}$** can be described by several canonical forms (Scheme 5): (i) a doubly protonated N-acyl iminium **[4]$^{2+}$**; (ii) a urea featuring two pendant imidazolium groups **[4]$^{2+}$a**; or (iii) a Lewis base stabilized CO dication **[4]$^{2+}$b**. It is noteworthy that **[4]$^{2+}$** is isostructural with the bis(NHI)-stabilized thioxoborane $[R_2B{=}S]^{+}$ cation reported by Inoue and coworkers.[9f]

An Alternative Route to an Acylium Ion

Given that superelectrophilic solvation of monoprotonated carbonyl compound **[3]$^{+}$** leads exclusively to superelectrophile **[4]$^{2+}$**, we sought an alternative pathway to access the Lewis base free acylium ion. Previously reported acylium ions have typically been generated by halide abstraction from their corresponding acyl halides.[4] Conveniently, as we had the NHI-substituted acyl chloride **1** in hand, we decided to adopt this method. Treatment of **1**

with Ag[SbF_6] (1 equiv.) in dichloromethane led to an instant colour change from pale yellow to amber (Scheme 6).



Scheme 6. Acylium ion **[5]**$^+$ (alternative canonical forms **[5]**$^+$**a** and **[5]**$^+$**b**), while not accessible via protonation chemistry, can be synthesized via chloride abstraction from **1**. Regeneration of **[3]**$^+$ from **[5]**$^+$.

Concentrating a solution of the product in dichloromethane at −30 °C afforded single crystals of the product. X-ray diffraction analysis unambiguously revealed that this is formed via abstraction of chloride from the carbonyl carbon to generate the desired acylium **[5]**$^+$ with $[SbF_6]^-$ as counteranion (Figure 2, right). **[5]**$^+$ can be thought of as a rare example of an acylium ion featuring a pendant heteroatom group. **[5]**$^+$ adopts a linear geometry about the central C1 [O1−C1−N1: 173.1(9)°] and is bent at N1 [C1−N1−C2: 135.9(8)°]. The C1−O1 bond distance is significantly reduced to 1.160(7) Å (cf. **[3]**$^+$: 1.216(2) Å) and is similar to that fund in carbon dioxide (1.16 Å),[7] but longer than those in previously reported acylium ions (1.10-1.13 Å).[6c] The N−C(O) distance is also remarkably shortened by ~0.11 Å to 1.219(8) Å (cf. **[3]**$^+$ N4−C1: 1.326(2) Å), and the N−C(N) distance concomitantly elongated to 1.372(6) Å (cf. **[3]**$^+$ N4−C5: 1.336(2) Å). The aforementioned structural changes from **[3]**$^+$ to **[5]**$^+$ are significant, and are presumably a manifestation of the reduced coordination number at carbonyl carbon from three to two. These structural features thus hint at an

alternative description of acylium ion **[5]**$^{+}$ in terms of a [C=N=C=O]$^{+}$ heterocumulene involving significant delocalization of electron density from the NHI into the C=O moiety.[6d-e,10] The acylium character of **[5]**$^{+}$ (albeit masked) is evident from the fact that reaction with IDippNH leads to coordination at the acylium carbon (C1) thereby regenerating the Lewis base stabilized acylium **[3]**$^{+}$ (Scheme 6). It is also implied by the fact that **[5]**$^{+}$ induces the polymerization of tetrahydrofuran at room temperature. **[5]**$^{+}$ might therefore be realistically described by a combination of limiting resonance forms (Scheme 6): (i) an acylium ion **[5]**$^{+}$; (ii) a [CNCO]$^{+}$ heterocumulene **[5]**$^{+}$**a**; and (iii) an isocyanate species with a pendant imidazolium unit **[5]**$^{+}$**b**.

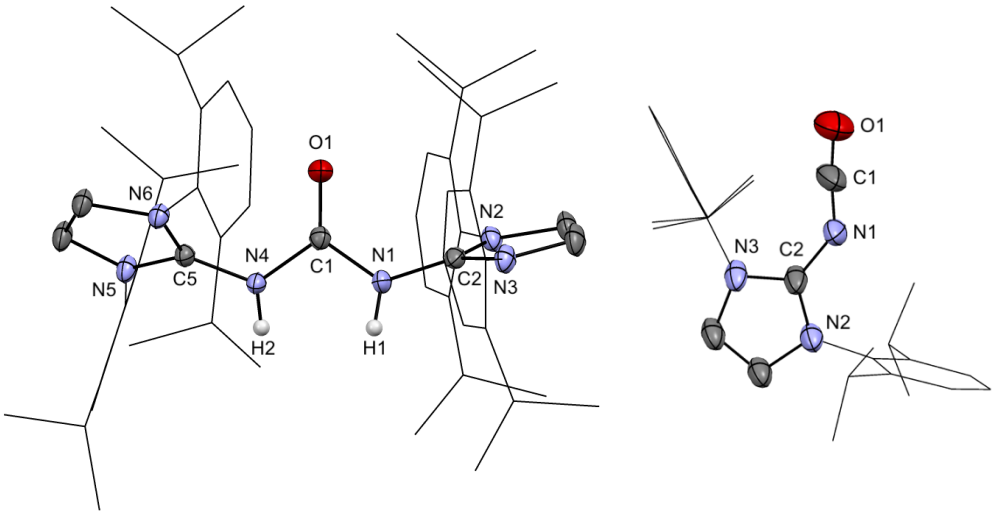


Figure 2. Solid-state structures of **[4]**$^{2+}$ (left) and **[5]**$^{+}$ (right). For clarity, [OTf]$^{-}$, [SbF_6]$^{-}$ and hydrogen atoms except H1 and H2 are omitted, Dipp groups are simplified as wireframes. Thermal ellipsoids set at 50% probability. Selected bond lengths (Å) and angles (°): **[4]**$^{2+}$: C1−O1 1.204(2), C1−N1 1.383(19), C1−N4 1.396(19), N1−C2 1.372(19), N4−C5 1.375(19). **[5]**$^{+}$: C1−O1 1.160(7), C1−N1 1.219(8), N1−C2 1.372(6), O1−C1−N1 173.1(9), C1−N1−C2 135.9(8).

Viewed from another perspective, while acylium ion **[5]**$^{+}$ is not directly obtained via NHI (leaving group) displacement from carbonyl **2** (Scheme 1, Path B), the sequence of

compounds **2**−**[3]**$^{+}$−**[5]**$^{+}$ can be regarded as structural models for this transformation. Hence, **[3]**$^{+}$ represents the proton-activated intermediate, a key structural snapshot which might offer important mechanistic insight into this fundamental reaction. The relevance of **[3]**$^{+}$ in this transformation sequence is further evidenced from the fact that the reaction can be reversed by reattaching the leaving group (IDippNH) to **[5]**$^{+}$ to regenerate **[3]**$^{+}$ (Scheme 6).

Analysis of C−O Stretching Frequencies

We probed the C−O stretching frequencies of the carbonyl compounds by IR spectroscopy (Table 1). From **2** to **[3]**$^{+}$ to **[4]**$^{2+}$, there is a stepwise increase in the stretching frequency from ~1574[a] cm^{-1} to 1703 cm^{-1} to 1752 cm^{-1}. We rationalized that upon successive N-protonation, the accumulation of positive charge on the central carbonyl carbon is quenched by enhanced π donation from the terminal oxygen. This results in a sequential increase in the C−O bond order, further evidenced by the dramatic shortening of the C1−O1 bond distances (Table 1). Consistently, **[5]**$^{+}$ has a C−O stretching frequency of 2253 cm^{-1}, which is within the range of known acylium ions (~2300 cm^{-1}),[6c] hence hinting at its CΞO triple bond character.

Table 1. C−O bond distances (Å) and IR stretching frequencies (cm^{-1}) for **2**, **[3]**$^{+}$, **[4]**$^{2+}$ and **[5]**$^{+}$.

	2	**[3]**$^{+}$	**[4]**$^{2+}$	**[5]**$^{+}$
C1−O1 (Å)	1.230(13)	1.216(2)	1.204(2)	1.160(7)
$\nu_{C=O}$ (cm^{-1})	~1574[a]	1703	1752	2253

[a] Three closely spaced bands are found in the range 1555-1593 cm^{-1} assigned to the C=O and symmetric/anti-symmetric C−N stretching modes.

DFT Analysis

To gain further insight into the electronic structure of **[5]⁺**, we carried out DFT calculations using the PBE1PBE exchange-correlation functional in combination with the def-TZVP basis set. The NPA charges calculated at both acylium carbon (C1) and carbenium carbon (C2) (+0.88 and +0.57, respectively) are consistent with the carbocationic $[CNCO]^+$ fragment, with distinct acylium character (Figure 3). The calculated Wiberg Bond Indices for O1−C1 (2.02), C1−N1 (1.71) and (to a lesser extent) N1−C2 (1.15) reflect delocalized character along the $[CNCO]^+$ fragment, in keeping with a cumulenic description in which the π systems of the acylium and NHI fragments are contiguous. Cumulenic ketones of the type $R_2C{=}C{=}C{=}O$ represent higher homologues of ketene, and are of fundamental interest, but have proved elusive to structural characterization.[11] Inspired by the isoelectronic relationship between the CCCO and $[CNCO]^+$ fragments, we carried out DFT calculations on the parent methylene ketene ($H_2C{=}C{=}C{=}O$) for comparison. The calculated LUMO and LUMO+1 of **[5]⁺** are the orthogonal $[CNCO]^+$ out-of-plane and in-plane π* orbitals, respectively (Figure 3). These orbitals are closely analogous to those calculated for the CCCO fragment of methylene ketene, and as such, DFT analysis provides further support for a description of **[5]⁺** as an acylium ion with cumulenic character.

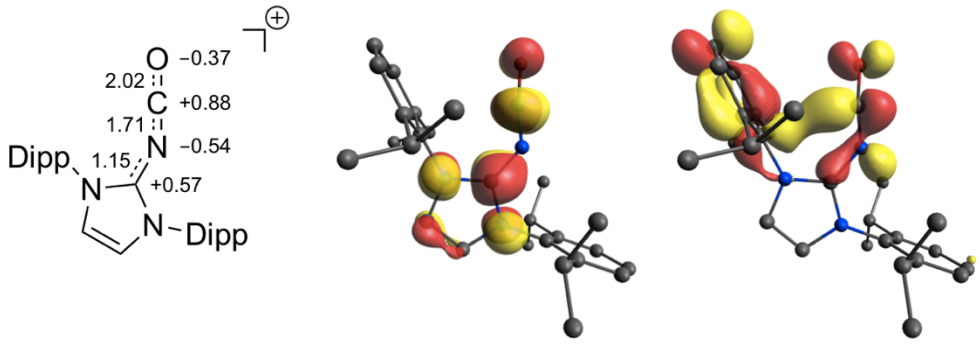


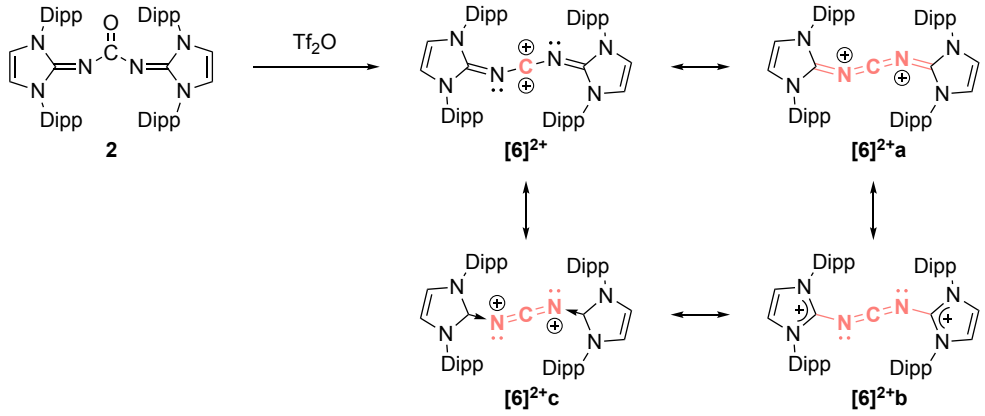
Figure 3. WBI bond order and NPA charges (left), LUMO (middle) and LUMO+1 (right) for **[5]⁺** (0.05 isosurface).

Conclusions

In conclusion, we describe the successful isolation and structural characterization of a rare singly protonated carbonyl monocation **[3]**$^{+}$ and the first example of a doubly protonated carbonyl dication (superelectrophile) **[4]**$^{2+}$ by successive protonation of bis(NHI)carbonyl compound **2**. Furthermore, we also report the preparation and structural characterization of the singly NHI derived acylium ion **[5]**$^{+}$ using an alternative halide abstraction protocol Crystallographic and DFT analysis shed light on the interaction between carbonyl and NHI fragments in **[5]**$^{+}$, which reveals that the $[CNCO]^{+}$ unit (isoelectronic with CCCO) can be described as an acylium ion masked as a cumulene. Additionally, the sequence of compounds **2**$-$**[3]**$^{+}-$**[5]**$^{+}$ can be regarded as structural models for leaving group elimination from a carbonyl in an acidic media, with **[3]**$^{+}$ as the key proton-activated intermediate. Building on the seminal work of Olah, our contribution demonstrates that highly reactive species once thought to be transient intermediates, can now not only be identified spectroscopically, but also isolated in a systematic fashion and structurally characterized. By employing the strongly donating and bulky steric profile of the NHI, a viable entry point to 'bottleable' carbonyl cations is provided.

Outlook

The pronounced basicity of the NHI substituents renders preferential protonation at the α-nitrogen instead of the carbonyl oxygen atom of bis(NHI)carbonyl **2**. As a possible extension of this work we sought to induce electrophilic attack at the terminal oxygen atom by selecting an oxophilic reagent. Treatment of neutral carbonyl **2** with excess Tf_2O in dichloromethane and subsequent layering with *n*-hexane results in the formation of yellow crystals (Scheme 7). X-ray diffraction analysis unambiguously revealed complete oxide ion (O^{2-}) abstraction from the carbonyl carbon atom to generate the dication **[6]**$^{2+}$ featuring a central two-coordinate carbon centre accompanied by two $[OTf]^-$ counteranions (Figure 4). While isolable two-coordinate carbocations such as the acylium ions,[6] nitrilium ions[12a] and vinyl cations[12b] have some precedence in the literature, they are exclusively monocations. Hence, **[6]**$^{2+}$ represents the first two-coordinate carbodication, isoelectronic with borinium ions.



Scheme 7. Oxide ion abstraction from **2** to give carbodication **[6]**$^{2+}$ (alternative canonical forms **[6]**$^{2+}$**a**, **[6]**$^{2+}$**b** and **[6]**$^{2+}$**c**).

Closer inspection of the structural parameters reveal a linear geometry (179.6(3)°) about the central carbon atom and bent geometries about the exocyclic nitrogen atoms of the NHI (mean: 145.98°). The C1−N1 and C1−N1' bond distances (mean: 1.2012 Å) are very short, which contrasts with the elongated N1−C2 and N1'−C2' bonds (mean: 1.347 Å). Furthermore, the capping NHC units adopt an essentially co-planar arrangement (mean torsion: 15.7°) with the central NCN unit, hinting at the extensive π delocalization of positive charges across the CNCNC system (Figure 4, right). Hence, its true nature can be described by a mixture of canonical forms (Scheme 7): (i) a carbodication **[6]**$^{2+}$; (ii) a $[CNCNC]^{2+}$ heterocumulene **[6]**$^{2+}$**a**; (iii) a carbodiimide species with pendant imidazolium units **[6]**$^{2+}$**b**; or (iv) an NHC-stabilized $[NCN]^{2+}$ fragment **[6]**$^{2+}$**c**.

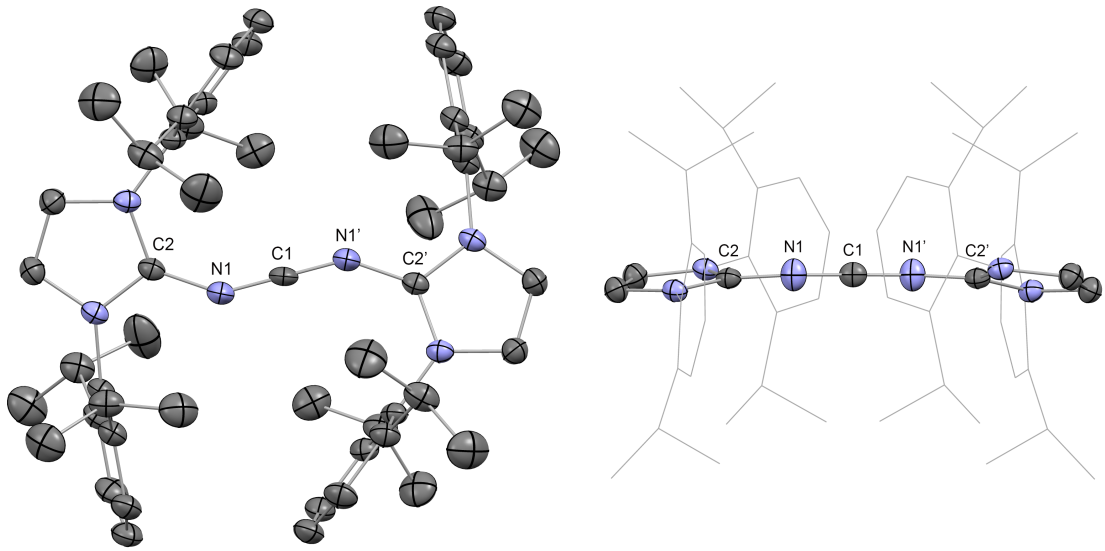


Figure 4. Solid-state structures of **[6]**$^{2+}$ (left) and sideview (right). For clarity, $[OTf]^-$ and hydrogen atoms are omitted, Dipp groups are simplified as wireframes. Thermal ellipsoids set at 40% probability. Selected bond lengths (Å) and angles (°): **[6]**$^{2+}$: C1−N1 1.2012(18), C1−N1' 1.2012(18), N1−C2 1.347(3), N1'−C2' 1.347(3), N1−C1−N1' 179.6(3), C2−N1−C1 145.98(17), C2'−N1'−C1 145.98(17).

To gain further insight into the electronic structure of **[6]**$^{2+}$, we carried out DFT calculations using the PBE1PBE exchange-correlation functional in combination with the def-TZVP basis set. The NPA charge calculated at the central carbon (C1) is +0.77 and the terminal carbon atoms (C2 and C2') each carry a charge of +0.56, consistent with the carbodicationic nature of the $[CNCNC]^{2+}$ fragment (Figure 5). The calculated Wiberg Bond Indices for C1−N1 (1.82), C1−N1' (1.82), N1−C2 (1.14) and N1'−C2' (1.14) reflect delocalized character along the $[CNCNC]^{2+}$ fragment, in keeping with a cumulenic description in which the π systems of the NCN and terminal NHC fragments are contiguous. The calculated LUMO and LUMO+1 of **[6]**$^{2+}$ are the orthogonal $[CNCNC]^{2+}$ out-of-plane and in-plane π* orbitals, respectively (Figure 5).

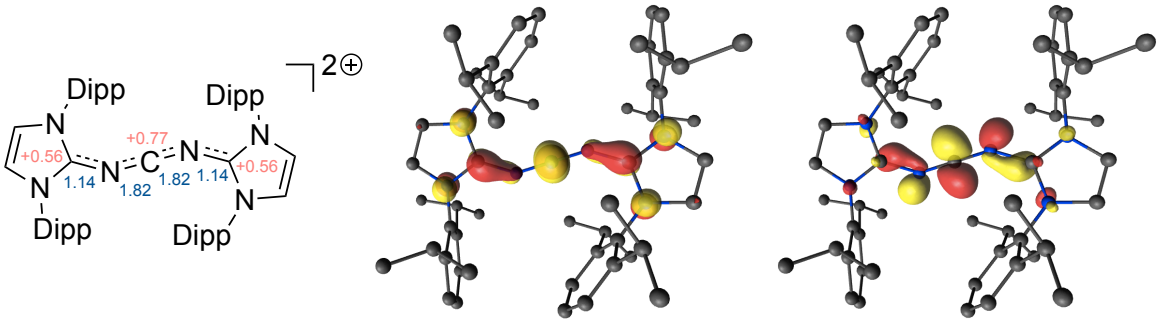


Figure 5. WBI bond order in red and NPA charges in blue (left), LUMO (middle) and LUMO+1 (right) for **[6]**$^{2+}$ (0.06 isosurface).

Based on the crystallographic and DFT analysis, **[6]**$^{2+}$ can be described as a carbodication masked as a cumulene, in a similar vein as **[5]**$^{+}$. However, a reliable synthesis is limited by its high sensitivity, thus **[6]**$^{2+}$ is still elusive towards complete characterization. Current efforts in our lab are aimed at an alternative protocol to access **[6]**$^{2+}$, with a view to exploring the reactivity patterns arising from its potent electrophilicity. Also of interest will be its reduction chemistry to access a radical cation and a superbasic bis(NHI)carbene.

Experimental

General Considerations and Starting Material Preparations

All manipulations were carried out using standard Schlenk line or dry-box techniques under an atmosphere of argon or dinitrogen. Solvents were degassed by sparging with argon and dried by passing through a column of the appropriate drying agent. NMR spectra were measured in benzene-d_6 (which was dried over potassium) or dichloromethane-d_2 (which was dried over CaH_2), with the solvent then being distilled under reduced pressure and stored under argon in Teflon valve ampoules. NMR samples were prepared under argon in 5 mm Wilmad 507-PP tubes fitted with J. Young Teflon valves. ^{1}H, $^{13}C\{^{1}H\}$ and $^{19}F\{^{1}H\}$ NMR spectra were recorded on Bruker Avance III HD nanobay 400 MHz or Bruker Avance 500 MHz spectrometer at ambient temperature and referenced internally to residual protio-solvent (^{1}H) or solvent (^{13}C) resonances and are reported relative to tetramethylsilane ($\delta = 0$ ppm). ^{19}F resonances are referenced externally to $CFCl_3$. Assignments were confirmed using two-dimensional ^{1}H-^{1}H and ^{13}C-^{1}H NMR correlation experiments. Chemical shifts are quoted in δ (ppm) and coupling constants in Hz. Elemental analyses were carried out by London Metropolitan University. IDippNSiMe$_3$ was prepared by the literature method.[13] All other reagents were used as received.

Synthetic, Spectroscopic and Analytical Data

Preparation of (IDippN)COCl (1). A solution of IDippNSiMe$_3$ (1.102 g, 2.32 mmol) in toluene (10 mL) was added to a solution of $(Cl_3CO)_2CO$ (0.229 g, 0.77 mmol) in toluene (10 mL) at room temperature. A white precipitate formed within the first 30 min and the reaction

mixture was left to stir overnight at room temperature. Volatiles were removed under vacuum. The residue was dissolved in benzene (20 mL) and filtered. The filtrate was dried under vacuum to yield (IDippN)COCl (**1**) (0.657 g, 61%) as an off-white powder. ^{1}H NMR (500 MHz, C_6D_6, 297 K): δ = 1.07 (d, $^{3}J_{HH}$ = 6.9 Hz, 12H, CH(CH_3)$_2$), 1.43 (d, $^{3}J_{HH}$ = 6.8 Hz, 12H, CH(CH_3)$_2$), 2.87 (sept, $^{3}J_{HH}$ = 6.8 Hz, 4H, C*H*(CH$_3$)$_2$), 6.05 (s, 2H, NC*H*), 7.06 (d, $^{3}J_{HH}$ = 7.8 Hz, 4H, Dipp-*m*-C*H*), 7.17 (t, $^{3}J_{HH}$ = 7.9 Hz, 2H, Dipp-*p*-C*H*); ^{13}C{^{1}H} NMR (126 MHz, C_6D_6): δ = 23.6 (CH(*C*H$_3$)$_2$), 24.8 (CH(*C*H$_3$)$_2$), 29.4 (*C*H(CH$_3$)$_2$), 117.8 (N*C*H), 124.6 (Dipp-*m*-*C*H), 130.9 (Dipp-*p*-*C*H), 131.7 (Dipp-*i*-*C*), 146.4 (Dipp-*o*-*C*), 148.2 (N$_2$*C*N), 149.4 (*C*O).

Preparation of (IDippN)$_2$CO (2). A solution of (Cl$_3$CO)$_2$CO (0.081 g, 0.28 mmol) in toluene (40 mL) was added to a solution of IDippNSiMe$_3$ (0.780 g, 1.64 mmol) also in toluene (10 mL) dropwise at 0 °C over a period of 45 min. While warming to room temperature, a white precipitate formed within the first 45 min, and the reaction was left to stir overnight at room temperature. Volatiles were removed under vacuum, and the residue dissolved in toluene (25 mL) and filtered. The filtrate was dried under vacuum to yield (IDippN)$_2$CO (**2**) (0.515 g, 76% yield) as an off-white powder. Single crystals suitable for X-ray diffraction analysis were obtained from a concentrated solution of **2** in toluene at 0 °C. ^{1}H NMR (500 MHz, C_6D_6, 297 K): δ = 1.16 (d, $^{3}J_{HH}$ = 7.0 Hz, 48H, CH(CH_3)$_2$), 3.02 (sept, $^{3}J_{HH}$ = 6.8 Hz, 8H, C*H*(CH$_3$)$_2$), 5.86 (s, 4H, NC*H*), 7.08 (d, $^{3}J_{HH}$ = 7.7 Hz, 8H, Dipp-*m*-C*H*), 7.23 (t, $^{3}J_{HH}$ = 7.7 Hz, 4H, Dipp-*p*-C*H*); ^{13}C{^{1}H} NMR (126 MHz, C_6D_6): δ = 24.0 (CH(*C*H$_3$)$_2$), 24.6 (CH(*C*H$_3$)$_2$), 29.0 (*C*H(CH$_3$)$_2$), 115.6 (N*C*H), 123.8 (Dipp-*m*-*C*H), 129.1 (Dipp-*p*-*C*H), 134.4 (Dipp-*i*-*C*), 147.4 (Dipp-*o*-*C*), 147.6 (N$_2$*C*N), 161.7 (*C*O); IR ν/cm^{-1} (Nujol): ~1574 (C=O); anal. calc. for $C_{55}H_{72}N_6O$: C 79.28%, H 8.71%, N 10.09%, found: C 79.31%, H 8.85%, N 10.21%.

Preparation of [(IDippN)(IDippNH)CO][OTf] [3][OTf]. To a mixture of **2** (50 mg, 0.06 mmol) and $C_5H_5NH.OTf$ (14 mg, 0.06 mmol) was added dichloromethane (2 mL) at room temperature and the reaction mixture agitated for 5 min at room temperature. All volatiles were removed under vacuum. The residue was dissolved in toluene (2 mL) and filtered to yield [(IDippN)(IDippNH)CO][OTf] **[3][OTf]** (39 mg, 67%) as an off-white powder. Single crystals suitable for X-ray diffraction analysis were obtained from layering a solution of **[3][OTf]** in 1,2-difluorobenzene with *n*-hexane at room temperature. ^{1}H NMR (500 MHz, CD_2Cl_2, 297 K): δ = 0.84 (d, $^{3}J_{HH}$ = 6.0 Hz, 24H, CH(CH_3)$_2$), 1.08 (d, $^{3}J_{HH}$ = 6.9 Hz, 12H, CH(CH_3)$_2$), 1.11 (d, $^{3}J_{HH}$ = 6.8 Hz, 12H, CH(CH_3)$_2$), 2.23 (sept, $^{3}J_{HH}$ = 6.9 Hz, 4H, C*H*(CH$_3$)$_2$), 2.43 (sept, $^{3}J_{HH}$ = 6.8 Hz, 4H, C*H*(CH$_3$)$_2$), 6.05 (s, 1H, N*H*), 6.67 (s, 2H, NC*H*), 6.99 (s, 2H, NC*H*), 7.11 (d, $^{3}J_{HH}$ = 7.7 Hz, 4H, Dipp-*m*-C*H*), 7.19 (d, $^{3}J_{HH}$ = 7.8 Hz, 4H, Dipp-*m*-C*H*), 7.39 (t, $^{3}J_{HH}$ = 7.8 Hz, 2H, Dipp-*p*-C*H*), 7.50 (t, $^{3}J_{HH}$ = 7.8 Hz, 2H, Dipp-*p*-C*H*); ^{13}C{^{1}H} NMR (126 MHz, CD_2Cl_2): δ = 23.4 (CH(*C*H$_3$)$_2$), 23.5 (CH(*C*H$_3$)$_2$), 24.5 (CH(*C*H$_3$)$_2$), 29.2 (*C*H(CH$_3$)$_2$), 29.6 (*C*H(CH$_3$)$_2$), 118.7 (N*C*H), 121.0 (N*C*H), 124.4 (Dipp-*m*-*C*H), 125.4 (Dipp-*m*-*C*H), 129.6 (Dipp-*i*-*C*), 130.7 (Dipp-*p*-*C*H),131.4 (Dipp-*i*-*C*), 132.2 (Dipp-*p*-*C*H), 141.9 (N$_2$*C*N), 145.6 (Dipp-*o*-*C*), 146.3 (Dipp-*o*-*C*), 148.8 (N$_2$*C*N), 148.9 (*C*O); ^{19}F{^{1}H} NMR (377 MHz, CD_2Cl_2): δ = −79.0; IR ν/cm^{-1} (Nujol): 1703 (C=O); anal. calc. for $C_{56}H_{73}F_3N_6O_4S$: C 68.40%, H 7.48%, N 8.55%, found: C 68.23%, H 7.64%, N 8.35%.

Preparation of [(IDippNH)$_2$CO][OTf]$_2$ [4][OTf]$_2$. To a suspension of **2** (50 mg, 0.06 mmol) in diethyl ether (5 mL) was added HOTf (0.10 mL, 1.13 mmol). The suspension was sonicated for 1 min, filtered and all volatiles removed under vacuum to yield [(IDippNH)$_2$CO][OTf]$_2$ **[4][OTf]$_2$** (41 mg, 61%) as a beige powder. Single crystals suitable for X-ray diffraction analysis were obtained from layering a solution of **[4][OTf]$_2$** in dichloromethane with *n*-hexane at room temperature. ^{1}H NMR (500 MHz, CD_2Cl_2, 297 K): δ

= 0.96 (d, $^{3}J_{HH}$ = 6.7 Hz, 24H, CH(CH_3)$_2$), 1.04 (d, $^{3}J_{HH}$ = 6.8 Hz, 24H, CH(CH_3)$_2$), 2.29 (sept, $^{3}J_{HH}$ = 6.8 Hz, 8H, CH(CH$_3$)$_2$), 7.26 (d, $^{3}J_{HH}$ = 7.9 Hz, 8H, Dipp-*m*-CH), 7.35 (s, 4H, NCH), 7.56 (t, $^{3}J_{HH}$ = 7.8 Hz, 4H, Dipp-*p*-CH), 10.19 (s, 2H, NH); ^{13}C{^{1}H} NMR (126 MHz, CD_2Cl_2): δ = 23.0 (CH(*C*H$_3$)$_2$), 25.5 (CH(*C*H$_3$)$_2$), 30.0 (*C*H(CH$_3$)$_2$), 125.1 (N*C*H), 125.8 (Dipp-*m*-*C*H), 129.6 (Dipp-*i*-*C*), 132.7 (Dipp-*p*-*C*H), 137.4 (N$_2$*C*N), 145.4 (Dipp-*o*-*C*), 148.5 (*C*O); ^{19}F{^{1}H} NMR (377 MHz, CD_2Cl_2): δ = −78.5; IR ν/cm^{-1} (Nujol): 1752 (C=O); anal. calc. for $C_{57}H_{74}F_6N_6O_7S_2$: C 60.41%, H 6.58%, N 7.42%, found: C 60.26%, H 6.54%, N 7.45%.

Preparation of [(IDippN)CO][SbF$_6$] [5][SbF$_6$]. To a mixture of **1** (150 mg, 0.32 mmol) and Ag[SbF_6] (37 mg, 0.32 mmol) was added dichloromethane (5 mL) at room temperature. A white precipitate formed immediately and the amber suspension was agitated for a further 5 min at room temperature. The suspension was filtered and all volatiles were removed under vacuum to yield [(IDippN)CO][SbF_6] **[5][SbF$_6$]** (165 mg, 77%) as an amber powder. Single crystals suitable for X-ray diffraction analysis were obtained from layering a solution of **[5][SbF$_6$]** in dichloromethane at −30 °C. ^{1}H NMR (400 MHz, CD_2Cl_2, 297 K): δ = 1.25 (d, $^{3}J_{HH}$ = 6.9 Hz, 12H, CH(CH_3)$_2$), 1.32 (d, $^{3}J_{HH}$ = 6.8 Hz, 12H, CH(CH_3)$_2$), 2.41 (sept, $^{3}J_{HH}$ = 6.8 Hz, 4H, CH(CH$_3$)$_2$), 7.49 (d, $^{3}J_{HH}$ = 7.9 Hz, 4H, Dipp-*m*-CH), 7.64 (s, 2H, NCH), 7.73 (t, $^{3}J_{HH}$ = 7.9 Hz, 2H, Dipp-*p*-CH); ^{13}C{^{1}H} NMR (126 MHz, CD_2Cl_2): δ = 23.9 (CH(*C*H$_3$)$_2$), 24.2 (CH(*C*H$_3$)$_2$), 29.9 (*C*H(CH$_3$)$_2$), 123.6 (N*C*H), 126.1 (Dipp-*m*-*C*H), 127.3 (Dipp-*i*-*C*), 134.1 (Dipp-*p*-*C*H), 135.5 (N$_2$*C*N), 146.3 (Dipp-*o*-*C*), 146.9 (*C*O); IR ν/cm^{-1} (Nujol): 2253 (C=O); anal. calc. for $C_{28}H_{36}F_6N_3OSb$: C 50.47%, H 5.45%, N 6.31%, found: C 50.36%, H 5.59%, N 6.21%.

NMR Spectra

(IDippN)COCl [1]

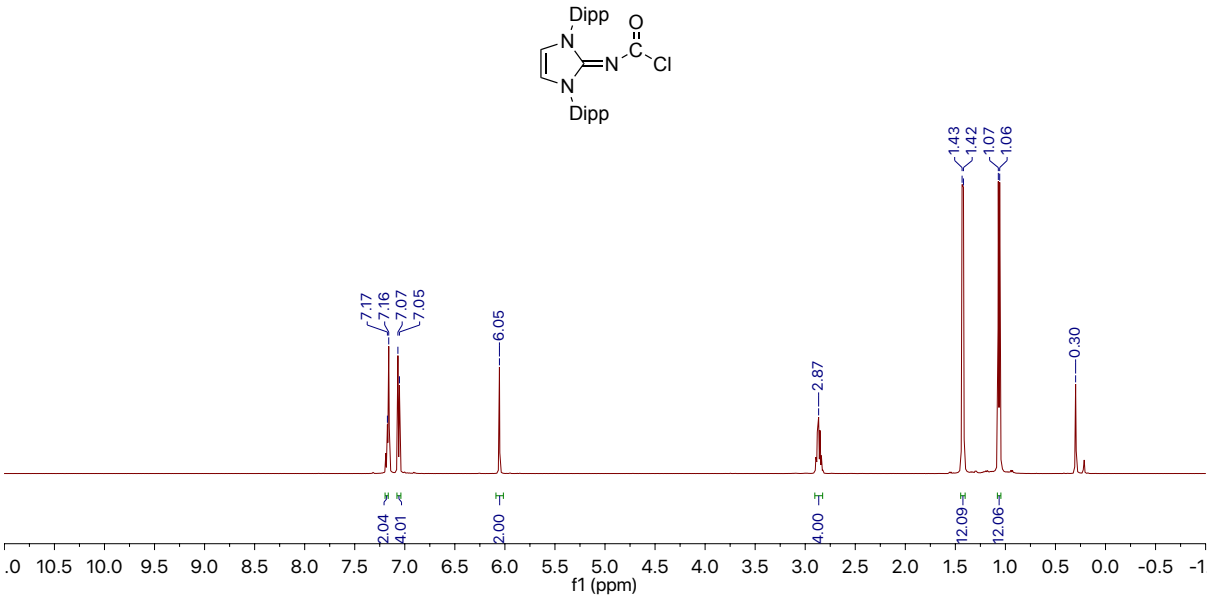


Figure 6. ^{1}H NMR spectrum of **1**.

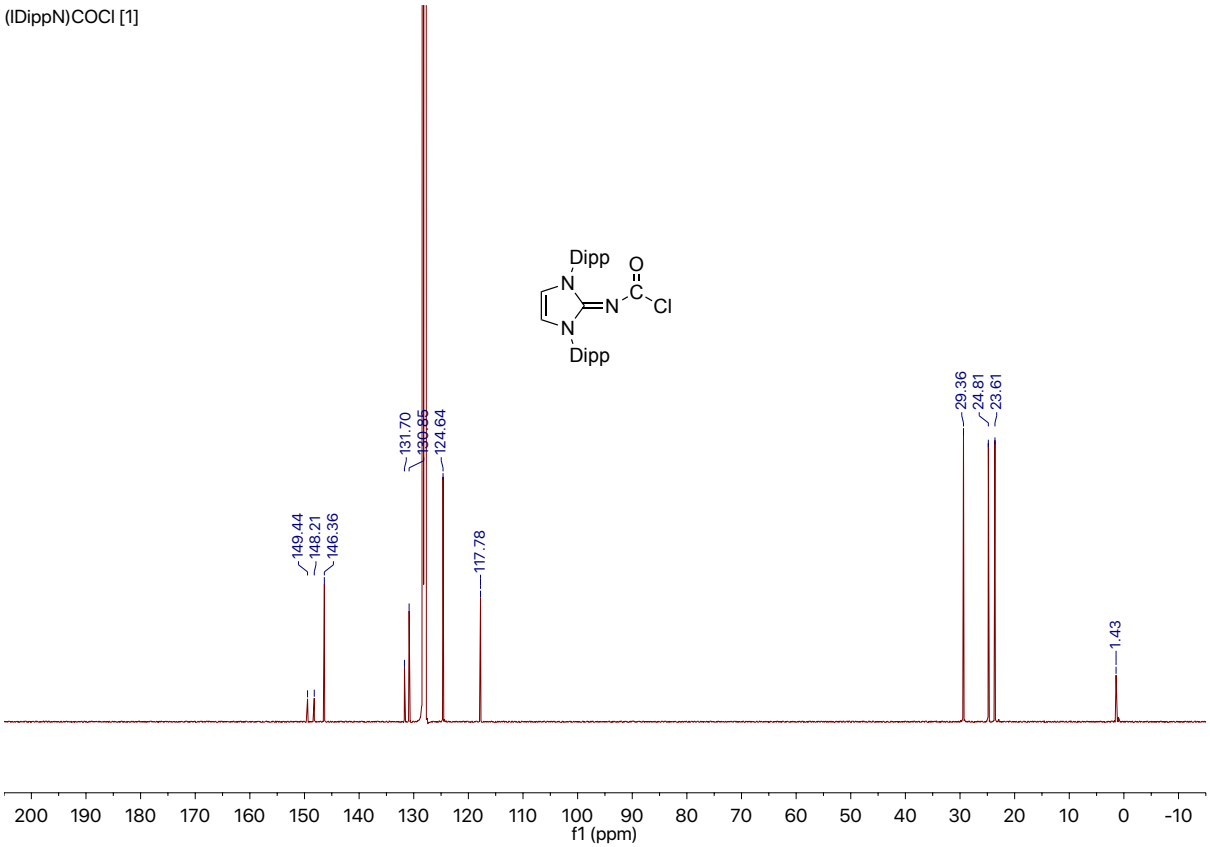


Figure 7. ^{13}C{^{1}H} NMR spectrum of **1**.

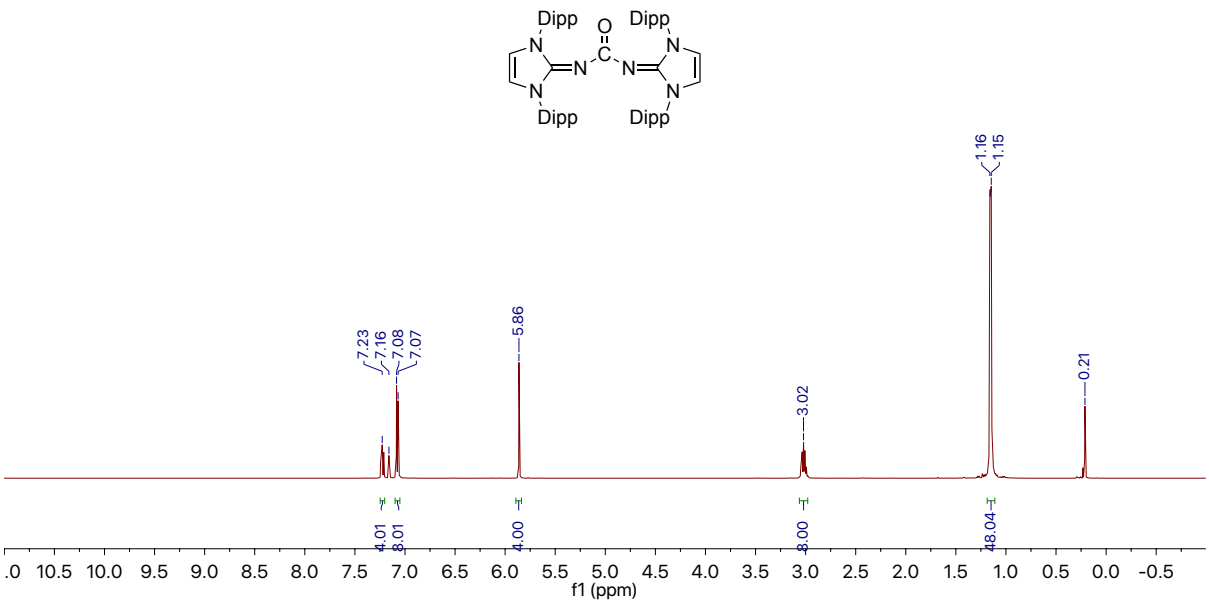


Figure 8. ^{1}H NMR spectrum of **2**.

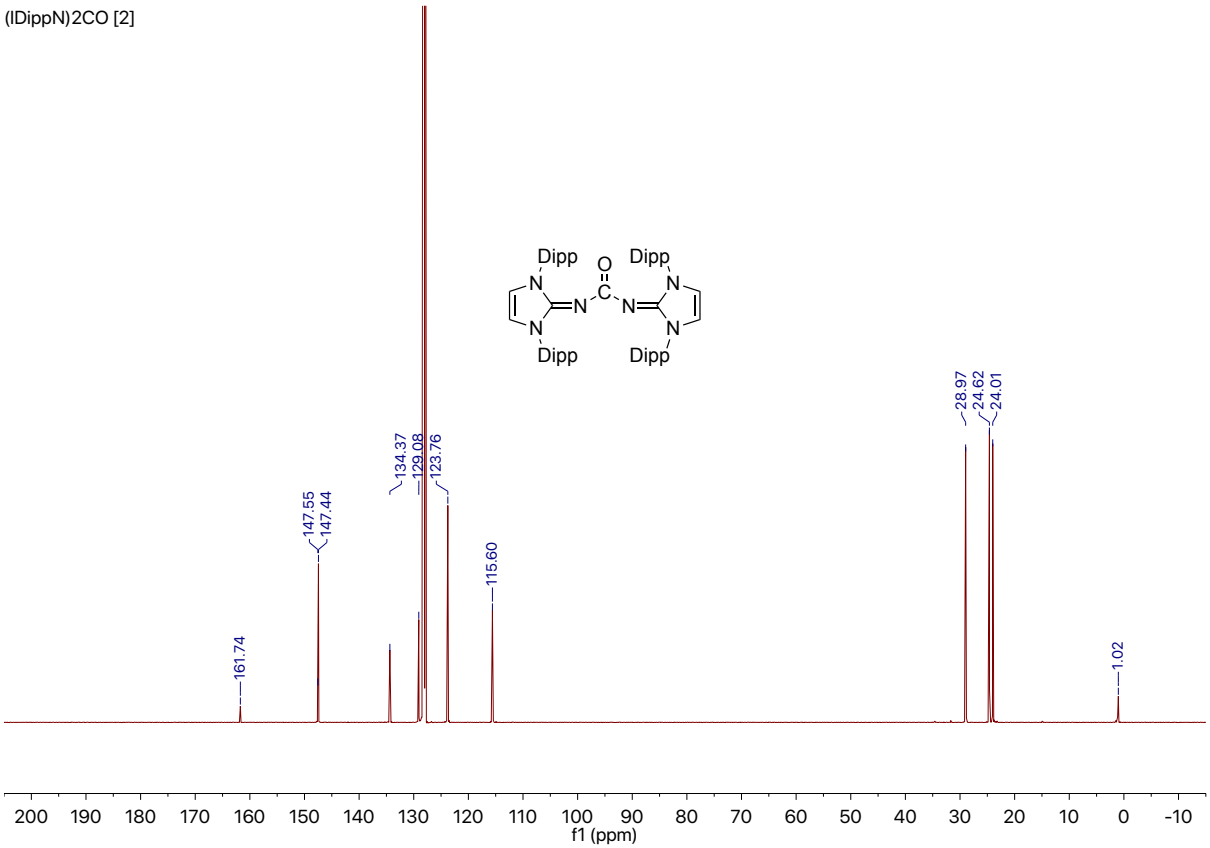


Figure 9. ^{13}C{^{1}H} NMR spectrum of **2**.

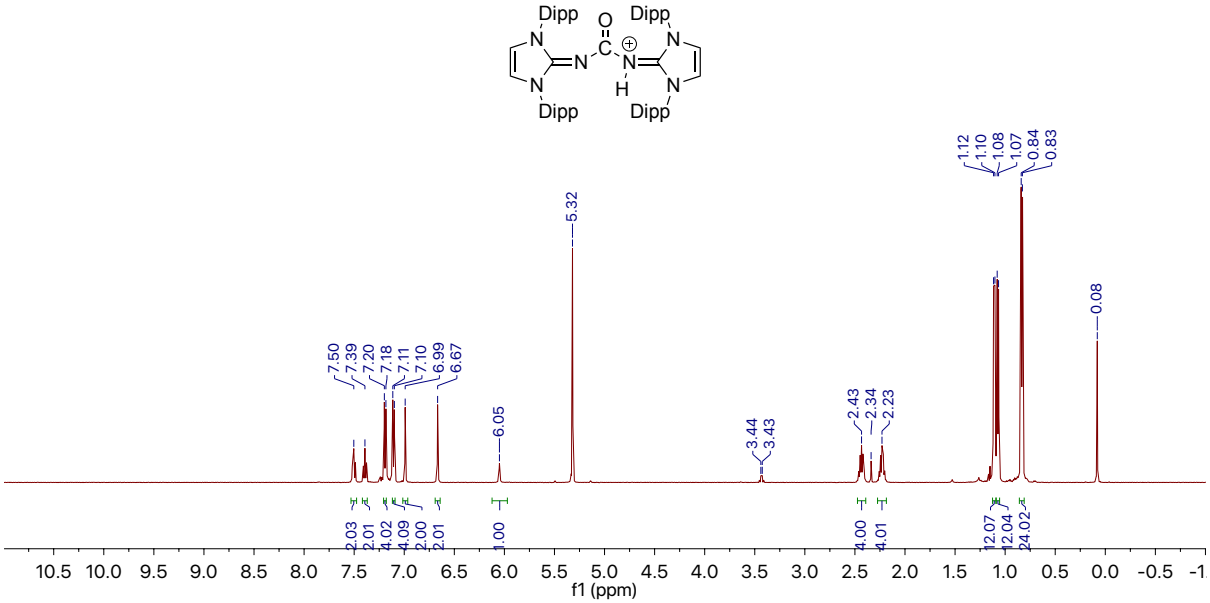


Figure 10. ^{1}H NMR spectrum of **[3][OTf]**.

(IDippN)(IDippNH)CO.OTf [3][OTf]

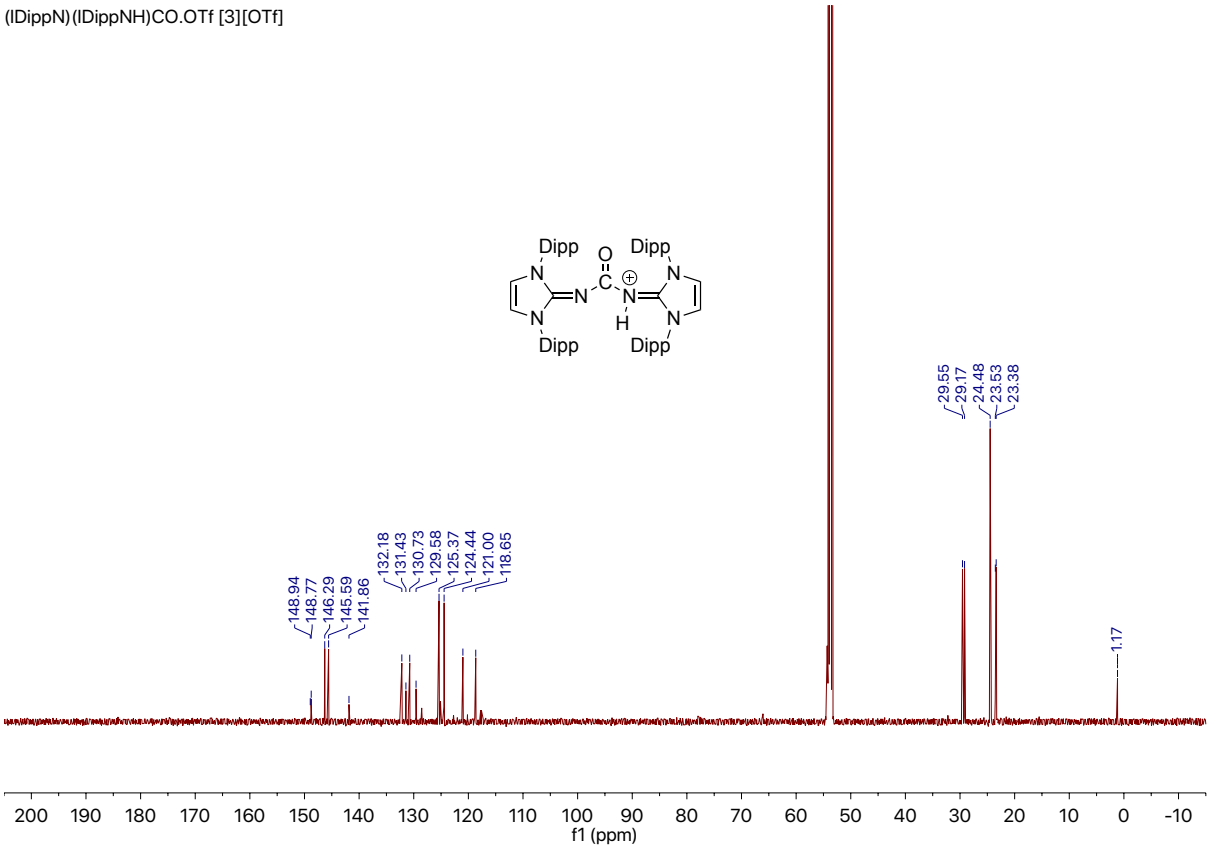


Figure 11. ^{13}C{^{1}H} NMR spectrum of **[3][OTf]**.

(IDippN)(IDippNH)CO.OTf [3][OTf]

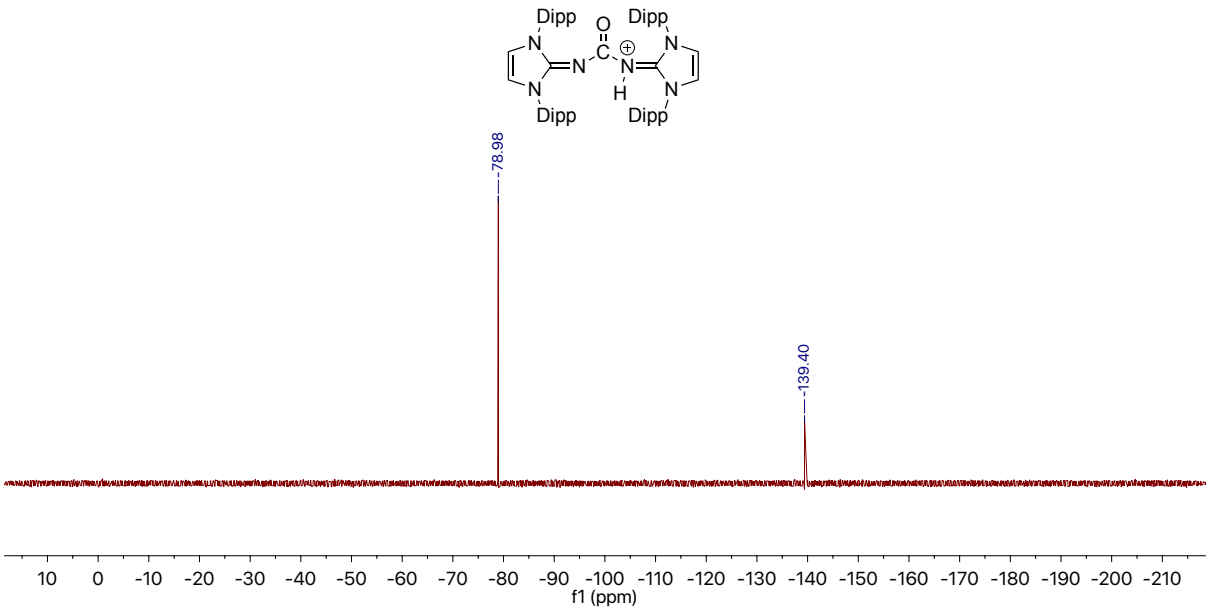


Figure 12. $^{19}F\{^{1}H\}$ NMR spectrum of **[3][OTf]**.

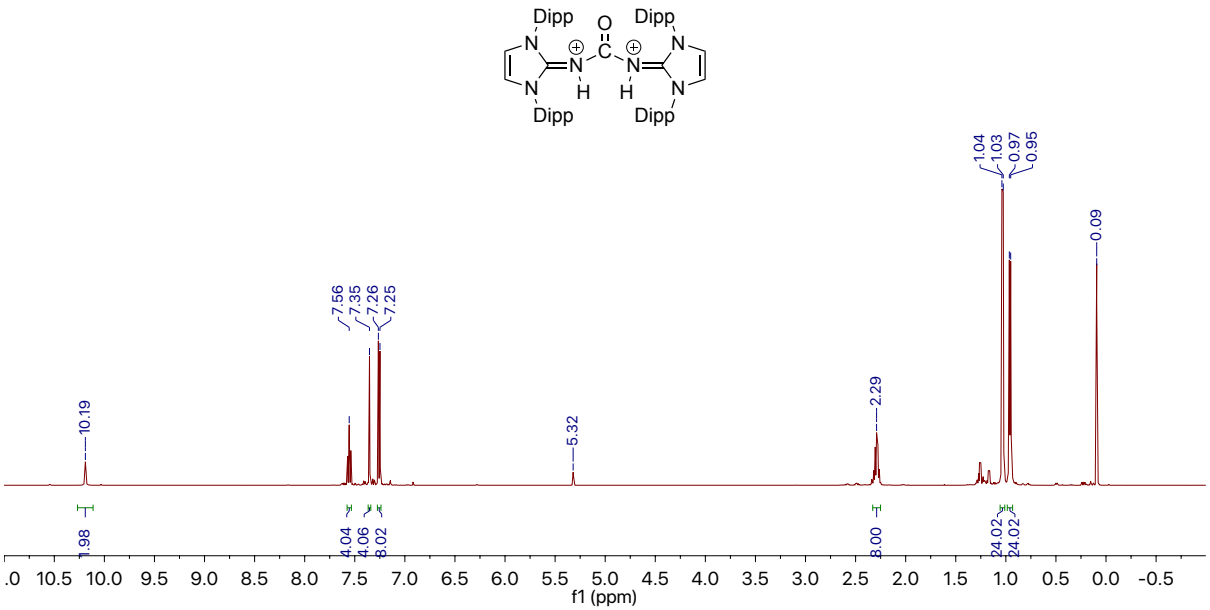


Figure 13. ^{1}H NMR spectrum of **[4][OTf]$_2$**.

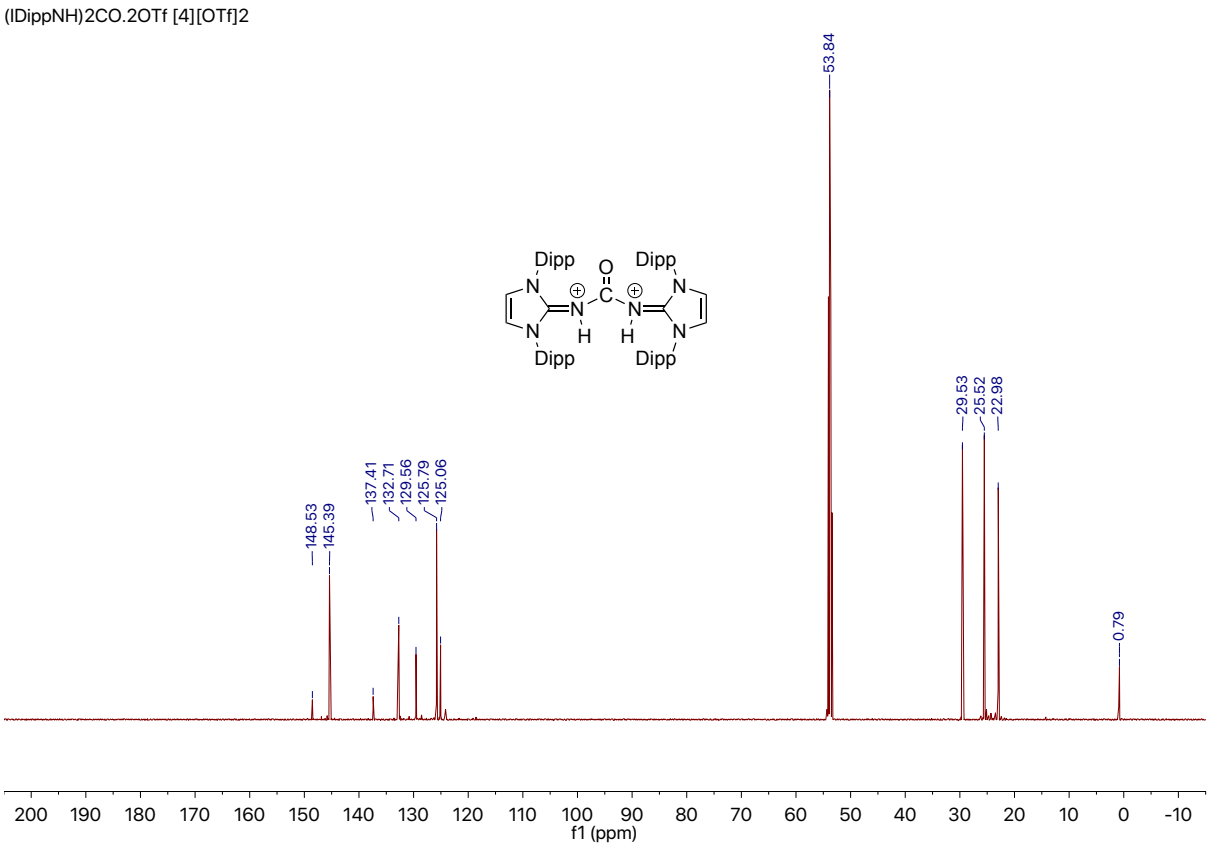


Figure 14. ^{13}C{^{1}H} NMR spectrum of **[4][OTf]$_2$**.

(IDippNH)2CO.2OTf [4][OTf]2

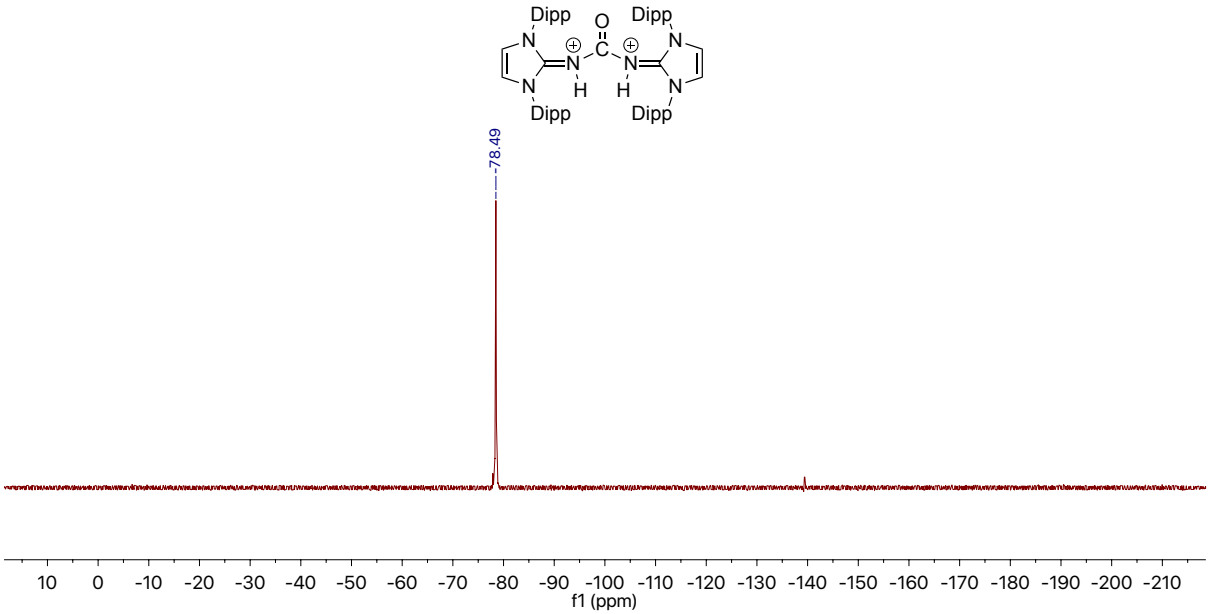


Figure 15. $^{19}F\{^{1}H\}$ NMR spectrum of **[4][OTf]$_2$**.

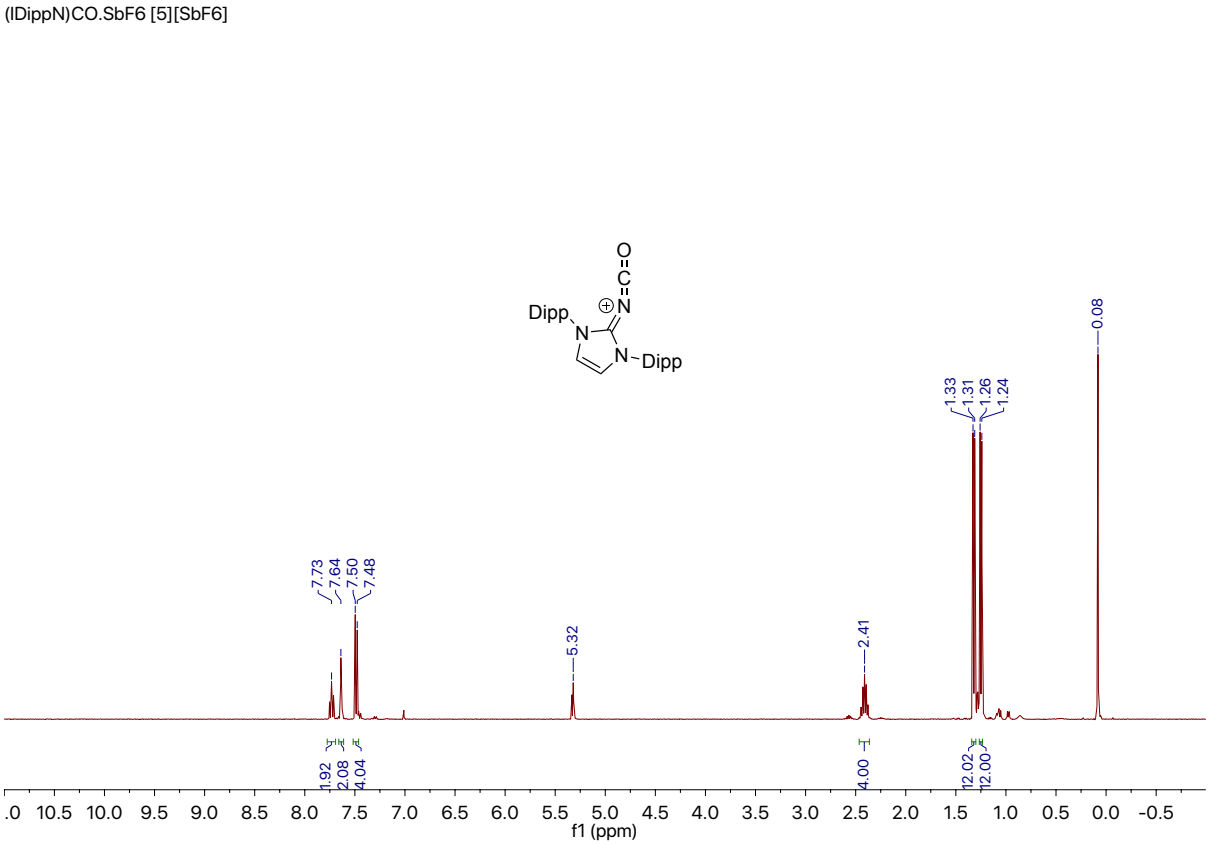


Figure 16. ^{1}H NMR spectrum of **[5][SbF$_6$]**.

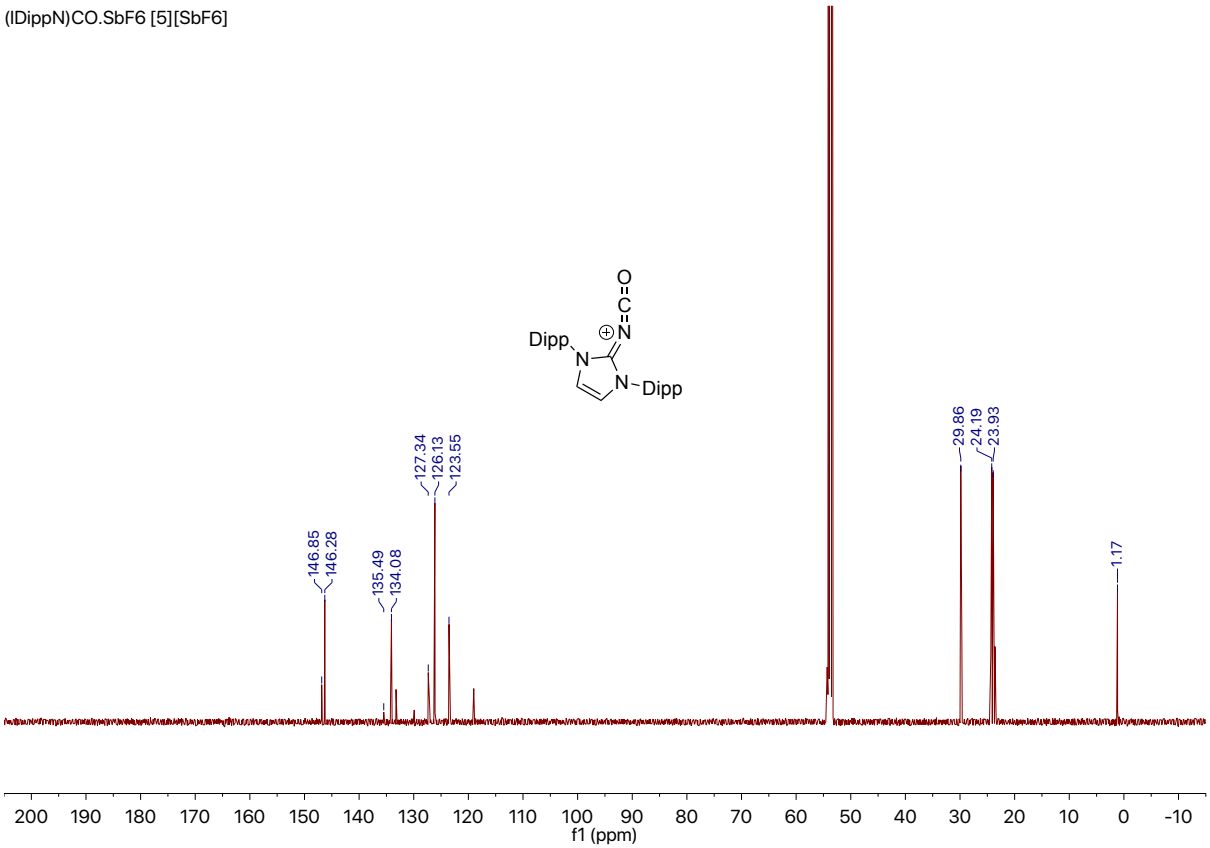


Figure 17. ^{13}C{^{1}H} NMR spectrum of **[5][SbF$_6$]**.

X-Ray Crystallographic Studies

Single-crystal X-ray diffraction data for **2–[6]$^{2+}$** were collected at 150 K on Oxford Diffraction/Agilent SuperNova diffractometers with Cu-$K\alpha$ (λ = 1.54184 Å) radiation equipped with nitrogen gas Oxford Cryosystems Cryostream unit.[14] Raw frame data were reduced using CrysAlisPro.[15] The structures were solved using SHELXT[16] and refined to convergence on F^2 and against all independent reflections by full-matrix least-squares using SHELXL[17] in combination with the SHELXLE[18] program. Distances and angles were calculated using the full covariance matrix. Restraints were used to maintain sensible geometries for the disordered groups and approximate the displacement parameters to typical values. For **2**, one 2,6-diisopropylphenyl group was modelled as disordered over two sites. For **[3]$^+$**, one molecule of [OTf]$^-$ and 1,2-difluorobenzene were modelled as disordered over two sites. For **[4]$^{2+}$**, one isopropyl group was modeled as disordered over two sites. For **[5]$^+$**, one $[SbF_6]^-$, one molecule of CH_2Cl_2 from crystallisation, one 2,6-diisopropylphenyl, two isopropyl groups and one NCO fragment were modeled as disordered over two sites. Selected crystallographic data are summarized in Table 2 and full details are given in the supplementary deposited CIF files (CCDC 1868070-1868073). These data can be obtained free of charge from the Cambridge Crystallographic Data Centre via http://www.ccdc.cam.ac.uk/data_request/cif.

Table 2. Selected crystallographic and refinement data for **2**–**[6]$^{2+}$**.

	2	**[3][OTf] ·½($C_6H_4F_2$)**	**[4][OTf]$_2$**	**[5][SbF_6] ·½(CH_2Cl_2)**	**[6][OTf]$_2$ ·2(CH_2Cl_2)**
Formula	C_{55} H_{72} N_6 O	C_{59} H_{75} F_4 N_6 O_4 S	C_{57} H_{74} F_6 N_6 O_7 S_2	C_{57} H_{74} Cl_2 F_{12} N_6 O_2 Sb_2	C_{59} H_{76} Cl_4 F_6 N_6 O_6 S_2
Fw	833.18	1040.31	1133.34	1417.62	1285.17
Cryst. System	Monoclinic	Monoclinic	Monoclinic	Monoclinic	Monoclinic
Space Group	P 21/c	P 2/c	C c	C 2/c	P 2/n
Wavelength/Å	1.54184	1.54184	1.54184	1.54178	1.54184
a/Å	21.0459(2)	20.9228(2)	14.17132(6)	18.6732(4)	25.6325(4)
b/Å	11.97190(10)	12.3724(2)	19.26524(8)	22.6905(2)	10.6261(1)
c/Å	19.8491(2)	23.0789(3)	21.81443(9)	17.5676(3)	25.9210(4)
α/°	90	90	90	90	90
β/°	99.1130(10)	99.8270(10)	93.3493(4)	119.325(2)	112.108(2)
γ/°	90	90	90	90	90
Volume/Å^3	4938.04(8)	5886.67(14)	5945.47(4)	6489.6(2)	6543.65(18)
Z	4	4	4	4	4
Temp./K	150(2)	150(2)	150(2)	150(2)	150(2)
Refls. Collect.	40318	44135	76725	25559	47475
$2\theta_{max}$	152.33	152.83	152.55	152.31	149.00
R_{int}	0.0301	0.0305	0.0310	0.0308	0.0429
Goodness of fit	1.031	1.037	1.016	1.041	1.026
$R[F^2>2\sigma]$, F	0.0390	0.0610	0.0238	0.0459	0.0619
R_w (all data), F^2	0.1050	0.1827	0.0627	0.1333	0.1926
CCDC ref	1868070	1868071	1868072	1868073	-

Computational Studies

All computational work reported here was carried out using density functional theory (DFT) within the Gaussian09 (Revision D.01) program package.[19] Geometry optimizations were performed with the PBE1PBE exchange-correlation functional using def-TZVP basis set.[20] In addition, Grimme's empirical dispersion correction scheme was employed.[21] The nature of the stationary points found (minima) were confirmed by full frequency calculations. The natural bond orbital (NBO) analysis was conducted to the optimized structure using NBO 3.1 as implemented in Gaussian09.[22]

References

(1) For carbonyl compounds in acidic media: (a) Clayden, J.; Greeves, N.; Warren S. *Organic Chemistry*; Oxford Press: Oxford, 2012. (b) Warren, S. *Chemistry of the Carbonyl Group*; Wiley-Blackwell: New York, 1974.

(2) For structures of protonated carbonyl compounds: (a) Tani, K.; Stoltz, B. M. Synthesis and structural analysis of 2-quinuclidoniumtetrafluoroborate. *Nature* **2006**, *441*, 731-734. (b) Komarov, I. V.; Yanik, S.; Ishchenko, A. Y.; Davies, A. J.; Goodman, J. M.; Kirby, A. J. The most reactive amide as a transition-state mimic for cis-trans interconversion. J. *Am. Chem. Soc.* **2015**, *137*, 926-930. (c) Szostak, M.; Yao, L.; Day, V. W.; Powell, D. R.; Aubé, J. Structural characterization of N-protonated amides: regioselective N-activation of medium-bridged twisted lactams. *J. Am. Chem. Soc.* **2010**, *132*, 8836-8837. (d) Cox, C.; Wack, H.; Lectka, T. Strong hydrogen bonding to the amide nitrogen atom in an "aimde proton sponge": consequences for structure and reactivity. *Angew. Chem., Int. Ed.* **1999**, *38*, 798-800. (e) Stuart, D.; Wetmore, S. D.; Gerken, M. Solid-state structure of protonated ketones and aldehydes. *Angew. Chem., Int. Ed.* **2017**, *56*, 16380-16384. (f) Tskhovrebov, A. G.; Vuichoud, B.; Solari, E.; Scopelliti, R.; Severin, K. Adducts of nitrous oxide and *N*-heterocyclic carbenes: syntheses, structures, and reactivity. *J. Am. Chem. Soc.* **2013**, *135*, 9486-9492.

(3) For superelectrophilic activation: (a) Olah, G. A.; Klumpp, D. A. *Superelectrophiles and Their Chemistry*; Wiley: New York, 2007. (b) Olah, G. A. Superelectrophiles. *Angew. Chem., Int. Ed.* **1993**, *32*, 767-922. (c) Olah, G. A.; Klumpp, D. A. Superelectrophilic solvation. *Acc. Chem. Res.* **2004**, *37*, 211-220. (d) Naredla, R. R.; Klumpp, D. A. Contemporary carbocation chemistry: applications in organic synthesis. *Chem. Rev.* **2013**, *113*, 6905-6948. (e) O'Connor, M. J.; Boblak, K. N.; Topinka, M. J.; Kindelin, P. J.; Briski, J. M.; Zheng, C.; Klumpp, D. A. Superelectrophiles and the effects of trifluoromethyl substituents. *J. Am. Chem. Soc.* **2010**, *132*, 3266-3267. (f) Naredla, R. R.; Zheng, C.; Lill, S. O. N.; Klumpp, D. A. Charge delocalization and enhanced acidity in tricationic superelectrophiles. *J. Am. Chem. Soc.* **2011**, *133*, 13169-13175. (g) Sai, K. K. S.; Tokarz, M. J.; Malunchuk, A. P.; Zheng, C.; Gilbert, T. M.; Klumpp, D. A. *N*-Heterocyclic superelectrophiles and evidence for single electron transfer chemistry. *J. Am. Chem. Soc.* **2008**, *130*, 14388-14389. (h)

Klumpp, D. A.; Zhang, Y.; O'Connor, M. J.; Esteves, P. M.; de Almeida, L. S. Aza-nazarov reaction and the role of superelectrophiles. *Org. Lett.* **2007**, *9*, 3085-3088.

(4) For theoretical, gas-phase and *in situ* studies of cations: (a) Olah, G. A.; Rasul, G.; Aniszfeld, R.; Prakash, G. K. S. Protonitronium dication (NO_2H^{2+}). *J. Am. Chem. Soc.* **1992**, *114*, 5608-5609. (b) Weiske, T.; Koch, W.; Schwarz, H. Experimental evidence for the existence of the protonitronium dication ($HONO^{2+}$) in the gas phase and ab initio molecular orbital calculations of its potential energy surface. *J. Am. Chem. Soc.* **1993**, *115*, 6312-6316. (c) Klumpp, D. A.; Zhang, Y.; Kindelin, P. J.; Lau, S. Superacid-catalyzed reactions of pyridinecarboxaldehydes. *Tetrahedron* **2006**, *62*, 5915-5921. (d) Olah, G. A.; Donovan, D. J.; Lin, H. C.; Mayr, H.; Andreozzi, P.; Klopman, G. Onium ions. 18. Static protonated and exchanging diprotonated ambivalent heteroorganic systems: hydroxylamines, acetone oxime, and dimethyl sulfoxide. *J. Org. Chem.* **1978**, *43*, 2268-2272. (e) Olah, G. A.; White, A. M. Stable carbonium ions. LXIX: protonation of ureas, guanidines, and biotin in super acid solution. *J. Am. Chem. Soc.* **1968**, *90*, 6087-6091. (f) Olah, G. A.; Kuhn, S. J.; Tolgyesi, W. S.; Baker, E. B. Stable carbonium ions. II. Oxocarbonium (acylium) tetrafluoroborates, hexafluorophosphates, hexafluoroantimonates and hexafluoroarsenates. Structure and chemical reactivity of acyl fluoride: Lewis acid fluoride complexes. *J. Am. Chem. Soc.* **1962**, *84*, 2733-2740.

(5) For Friedel-Crafts chemistry: a) Olah, G. A. *Friedel-Crafts and Related Reactions*, *Vol. 3*; Interscience: New York, 1964. (b) Olah, G. A. *Friedel-Crafts Chemistry*; Wiley: New York, 1973. (c) Olah, G. A.; Molnar, A. *Hydrocarbon Chemistry*; Wiley-Interscience: Hoboken, New Jersey, 2003.

(6) For structures of acylium ions: (a) Boer, F. P. The crystal structure of $CH_3CO^+SbF_6^-$. *J. Am. Chem. Soc.* **1966**, *88*, 1572-1574. (b) Chevrier, B.; Le Carpentier, J.; Weiss, R. Synthesis of two crystalline species of the Friedel-Crafts intermediate antimony penta-p-toluoyl chloride. Crystal structures of the donor-acceptor complex and of the ionic salt. *J. Am. Chem. Soc.* **1972**, *94*, 5718-5723. (c) Davlieva, M. G.; Lindeman, S. V.; Neretin, I. S.; Kochi, J. K. Isolation, X-ray structures, and electronic spectra of reactive intermediates in Friedel-Crafts acylations. *J. Org. Chem.* **2005**, *70*, 4013-4021. (d) Al-Talib, M.; Jibril, I.; Jochims, J. C.; Huttner, G. Synthesis and structures of heterocumulenes with $>C=N^+=C=O$ and $>C=N^+=C=S$ units. *Chem. Ber.* **1984**, *117*, 3211-3221. (e) Müller, E.; Orama, O.; Huttner, G.; Jochims, J. C. Amino substituted 1-oxa-3-azabutatrienium salts: preparation, structure and reaction with carbonyl compounds. *Tetrahedron*, **1985**, *41*, 5901-5912.

(7) For C=O bond distances: (a) Glocker, G. Carbon−oxygen bond energies and bond distances. *J. Phys. Chem.* **1958**, *62*, 1049-1054. (b) Gordy, W. *Microwave Spectroscopy*; Wiley: New York, 1953. (c) Allen, P. W.; Bowen, H. J.; Sutton, L. E.; Bastiansen, O. The molecular struture of acetone. *Trans. Faraday Soc.* **1952**, *48*, 991-995. (d) Herzberg, G. *Infrared and Raman Spectra of Polyatomic Molecules*; D. Van Nostrand Co. Inc.: New York, 1945.

(8) For reviews on NHIs: (a) Ochiai, T.; Franz, D.; Inoue, S. Applications of N-heterocyclic imines in main group chemistry. *Chem. Soc. Rev.* **2016**, *45*, 6327-6344. (b) Wu, X.; Tamm, M. Transition metal complexes supported by highly basic imidazolin-2-iminato and imidazolin-2-imine N-donor ligands. *Coord. Chem. Rev.* **2014**, *260*, 116-138. (c) Trambitas, A. G.; Panda, T. K.; Tamm, M. Rare earth metal complexes supported by ancillary imidazolin-2-iminato ligands. *Z. Anorg. Allg. Chem.* **2010**, *636*, 2156-2171.

(9) For NHI-stabilized multiply bonded main group compounds: (a) Wendel, D.; Reiter, D.; Porzelt, A.; Altmann, P. J.; Inoue, S.; Rieger, B. Silicon and oxygen's bond of affection: an acyclic three-coordinate silanone and its transformation to an iminosiloxysilylene. *J. Am. Chem. Soc.* **2017**, *139*, 17193-17198. (b) Wunsche, M.; Witteler, T.; Dielmann, F. Lewis base free oxophosphonium ions: tunable, trigonal-planar Lewis acids. *Angew. Chem., Int. Ed.* **2018**, *57*, 7234 -7239. (c) Dielmann, F.; Back, O.; Henry-Ellinger, M.; Jerabek, P.; Frenking, G.; Bertrand, G. A crystalline singlet phosphinonitrene: a nitrogen atom-transfer agent. *Science* **2012**, *337*, 1526-1528. (d) Dielmann, F.; Moore, C. E.; Rheingold, A. L.; Bertrand, G. Crystalline, Lewis base-free, cationic phosphoranimines (iminophosphonium salts). *J. Am. Chem. Soc.* **2013**, *135*, 14071-14073. (e) Franz, D.; Szilvási, T.; Irran, E.; Inoue, S. A monotopic aluminum telluride with an Al=Te double bond stabilized by *N*-heterocyclic carbenes. *Nat. Commun.* **2015**, *6*, 10037. (f) Franz, D.; Irran, E.; Inoue, S. Isolation of a three-coordinate boron cation with a boron−sulfur double bond. *Angew. Chem., Int. Ed.* **2014**, *53*, 14264-14268. (g) Wendel, D.; Szilvási, T.; Henschel, D.; Altmann, P. J.; Jandl, C.; Inoue, S.; Rieger, B. Twist of a silicon−silicon double bond: selective *anti*-addition of hydrogen to an iminodisilene. *J. Am. Chem. Soc.* **2017**, *139*, 9156-9159. (h) Wendel, D.; Szilvási, T.; Henschel, D.; Altmann, P. J.; Jandl, C.; Inoue, S.; Rieger, B. Precise activation of ammonia and carbon dioxide by an iminodisilene. *Angew. Chem., Int. Ed.* **2018**, *57*, 14575-14579.

(10)For structures of Ar−N=C=O: (a) Barnett, B. R.; Labios, L. A.; Moore, C. E.; England, J.; Rheingold, A. L.; Wieghardt, K.; Figueroa, J. S. Solution dynamics of redox noninnocent nitrosoarene ligands: mapping the electronic criteria for the formation of persistent metal-coordinated nitroxide radicals. *Inorg. Chem.* **2015**, *54*, 7110-7121. (b) Wilson, R. B.; Chen, Y.; Paul, I. C.; Curtin, D. Y. Crystal structure and solid-state reactivity of 4,4'-methylenediphenyl isocyanate (MDI). *J. Am. Chem. Soc.* **1983**, *105*, 1672-1674. (c) Zitt, H.; Dix, I.; Hopf, H.; Jones, P. G. 4,15-Diamino[2.2]paracyclophane, a reusable template for topochemical reaction control in solution. *Eur. J. Org. Chem.* **2002**, 2298-2307. (d) Hopf, H.; Narayanan, S. V.; Jones, P. G. The preparation of new functionalized [2.2]paracyclophane derivatives with *N*-containing functional groups. *Beilstein J. Org. Chem.* **2015**, *11*, 437-445.

(11)For theoretical analyses of cumulene ketones: (a) Weinhold, F. Why do cumulene ketones kink? *J. Org. Chem.* **2017**, *82*, 12238-12245. (b) Scheiner, A. C.; Schaefer III, H. F. Cyclopentadienylideneketene: theoretical consideration of an infrared spectrum frequently mistaken for that of benzyne. *J. Am. Chem. Soc.* **1992**, *114*, 4758-4762. (c) Radziszewski, J. G.; Kaszynski, P.; Friderichsen, A.; Abildgaard, J. Bent Cyclopenta-2,4-dienylideneketene: spectroscopic and *ab initio* study of reactive intermediate. *Collect. Czech. Chem. Commun.* **1998**, *63*, 1094-1106.

(12)For nitrilium ions and vinyl cations: (a) van Dijk, T.; Burck, S.; Rong, M. K.; Rosenthal, A. J.; Nieger, M.; Slootweg, J. C.; Lammertsma, K. Facile synthesis of phosphaamidines and phosphaamidinates using nitrilium ions as an imine synthon. *Angew. Chem., Int. Ed.* **2014**, *53*, 9068-9071. (b) Müller, T.; Meyer, R.; Lennartz, D.; Siehl, H. Unusually stable vinyl cations. *Angew. Chem., Int. Ed.* **2000**, *39*, 3074-3077.

(13)For preparation of IDippNSiMe$_3$: Imidazolin-2-iminato titanium complexes: synthesis, structure and use in ethylene polymerization catalysis. Tamm, M.; Randoll, S.; Herdtweck, E.; Kleigrewe, N.; Kehr, G.; Erker, G.; Rieger, B. *Dalton Trans.* **2006**, 459-467.

(14)Cosier, J.; Glazer, A. M. A nitrogen-gas-stream cryostat for general X-ray diffrcaction studies. *J. Appl. Cryst.* **1986**, *19*, 105-107.

(15)CrysAlisPro, Agilent Technologies, Version 1.171.35.8.

(16)Sheldrick, G. M. SHELXT - Integrated space-group and crystal structure determination. *Acta Cryst. Sect. A* **2015**, *71*, 3-8.

(17)Sheldrick, G. M. *Acta Cryst. Sect. A* **2008**, *64*, 112-122.

(18)Hübschle, C. B.; Sheldrick, G. M.; Dittrich, B. ShelXle: a Qt graphical user interface for SHELXL. *J. Appl. Cryst.* **2011**, *44*, 1281-1284.

(19)Frisch, M. J.; Trucks, G. W.; Schlegel, H. B.; Scuseria, G. E.; Robb, M. A.; Cheeseman, J. R.; Scalmani, G.; Barone, V.; Mennucci, B.; Petersson, G. A.; Nakatsuji, H.; Li, X.; Caricato, M.; Li, X.; Hratchian, H. P.; Izmaylov, A. F.; Bloino, J.; Zheng, G.; Sonnenberg, J. L.; Hada, M.; Ehara, M.; Toyota, K.; Fukuda, R.; Hasegawa, J.; Ishida, M.; Nakajima, T.; Honda, Y.; Kitao, O.; Nakai, H.; Vreven, T.; Montgomery, J. A., Jr.; Peralta, J. E.; Ogliaro, F.; Bearpark, M. J.; Heyd, J. J.; Brothers, E. N.; Kudin, K. N.; Staroverov, V. N.; Kobayashi, R.; Normand, J.; Raghavachari, K.; Rendell, A. P.; Burant, J. C.; Iyengar, S. S.; Tomasi, J.; Cossi, M.; Rega, N.; Millam, J. M.; Klene, M.; Adamo, C.; Jaramillo, J.; Gomperts, R.; Stratmannm R. E.; Yazyev, O; Austin, A.J.; Cammi, R.; Pomelli, C.; Ochterski, J. W.; Martin, R. L.; Morokuma, K.; Zakrzewski, V. G.; Voth, G. A.; Salvador, P; Dannenberg, J. J.; Dapprich, S.; Daniels, A. D.; Farkas, O.; Foresman, J. B.; Ortiz, J. V.; Cioslowski, J.; Fox, D. J. *Gaussian 09*, *Revision D.01*, Gaussian, Inc., Wallingford, CT **2009**.

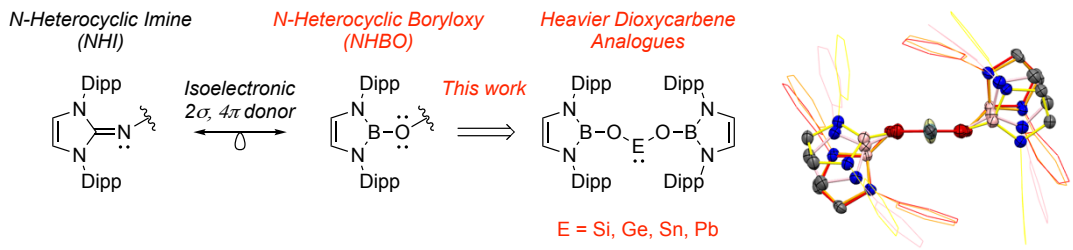
(20)(a) Perdew, J. P.; Burke, K.; Ernzerhof, M. *Phys. Rev. Lett.* **1996**, *77*, 3865-3868. (b) Perdew, J. P.; Ernzerhof, M.; Burke, K. *J. Chem. Phys.* **1996**, *105*, 9982-9985. (c) Adamo, C.; Barone, V. *J. Chem. Phys.* **1999**, *110*, 6158-6170. (d) Perdew, J. P.; Burke, K.; Ernzerhof, M. *Phys. Rev. Lett.* **1997**, *78*, 1396. (e) Schäfer, A.; Huber, C.; Ahlrichs, R. *J. Chem. Phys.* **1994**, *100*, 5829-5835.

(21)(a) Grimme, S.; Antony, J.; Ehrlich, S.; Krieg, H. *J. Chem. Phys.* **2010**, *132*, 154104-154119. (b) Grimme, S.; Ehrlich, S.; Goerigk, L. *J. Comput. Chem.* **2011**, *32*, 1456-1465.

(22)Glendening, E. D.; Reed, A. E.; Carpenter, J. E.; Weinhold,F. NBO Version 3.1.

Chapter 3

An N-Heterocyclic Boryloxy Ligand Isoelectronic with N-Heterocyclic Imines: Access to an Acyclic Dioxysilylene and its Heavier Congeners



Loh, Y. K.; Ying, L.; Fuentes, M. A.; Do, D. C. H.; Aldridge, S.

Angew. Chem., Int. Ed. **2019**, *58*, 4847-4851.

CONTENTS

Introduction 1

Oxygen-based Ligands 1

N-Heterocyclic Imine Ligands 2

N-Heterocyclic Boryl Anions 4

N-Heterocyclic Boryloxy Ligand 5

Results and Discussion 9

Synthesis of the NHBO Ligand 9

Acyclic Two-coordinate Silylenes 10

Synthesis of a bis(NHBO)Silylene 11

Synthesis of the Heavier Congeners (Ge, Sn, Pb) 12

Periodic Trends 14

DFT Analysis 16

Conclusions 18

Experimental 19

References 37

Introduction

Oxygen-based Ligands

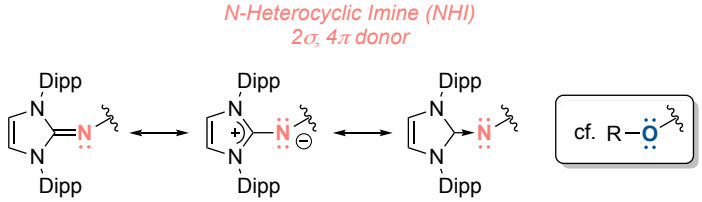
Oxygen-based ligands constitute a family of donors that are prevalent in coordination chemistry, particularly that of the harder metals.[1a] Among the most common of this family are alkoxy (RO−) ligands, formally derived from alcohols − which are widely applied, for example as supporting ligands for alkene and alkyne metathesis catalysts. This ligand class stands out for the fact that they have only one substituent, giving them the potential to contribute $2\sigma + 4\pi$ electrons to the metal centre − the maximum for any η^1 ligand. However, limited steric protection in the vicinity of the metal centre typically leads to bridging modes of coordination through oxygen to form aggregated clusters.[1b] This is clearly undesirable for applications which involve low coordinate metal centres, for example ambiphilic main group species (e.g. silylenes and their heavier congeners) which are of interest in small molecule activation chemistry.[2] An approach to counter this problem is to utilize *ortho*-substituted aryloxy (ArO−) ligands, making it possible to extend the degree of steric protection towards the metal centre. This strategy has enabled the isolation of monomeric species of the type $(ArO)_2E$ (E = Ge, Sn, Pb) by the groups of Lappert and Power.[1c-e] However, further chemistry with these systems typically involves the ligands acting as leaving groups with the aryloxide ligand being substituted by a stronger donor (cf. *p*Ka of phenol = ~9).[1f]

A potential strategy to circumvent this is to exploit the electropositive nature of boron and replace the O-bound substituent with a boryl (R_2B−) functionality.[3] However, the boryloxy (R_2BO−) ligand is considered an *electron deficient* alkoxide variant when R = alkyl or aryl, due to the formally empty *p* orbital on boron rendering the boryloxy fragment a weak π donor. Applications in main group element compounds are scarce and are limited to

complexes of the groups 1, 2 and 13 metals.[3b-d] Very recently, Sarazin and co-workers reported the examples of monomeric main group species of the form $(R_2BO)_2E$ (E = Sn, Pb, Ba) by employing the bulky R = $(Me_3Si)_2HC$ group to inhibit dimerization.[2e-f] Hence, it was viewed as highly desirable from a main group coordination chemistry perspective to design a synthetically facile and widely applicable, strong O-donor ligand with a large steric profile.

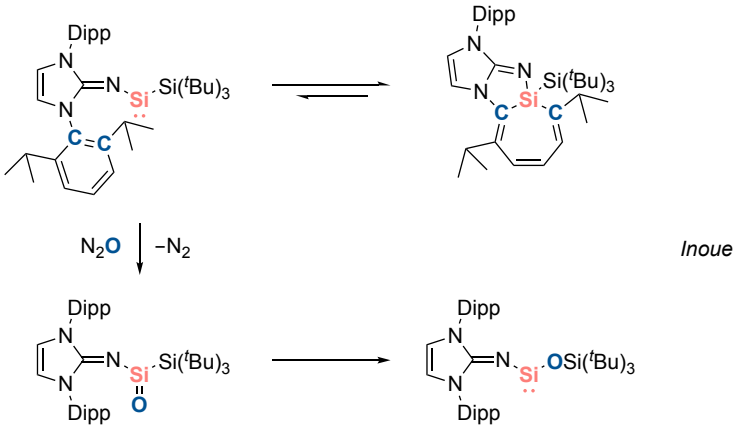
N-Heterocyclic Imine Ligands

The N-heterocyclic imine (NHI) represents another class of anionic iminato ligand featuring a single substituent, thus they have the propensity to donate 2σ, 4π electrons, making them isolobal with alkoxide/aryloxide ligands (Scheme 1; Chapters 1 and 2).[4] These systems are based on the well-known N-heterocyclic carbene (NHC) framework, which acts as the sole N-bound substituent. Harnessing the strongly electron-releasing properties of the NHC moiety, the exocyclic C=N double bond is highly polarized in an ylidic fashion ($C^{\delta+}-N^{\delta-}$), rendering the NHI family strong donor ligands. Aside from its highly basic nature, the NHC framework also provides a potentially very large steric profile, making them ideally suited for applications in low-coordinate main group chemistry.[5] Recently, our group exploited the NHI as a surrogate for O-based ligands to tame hitherto unknown organic electrophiles (Chapter 2).[5e]



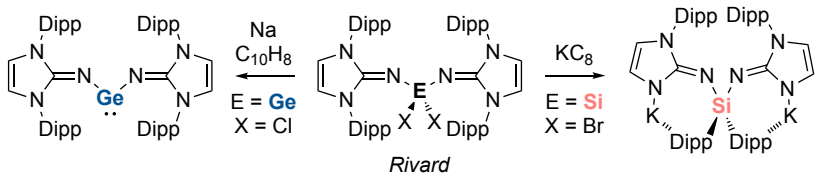
Scheme 1. Canonical forms of the NHI ligand which is isolobal with conventional O-based ligands.

In addition to carbon-based species, the NHI family has also proved its effectiveness in supporting compounds featuring the heavier group 14 elements.[5f-j, 6d-e] Most notably, the Inoue group has explored the strong σ and π donor abilities of NHIs in the synthesis of silylenes, such as an acyclic iminosilylene, NHI(Cp*)Si.[6a] More recently, in 2017, they reported that an imino(silyl)silylene, NHI(SiR_3)Si, reversibly inserts into an aromatic C=C double bond in an intramolecular fashion to form a silepin (Scheme 2; Chapter 1).[6b] While Si(II)-to-Si(IV) oxidative addition is well documented, this work by Inoue and co-workers opens the door to Si(IV)-to-Si(II) reductive elimination – a process which has been a long standing goal in the development of potential catalytic processes involving silicon centres. Most remarkably, this silepin could further act as a "masked" silylene in the presence of N_2O, allowing the isolation of a long-sought-after acyclic silanone containing a Si=O double bond.[6c] Key to this landmark achievement is the strong π donation from the single NHI substituent attached to the electron-deficient silicon center. The highly oxophilic nature of silicon coupled with its strong desire to form Si–O single bonds (rather than a Si=O double bond) induces thermal rearrangement of the silanone to an imino(siloxy)silylene, again reversing the oxidation from Si(IV)-to-Si(II).



Scheme 2. Oxidation of a "masked" imino(silyl)silylene to an acyclic silanone and subsequent thermal rearrangement to an imino(siloxy)silylene.

Employing NHI as substituent has a profound influence on the reactivity of silylenes, which led us to wonder whether a homoleptic bis(NHI)silylene is a viable synthetic target for exploring new modes of reactivity. While the Rivard group recently reported the successful synthesis of a homoleptic bis(NHI)germylene complex, the attempted synthesis of the analogous bis(NHI)silylene resulted in ligand rearrangement (Scheme 3).[5f] They attributed this to the strongly donating nature of the NHI, rendering the silicon center too electron rich. Hence, we believed that an O-based analogue of the NHI $[(HCDippN)_2CN]^-$ (i.e. $[(HCDippN)_2BO]^-$) bearing a more electronegative oxygen donor might be better suited to stabilize the Si(II) center. Furthermore, the newly designed N-heterocyclic boryloxy (NHBO) ligand is isoelectronic and isostructural with the NHI family, which might inherit strong O-donor traits and a huge steric profile (features which are absent from currently available O-based ligands), making it a potential candidate for a dioxysilylene and its heavier congeners.

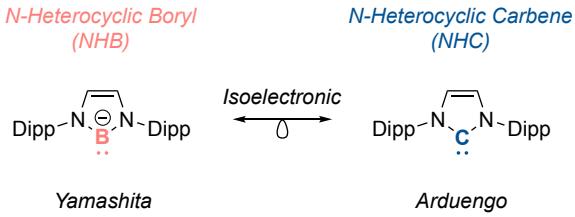


Scheme 3. Rivard's synthesis of a bis(NHI)germylene and attempted synthesis of a bis(NHI)silylene.

N-Heterocyclic Boryl Anions

The N-heterocyclic boryl (NHB) unit, $[(HCDippN)_2B]^-$, was first reported by Yamashita and co-workers in 2006 (Scheme 4; Chapter 1).[7] This boryl anion is isoelectronic with classical NHCs, and can be regarded as an anionic group 13 carbene analogue.[8] It shares similar traits with NHCs, such as its singlet ground state, with a lone pair of electrons in a σ orbital and a formally vacant $p\pi$ orbital, thus making it somewhat ambiphilic as well.

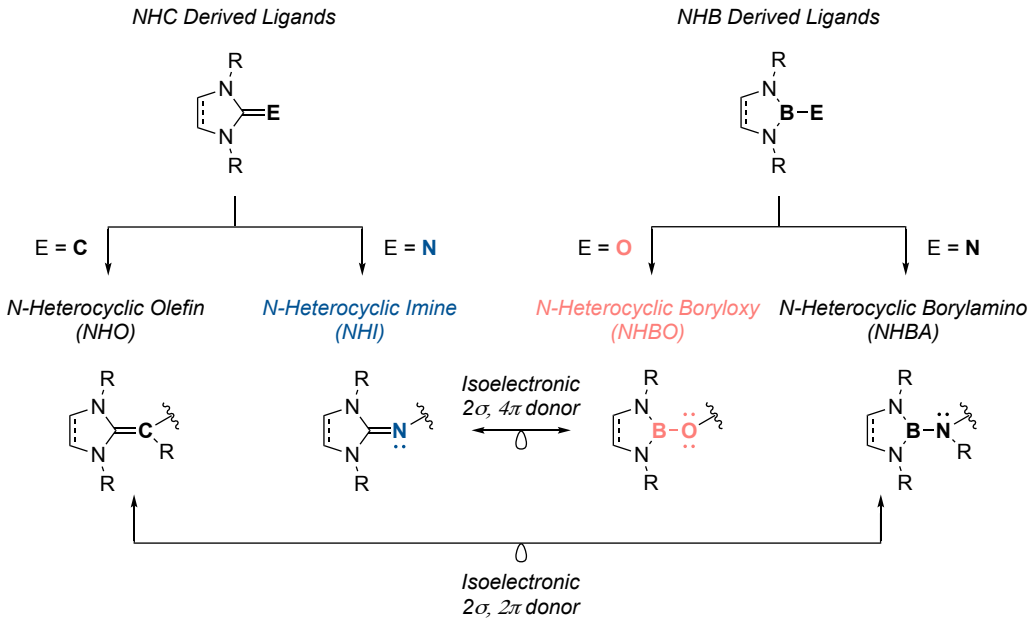
However, the NHB is predominantly more nucleophilic than electrophilic, a feature in common with the NHCs, presumably due to the contribution of the 6π aromatic form induced by the diazabutadiene ligand scaffold. Also, the NHB contains an electropositive boron, coupled with its anionic nature, renders it a stronger σ donor ligand than the NHCs.[9]



Scheme 4. N-Heterocyclic boryl (NHB) and its isoelectronic analogy with the classical N-heterocyclic carbene (NHC).

N-Heterocyclic Boryloxy Ligand

The NHB ligand features strong σ donor and weak π acceptor properties complemented by a sterically demanding profile, in analogy with classical NHCs. We believe that the NHB could also transfer its electronic and steric properties to an appended exocyclic moiety, to act as a platform for new ligand design (Scheme 5; Chapter 1). Thus, having the NHB fragment as the O-bound substituent of an N-heterocyclic boryloxy (NHBO) system would give rise to a strong O-donor ligand with a high degree of steric hindrance, in a manner reminiscent of NHI ligands having an NHC as the N-bound substituent. While the isoelectronic analogy relates NHBO with NHI, the NHBO can also be viewed as under a family of NHB derived ligands, with the N-heterocyclic borylamino (NHBA)[10e] ligand [which is isoelectronic with N-heterocyclic olefins (NHO)][11] also a member of this ligand class (Scheme 5; Chapter 1).



Scheme 5. N-Heterocyclic boryloxy (NHBO) ligands, isoelectronic with N-heterocyclic imines (NHI) and closely related to N-heterocyclic borylamino (NHBA) ligands.

With this new ligand design in mind, we first probed the donor capacity of the NHBO ligand with respect to other O-based ligands and NHI (Figure 1). DFT calculations using the PBE1PBE hybrid exchange-correlation functional in combination with the SVP basis set carried out on the 'free' ligand anions are consistent with the isolobal nature of these systems. The frontier orbitals (HOMO, HOMO−1) are comprised of the orthogonal in-plane and out-of-plane π donor orbitals. In general, the relative energies of the donor orbitals rise in the order $[\{(Me_3Si)_2HC\}_2BO]^-$< $[(2,6\text{-}Dipp_2C_6H_3)O]^-$< $[(HCDippN)_2BO]^-$< $[(HCDippN)_2CN]^-$, reflecting successively enhanced π donor abilities. Consistently, the relative energies of the σ donor orbitals assume a similar trend.

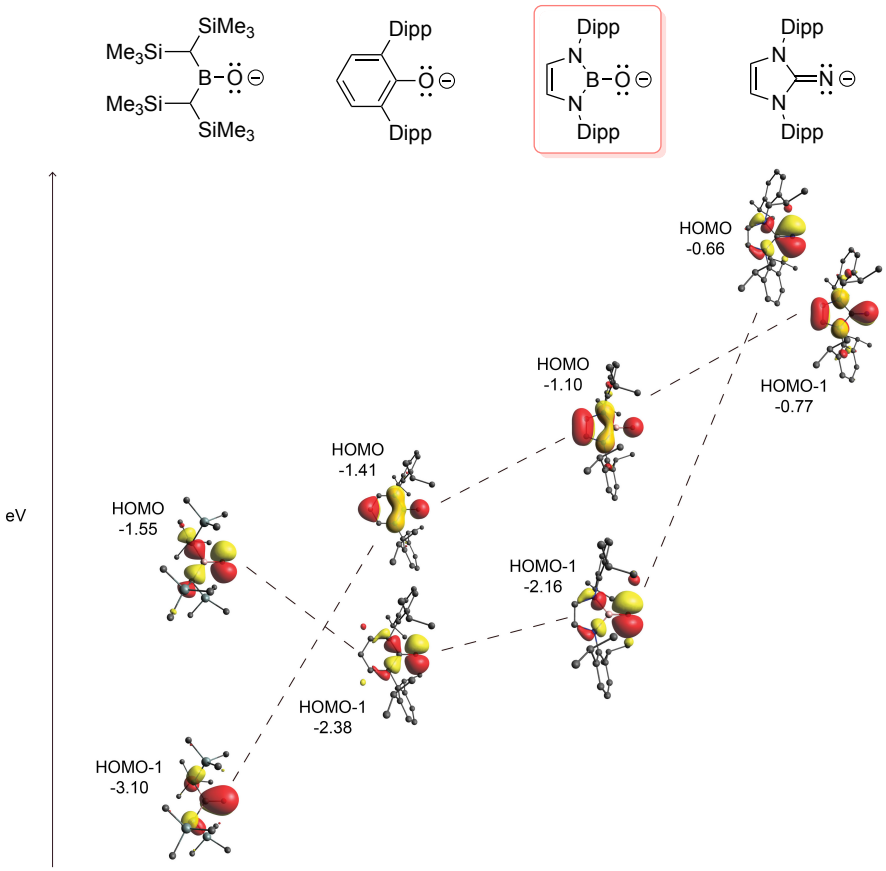
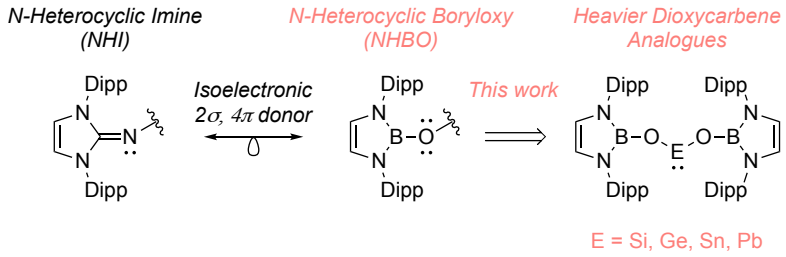


Figure 1. π-Symmetry frontier orbitals and their relative energies for $[\{(Me_3Si)_2HC\}_2BO]^-$, $[(2,6\text{-}Dipp_2C_6H_3)O]^-$, $[(HCDippN)_2BO]^-$ and $[(HCDippN)_2CN]^-$ (isosurface 0.04).

Hence, these calculations would seem to indicate that the NHBO is indeed a strong O-donor ligand, yet not as strong a donor as the NHI. Since a wholly NHI supported silylene does not seem to be viable, the NHBO ligand appears to be an ideal candidate for a uniquely isoelectronic silylene. Herein, we introduce a new class of strongly donating NHBO ligand, isoelectronic with the NHI which allows access to the first acyclic two-coordinate dioxysilylene and its heavier (Ge, Sn, Pb) congeners, presenting the complete series of homoleptic group 14 heavier dioxycarbene analogues (Scheme 6).

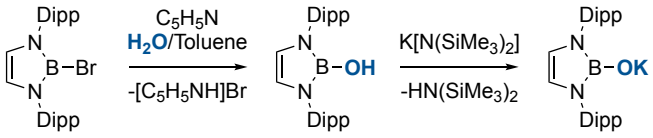


Scheme 6. The isoelectronic relationship between NHI and NHBO ligands, and syntheses of heavier dioxycarbene analogues (Si, Ge, Sn, Pb).

Results and Discussion

Synthesis of the NHBO Ligand

We set out to develop a convenient synthesis for borinic acid ("protio ligand") **1** (Scheme 7), hypothesizing that deprotonation would then offer a straightforward route to the formally anionic NHBO target system.[7b] Treatment of the corresponding bromoborane in a biphasic water/toluene mixture using pyridine as the base leads to facile introduction of the exocyclic OH group in 66% yield. Subsequent deprotonation was achieved by treating **1** with K[N(SiMe$_3$)$_2$] to afford K[(HCDippN)$_2$BO], **2**, which gives rise to a signal at 22.8 ppm in the ^{11}B{^{1}H} NMR spectrum. Single crystals obtained by slow evaporation of a concentrated *n*-hexane solution allowed X-ray diffraction analysis to determine its structure to be dimeric in the solid-state, with potassium ions sandwiched between the two arene π systems (Figure 2). As a library of diazaborolyl frameworks featuring a variety of substitution patterns has been documented, there is a potential for fine-tuning of the electronics and steric properties of the NHBO ligand.



1 **2**

Scheme 7. Syntheses of (HCDippN)$_2$BOH (**1**) and K[(HCDippN)$_2$BO] (**2**).

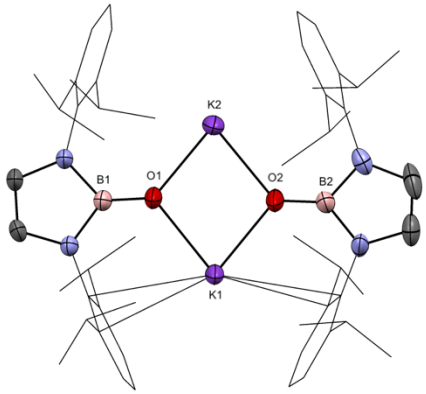
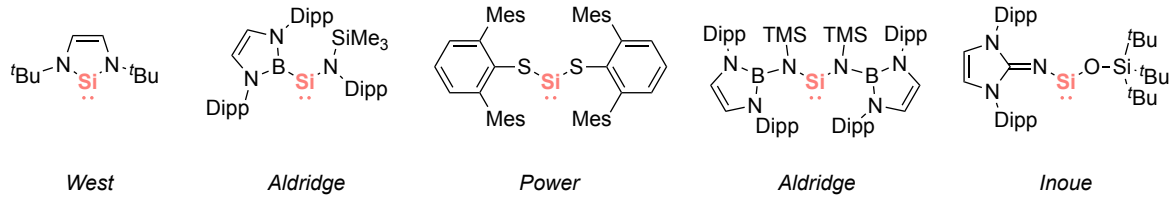


Figure 2. Solid-state structure of **2** as determined by X-ray crystallography. For clarity, hydrogen atoms are omitted and Dipp groups shown in wireframe format. Thermal ellipsoids are set at 40% probability. Selected bond lengths (Å): **2**: B1−O1 1.301(3), B2−O2 1.299(3), O1−K1 2.5400(18), O1−K2 2.4934(19), O2−K1 2.539(2), O2−K2 2.515(2).

Acyclic Two-coordinate Silylenes

Silylenes are the heavier relatives of carbenes, and have garnered immense interest in the field of main group chemistry. In 1994, West reported the seminal discovery of an isolable N-heterocyclic silylene (NHSi) that is valence isoelectronic with the NHC class of compound (Scheme 8).[10a] While the chemistry of cyclic silylenes developed subsequently by varying the ancillary ligands and coordination number at the silicon centre, acyclic silylenes remained notoriously challenging synthetic targets. In 2012, our group reported the successful synthesis of the first acyclic two-coordinate silylene, featuring pendant boryl and amido substituents.[10b] The narrow singlet-triplet gap of 103.9 kJ mol^{-1} enables facile single site activation of H_2. This fundamental mode of reactivity, more akin to transition metal systems was observed at a Si(II) centre for the first time. Shortly after, the Power group reported another acyclic silylene supported by thiolato ligands, which interestingly binds ethylene reversibly.[10c] While the chemistry of acyclic two-coordinate silylenes has gained much attention and new systems have been subsequently developed (vide supra), to date only

a handful of them have been isolated and among this group, dioxysilylenes remain conspicuously absent.

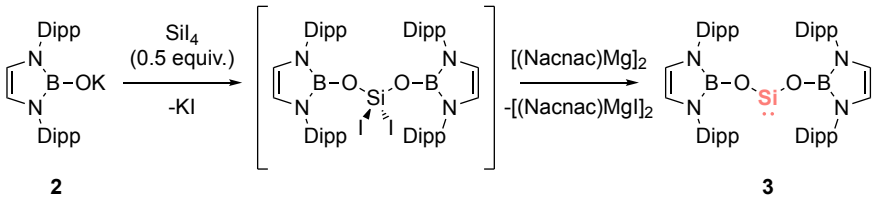


Scheme 8. Examples of two-coordinate cyclic and acyclic silylenes.

Synthesis of a bis(NHBO)Silylene

Treatment of **2** with SiI_4 (0.5 equiv.) initially forms the intermediate $[(HCDippN)_2BO]_2SiI_2$ which could subsequently be reduced at 80 °C with Jones' reagent, $[(Nacnac)Mg]_2$ (Nacnac = $HC(MeCMesN)_2$; Mes = 2,4,6-$Me_3C_6H_2$), to afford the target bis(NHBO)silylene system **3** in 87% isolated yield (Scheme 9). The $^{29}Si\{^1H\}$ NMR spectrum of **3** displays a signal at 35.5 ppm, significantly high-field shifted compared to the acyclic two-coordinate diamino- (204.6 ppm)[10e] and dithiolatosilylenes (285.5 ppm),[10c] but close to Inoue's imino(siloxy)silylene (58.9 ppm).[6c] Slow evaporation of a solution of **3** in *n*-pentane afforded colourless crystals, and X-ray diffraction analysis unambiguously confirmed the molecular structure of **3** as featuring a two-coordinate Si(II) centre; **3** therefore represents the first example of an acyclic two-coordinate dioxysilylene (Figure 3). The central Si1 atom is bent at an angle of 100.02(8)°, a value which is intermediate between that of West's cyclic NHSi (88.6°)[10a] and the acyclic amino(boryl)silylene (109.7(1)°)[10b] from our group. The angle resembles that determined for Inoue's imino(siloxy)silylene (103.56(8)°),[6c] further suggesting the similar electronic effect exerted on the Si(II) center by NHBO and NHI. However, the Si−O bond distances (mean: 1.606(1) Å) are significantly shorter than that found in Inoue's

imino(siloxy)silylene (1.643(1) Å),[6c] presumably reflecting the fact that the NHI is the dominant electron-releasing component in Inoue's system.



Scheme 9. Synthesis of $[(HCDippN)_2BO]_2Si$ (**3**).

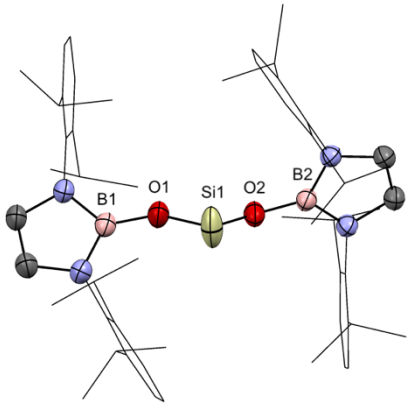
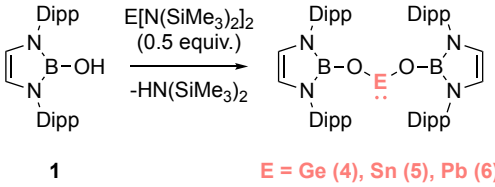


Figure 3. Solid-state structures of **3** as determined by X-ray crystallography. For clarity, hydrogen atoms are omitted and Dipp groups shown in wireframe format. Thermal ellipsoids are set at 40% probability. Selected bond lengths (Å) and angles (°): **3**: Si1−O1 1.6074(14), Si1−O2 1.6052(14), O1−B1 1.373(2), O2−B2 1.375(2), O1−Si1−O2 100.02(8).

Synthesis of the Heavier Congeners (Ge, Sn, Pb)

Motivated by the successful isolation of a dioxysilylene featuring the NHBO ligand, we turned our attention to its heavier congeners. An alternative approach to access heavier carbene analogues (Ge, Sn, Pb) is via protonolysis. Accordingly, direct treatment of borinic acid **1** with $E[N(SiMe_3)_2]_2$ (E = Ge, Sn, Pb) (0.5 equiv.) led to facile formation of the target systems $(NHBO)_2E$ in good yields (**4**: E = Ge (86%), **5**: E = Sn (88%), **6**: E = Pb (78%);

Scheme 10). In the case of **5**, the $^{119}Sn\{^{1}H\}$ NMR spectrum displays a signal at −109.0 ppm, which is downfield shifted from the resonances reported for $[\{(Me_3Si)_2HC\}_2BO]_2Sn$ (−186 ppm)[3e] and $[(2,6\text{-}Dipp_2C_6H_3)O]_2Sn$ (−289.7 ppm).[1d] A similar trend is observed for **6** in the $^{207}Pb\{^{1}H\}$ NMR spectrum, which gives rise to a signal at 1885 ppm, i.e. downfield shifted compared to those of $[\{(Me_3Si)_2HC\}_2BO]_2Pb$ (1805 ppm)[3e] and $[(2,6\text{-}Dipp_2C_6H_3)O]_2Pb$ (1070 ppm).[1e]



Scheme 10. Syntheses of $[(HCDippN)_2BO]_2E$ (E = Ge (**4**), Sn (**5**), Pb (**6**)) via protonolysis.

Concentrating solutions of **4**, **5** or **6** in benzene afforded single crystals in all three cases. X-ray diffraction analysis unambiguously revealed the heavier analogues $(NHBO)_2Ge$ (**4**), $(NHBO)_2Sn$ (**5**), $(NHBO)_2Pb$ (**6**) to be isostructural to $(NHBO)_2Si$ (**3**) in the solid-state (Figure 4). In germylene **4**, the central Ge(II) center is bent at an angle of 93.56(7)°, i.e. marginally wider than that of $[(2,6\text{-}Dipp_2C_6H_3)O]_2Ge$ (92.54(6)°),[1d] but narrower than that of Rivard's $(NHI)_2Ge$ system (99.48(10)°).[5f] The Ge−O bond distance (mean: 1.778(2) Å) is significantly shorter than that found in $[(2,6\text{-}Dipp_2C_6H_3)O]_2Ge$ (mean: 1.827 Å)[1d] suggesting the presence of a relatively strong Ge−O π interaction. These structural parameters support the donor capacity of the NHBO ligand being intermediate of the aryloxy ligand and the NHI. For stannylene **5** and plumbylene **6**, a similar trend can be observed whereby the Sn−O (mean: 2.015(2) Å) and Pb−O distances (mean: 2.131(2) Å) are considerably shorter than their aryloxy counterparts $[(2,6\text{-}Dipp_2C_6H_3)O]_2Sn$ (mean: 2.047 Å)[1d] and $[(2,6\text{-}Dipp_2C_6H_3)O]_2Pb$ (mean: 2.216 Å).[1e]

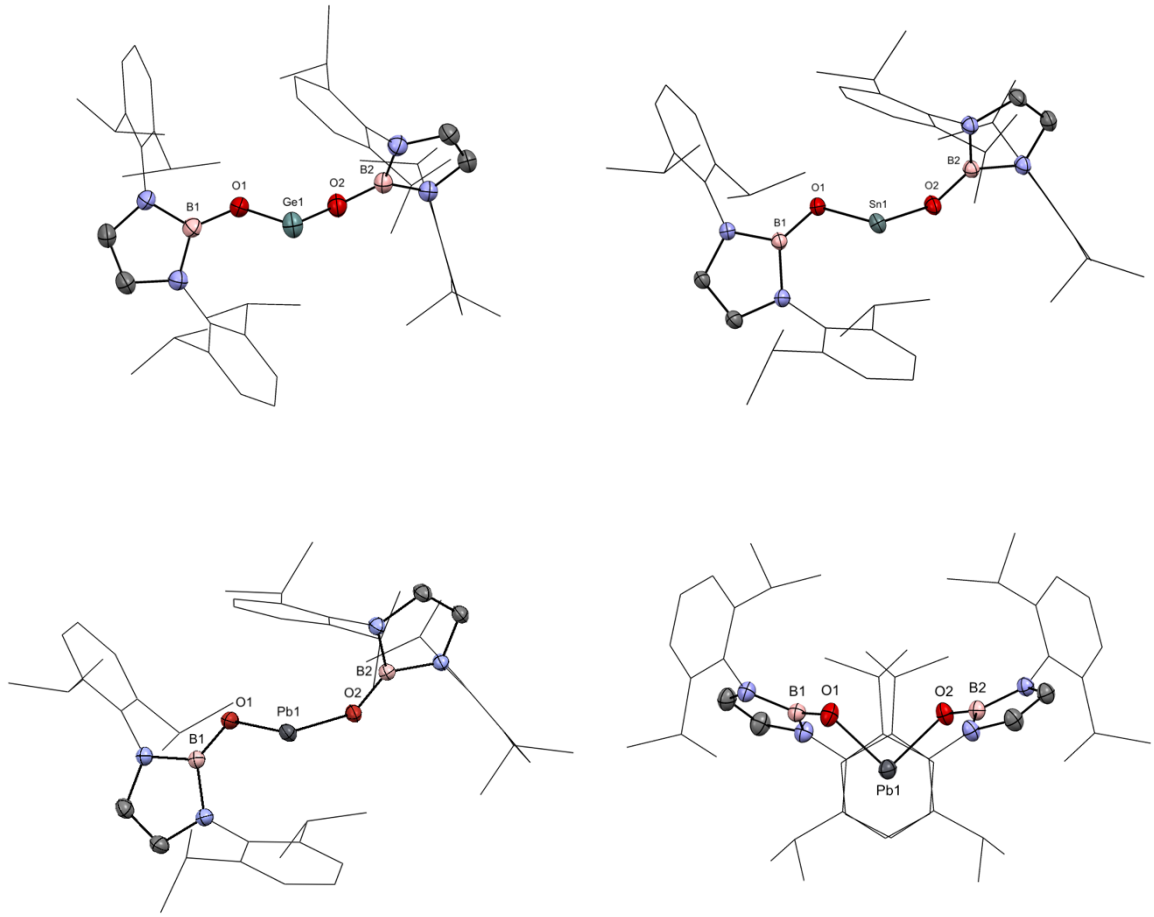


Figure 4. Solid-state structures of **4** (top left), **5** (top right), **6** (bottom left) and top view **6** (bottom right) as determined by X-ray crystallography. For clarity, hydrogen atoms are omitted and Dipp groups shown in wireframe format. Thermal ellipsoids are set at 40% probability. Selected bond lengths (Å) and angles (°): **4**: Ge1–O1 1.7768(16), Ge1–O2 1.7786(16), O1–B1 1.360(3), O2–B2 1.364(3), O1–Ge1–O2 93.56(7). **5**: Sn1−O1 2.0184(18), Sn1−O2 2.0125(19), O1−B1 1.355(3), O2−B2 1.350(3) O1–Sn1–O2 93.25(8). **6**: Pb1−O1 2.1319(16), Pb1−O2 2.1304(15), O1−B1 1.341(3), O2−B2 1.344(3) O1–Pb1–O2 92.66(6).

Periodic Trends

With a complete homoleptic series of group 14 heavier dioxycarbene analogues of the type $(NHBO)_2E$ (E = Si, Ge, Sn, Pb) in hand, some periodic trends in their structural properties could be discerned. Descending down the group, the O−E−O angle becomes more acute, gradually approaching 90°, reflecting the less effective *s*-*p* hybridization commonly

observed in heavier main group elements (Table 1).[2] In addition, the B−O distances shorten, consistent with increasing π donation from oxygen to boron as the competing O-to-E π interaction becomes less efficient. Thus, the B−O distances measured for silylene **3** (mean: 1.374(2) Å), are essentially identical to the B−O single bond distance (1.373(3) Å) in borinic acid **1**;[7b] this distance progressively shortens to plumbylene **6** (mean: 1.343(3) Å), hinting at the gradually accruing B=O double bond character.[12] Lastly, the B−O−E−O torsion angle narrows as E becomes heavier, swiveling the NHBO ligands above and below the central O−E−O plane (Figure 5). This enables enhanced arene π interactions between the Dipp groups and the formally vacant *p*π orbital of the central E(II) centre, which is further underscored by the progressive shortening of the C_{ipso}−E distances.[13] This sandwich type π interaction is most prominent in plumbylene **6** (Figure 4, bottom right), with an average C_{ipso}−E distance of 3.095(2) Å. Viewed from another perspective, the NHBO ligand can be regarded as showing signs of ambidentate behavior, switching from hard O-donor to the soft arene π system, upon descending the group, from the hard Si(II) in **3** to the softer Pb(II) centre in **6** (Figure 5).

Table 1. Selected bond distances (Å) and angles (°) for $(NHBO)_2E$ (E = Si, Ge, Sn, Pb).

E	O−E−O	E−O[a]	B−O[a]	B−O−E−O[a]	E−C_{ipso}[a]
Si (**3**)	100.02(8)	1.606(1)	1.374(2)	159.48(1)	3.576(2)
Ge (**4**)	93.56(7)	1.778(2)	1.362(3)	144.45(1)	3.421(2)
Sn (**5**)	93.25(8)	2.015(2)	1.353(3)	123.40(1)	3.123(2)
Pb (**6**)	92.66(6)	2.131(2)	1.343(3)	120.37(1)	3.095(2)

[a] Mean values.

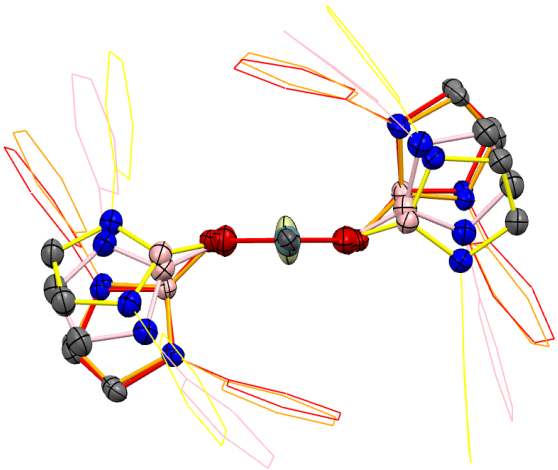


Figure 5. Solid-state structures of **3** (yellow), **4** (pink), **5** (orange) and **6** (red) overlaid. For clarity, hydrogen atoms and ^{i}Pr groups are omitted and Dipp groups shown in wireframe format. Thermal ellipsoids are set at 40% probability.

DFT Analysis

To gain further insights into the role of the NHBO ligand in the series of heavier dioxycarbene analogues **3**–**6**, in particular its ability to stabilize an unprecedented class of silylene, we subjected these systems to DFT analysis using the PBE1PBE hybrid exchange-correlation functional. Calculations reveal the LUMO for each case to be comprised mainly of the E p_z character, with decreasing O p_z contributions down the group, consistent with less effective O-to-E π interactions (Figure 6, silylene **3**). While the HOMO is typically ligand-based, the orbital with E(II) lone pair character is located in the HOMO−2 for (E = Si, Ge, Sn), due to the influence of the highly electronegative O-donors. Interestingly, when E = Pb, this orbital can be found in the HOMO−10, probably due to the additional influence of relativistic effects leading to stabilization of the Pb 6*s* orbital. The energy gap between the E(II)-centred lone pair orbital and the formally vacant *p*π orbital is very large for all of Si, Ge, Sn and Pb. In particular, bis(NHBO)silylene **3** has an energy gap of 5.45 eV, which is

considerably larger than those of reported acylic silylenes (eg. imino(siloxy)silylene: 4.33 eV,[6c] dithiolatosilylene: 4.23 eV).[10c]

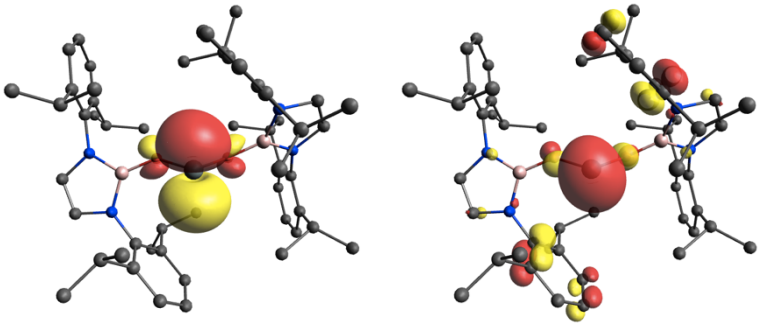


Figure 6. LUMO (left) and HOMO−2 (right) of bis(NHBO)silylene **3** (isosurface 0.05).

Conclusions

In conclusion, we report on the development of a new class of strongly donating N-heterocyclic boryloxy (NHBO) ligand, isoelectronic with the well-known NHI donor class. Employment of the NHBO ligand has enabled the successful stabilization of the first acyclic two-coordinate dioxysilylene and its heavier (Ge, Sn, Pb) congeners. This represents the first complete series of heavier dioxycarbene analogues, fully characterized by X-ray crystallography and DFT calculations. Analysis of periodic structural trends shed light on the ambident nature of the NHBO ligand, provided by snapshots of its gradual transition from O-donor (hard) to arene π donor (soft) upon descending the group from Si (hard) to Pb (soft). While monomeric low-coordinate main group species are predominantly supported by N-based ligands, those with O-based ligands are conspicuously rarer. We hope that this class of NHBO ligand, with its strong donor capacity and large steric profile will provide an entry point to access further examples of unprecedented oxy-stabilized main group species. Current interest in our lab is looking at incorporating the NHBO as substituents for a dioxycarbene.

Experimental

General Considerations and Starting Material Preparations

All manipulations were carried out using standard Schlenk line or dry-box techniques under an atmosphere of argon or dinitrogen. Solvents were degassed by sparging with argon and dried by passing through a column of the appropriate drying agent. NMR spectra were measured in benzene-d_6 (which was dried over potassium), with the solvent then being distilled under reduced pressure and stored under argon in Teflon valve ampoules. NMR samples were prepared under argon in 5 mm Wilmad 507-PP tubes fitted with J. Young Teflon valves. ^{1}H, ^{13}C{^{1}H}, ^{11}B{^{1}H}, ^{29}Si{^{1}H}, ^{119}Sn{^{1}H} and ^{207}Pb{^{1}H} NMR spectra were recorded on Bruker Avance III HD nanobay 400 MHz or Bruker Avance 500 MHz spectrometer at ambient temperature and referenced internally to residual protio-solvent (^{1}H) or solvent (^{13}C) resonances and are reported relative to tetramethylsilane (δ = 0 ppm). ^{29}Si resonances are referenced externally to dilute tetramethylsilane in chloroform-d_3. ^{119}Sn resonances are referenced externally to 90% tetramethylstannane in benzene-d_6. ^{207}Pb resonances are referenced externally to 5% tetramethylplumbane in benzene-d_6. Assignments were confirmed using two-dimensional ^{1}H-^{1}H and ^{13}C-^{1}H NMR correlation experiments. Chemical shifts are quoted in δ (ppm) and coupling constants in Hz. Elemental analyses were carried out by London Metropolitan University. UV-Vis samples were prepared by dissolving the compound in *n*-hexane (0.5 mM) and transfering the stock solution into cuvettes (l = 1.0 mm) fitted with Teflon valves. UV-Vis spectra were recorded on a Perkin Elmer Lambda 19 UV/vis/NIR spectrometer. $(HCDippN)_2BBr$,[14] $[HC(MeCMesN)_2Mg]_2$,[15] and $E[N(SiMe_3)_2]_2$ (E = Ge, Sn, Pb)[16] were prepared by literature methods. All other reagents were used as received.

Synthetic, Spectroscopic and Analytical Data

Preparation of (HCDippN)$_2$BOH (1). To a solution of (HCDippN)$_2$BBr (3.0 g, 6.4 mmol) in toluene (25 mL) was added water (25 mL) and pyridine (3 mL). The biphasic mixture was stirred overnight at room temperature. The layers were separated and the organic layer was dried over anhydrous magnesium sulfate and filtered. The filtrate was dried under vacuum to yield (HCDippN)$_2$BOH (**1**) (1.7 g, 66%) as a pale yellow powder. ^{1}H and ^{11}B NMR data matches previously reported literature values.[4d]

Preparation of K[(HCDippN)$_2$BO] (2). To a mixture of **1** (3.0 g, 7.4 mmol) and K[(NSiMe$_3$)$_2$] (1.5 g, 7.4 mmol) was added toluene (20 mL) and stirred for 5 min at room temperature. Volatiles were removed under vacuum to yield K[(HCDippN)$_2$BO] (**2**) (3.1 g, 95% yield) as a pale yellow powder. Single crystals suitable for X-ray diffraction analysis were obtained from slow evaporation of a concentrated solution of **2** in *n*-hexane at room temperature. ^{1}H NMR (400 MHz, C$_6$D$_6$, 297 K): δ = 1.16 (d, $^3J_{HH}$ = 6.9 Hz, 24H, CH(C*H*$_3$)$_2$), 1.26 (d, $^3J_{HH}$ = 6.9 Hz, 24H, CH(C*H*$_3$)$_2$), 3.62 (sept, $^3J_{HH}$ = 6.7 Hz, 8H, C*H*(CH$_3$)$_2$), 6.03 (s, 4H, NC*H*), 7.06 (m, 12H, Dipp-C*H*); ^{13}C{^{1}H} NMR (101 MHz, C$_6$D$_6$): δ = 24.0 (CH(*C*H$_3$)$_2$), 24.2 (CH(*C*H$_3$)$_2$), 28.4 (*C*H(CH$_3$)$_2$), 115.0 (N*C*H), 123.3 (Dipp-*m*-*C*H), 126.1 (Dipp-*p*-*C*H), 143.4 (Dipp-*i*-*C*), 148.0 (Dipp-*o*-*C*); ^{11}B{^{1}H} NMR (128 MHz, C$_6$D$_6$): δ = 22.8; anal. calc. for C$_{26}$H$_{36}$BKN$_2$O: C 70.57%, H 8.20%, N 6.33%, found: C 70.44%, H 8.38%, N 6.23%.

Preparation of [(HCDippN)$_2$BO]$_2$Si (3). To a mixture of **2** (83 mg, 0.19 mmol) and SiI$_4$ (50 mg, 0.09 mmol) was added benzene (10 mL) and the reaction mixture stirred overnight at room temperature. Volatiles were removed under vacuum. [HC(MeCMesN)$_2$Mg]$_2$ (100 mg, 0.14 mmol) and benzene (10 mL) were then added and the solution stirred at 80 °C overnight.

Volatiles were again removed under vacuum. To the residue was added *n*-pentane (10 mL) and the mixture filtered. The filtrate was dried under vacuum to yield $[(HCDippN)_2BO]_2Si$ (**3**) (70 mg, 87% yield) as an off-white powder. Single crystals suitable for X-ray diffraction analysis were obtained from a concentrated solution of **3** in *n*-pentane at room temperature. ^1H NMR (400 MHz, C_6D_6, 297 K): δ = 1.06 (d, $^3J_{HH}$ = 6.7 Hz, 24H, $CH(CH_3)_2$), 1.18 (d, $^3J_{HH}$ = 6.6 Hz, 24H, $CH(CH_3)_2$), 3.15 (m, 8H, $CH(CH_3)_2$), 5.90 (s, 4H, NC*H*), 7.09 (d, $^3J_{HH}$ = 7.5 Hz, 8H, Dipp-*m*-C*H*), 7.21 (t, $^3J_{HH}$ = 7.6 Hz, 4H, Dipp-*p*-C*H*); $^{13}C\{^1H\}$ NMR (101 MHz, C_6D_6): δ = 24.0 ($CH(CH_3)_2$), 24.5 ($CH(CH_3)_2$), 28.7 ($CH(CH_3)_2$), 116.6 (NCH), 123.6 (Dipp-*m*-CH), 127.7 (Dipp-*p*-CH), 137.5 (Dipp-*i*-*C*), 146.8 (Dipp-*o*-*C*); $^{11}B\{^1H\}$ NMR (128 MHz, C_6D_6): δ = 20.1; $^{29}Si\{^1H\}$ NMR (80 MHz, C_6D_6): δ = 35.5; UV-vis (*n*-hexane, λ_{max}): 348 nm (ε = 59706 $L{\cdot}mol^{-1}{\cdot}cm^{-1}$); anal. calc. for $C_{52}H_{72}B_2N_4O_2Si$: C 74.81%, H 8.69%, N 6.71%, found: C 74.60%, H 8.90%, N 6.54%.

Preparation of [(HCDippN)$_2$BO]$_2$Ge (4). To a mixture of **1** (107 mg, 0.26 mmol) and $Ge[N(SiMe_3)_2]_2$ (52 mg, 0.13 mmol) was added benzene (1 mL) and the reaction mixture agitated for 5 min at room temperature to form an orange solution. Volatiles were removed under vacuum to yield $[(HCDippN)_2BO]_2Ge$ (**4**) (100 mg, 86% yield) as an orange powder. Single crystals suitable for X-ray diffraction analysis were obtained from a concentrated solution of **3** in benzene at room temperature. ^1H NMR (500 MHz, C_6D_6, 297 K): δ = 1.06 (d, $^3J_{HH}$ = 6.9 Hz, 24H, $CH(CH_3)_2$), 1.18 (d, $^3J_{HH}$ = 6.9 Hz, 24H, $CH(CH_3)_2$), 3.19 (sept, $^3J_{HH}$ = 6.9 Hz, 8H, $CH(CH_3)_2$), 5.92 (s, 4H, NC*H*), 7.09 (d, $^3J_{HH}$ = 7.6 Hz, 8H, Dipp-*m*-C*H*), 7.18 (t, $^3J_{HH}$ = 7.7 Hz, 4H, Dipp-*p*-C*H*); $^{13}C\{^1H\}$ NMR (126 MHz, C_6D_6): δ = 23.8 ($CH(CH_3)_2$), 24.5 ($CH(CH_3)_2$), 28.7 ($CH(CH_3)_2$), 116.3 (NCH), 123.8 (Dipp-*m*-CH), 127.6 (Dipp-*p*-CH), 138.3 (Dipp-*i*-*C*), 147.1 (Dipp-*o*-*C*); $^{11}B\{^1H\}$ NMR (160 MHz, C_6D_6): δ = 22.7; UV-vis (*n*-hexane,

λ_{max}): 350 nm (ε = 9657 L·mol^{-1}·cm^{-1}); anal. calc. for $C_{52}H_{72}B_2GeN_4O_2$: C 71.02%, H 8.25%, N 6.37%, found: C 70.85%, H 8.12%, N 6.21%.

Preparation of [(HCDippN)$_2$BO]$_2$Sn (5). To a mixture of **1** (120 mg, 0.30 mmol) and Sn[N(SiMe$_3$)$_2$]$_2$ (66 mg, 0.15 mmol) was added benzene (1 mL) and the reaction mixture agitated for 5 min at room temperature to form an orange solution. Volatiles were removed under vacuum to yield [(HCDippN)$_2$BO]$_2$Sn (**5**) (112 mg, 88% yield) as an orange powder. Single crystals suitable for X-ray diffraction analysis were obtained from a concentrated solution of **5** in benzene at room temperature. ^{1}H NMR (500 MHz, C_6D_6, 297 K): δ = 1.14 (d, $^3J_{HH}$ = 6.9 Hz, 24H, CH(C*H*$_3$)$_2$), 1.20 (d, $^3J_{HH}$ = 6.9 Hz, 24H, CH(C*H*$_3$)$_2$), 3.30 (sept, $^3J_{HH}$ = 6.8 Hz, 8H, C*H*(CH$_3$)$_2$), 5.98 (s, 4H, NC*H*), 7.12-7.13 (m, 8H, Dipp-*m*-C*H*), 7.16-7.19 (m, 4H, Dipp-*p*-C*H*); ^{13}C{^{1}H} NMR (126 MHz, C_6D_6): δ = 23.6 (CH(*C*H$_3$)$_2$), 24.5 (CH(*C*H$_3$)$_2$), 28.7 (*C*H(CH$_3$)$_2$), 115.8 (N*C*H), 124.3 (Dipp-*m*-*C*H), 127.5 (Dipp-*p*-*C*H), 139.6 (Dipp-*i*-*C*), 147.6 (Dipp-*o*-*C*); ^{11}B{^{1}H} NMR (160 MHz, C_6D_6): δ = 22.5; ^{119}Sn{^{1}H} NMR (186 MHz, C_6D_6): δ = −109.0; UV-vis (*n*-hexane, λ_{max}): 355 nm (ε = 6120 L·mol^{-1}·cm^{-1}); anal. calc. for $C_{52}H_{72}B_2N_4O_2Sn$: C 67.48%, H 7.84%, N 6.05%, found: C 67.23%, H 7.73%, N 5.94%.

Preparation of [(HCDippN)$_2$BO]$_2$Pb (6). To a mixture of **1** (120 mg, 0.30 mmol) and Pb[N(SiMe$_3$)$_2$]$_2$ (66 mg, 0.15 mmol) was added benzene (1 mL) and the reaction mixture agitated for 5 min at room temperature to form an orange solution. Volatiles were removed under vacuum to yield [(HCDippN)$_2$BO]$_2$Pb (**6**) (117 mg, 78% yield) as a yellow powder. Single crystals suitable for X-ray diffraction analysis were obtained from a concentrated solution of **6** in benzene at room temperature. ^{1}H NMR (500 MHz, C_6D_6, 297 K): δ = 1.19-1.21 (m, 48H, CH(C*H*$_3$)$_2$), 3.38 (sept, $^3J_{HH}$ = 6.9 Hz, 8H, C*H*(CH$_3$)$_2$), 6.04 (s, 4H, NC*H*), 7.14 (s, 12H, Dipp-C*H*); ^{13}C{^{1}H} NMR (126 MHz, C_6D_6): δ = 23.6 (CH(*C*H$_3$)$_2$), 24.5 (CH(*C*H$_3$)$_2$),

28.7 (*C*H(CH_3)$_2$), 115.6 (N*C*H), 124.4 (Dipp-*m*-*C*H), 127.2 (Dipp-*p*-*C*H), 140.3 (Dipp-*i*-*C*), 148.0 (Dipp-*o*-*C*); $^{11}B\{^1H\}$ NMR (160 MHz, C_6D_6): δ = 24.8; $^{207}Pb\{^1H\}$ NMR (105 MHz, C_6D_6): δ = 1885; UV-vis (*n*-hexane, λ_{max}): 370 nm (ε = 8486 L·mol^{-1}·cm^{-1}); anal. calc. for $C_{52}H_{72}B_2N_4O_2Pb$: C 61.60%, H 7.16%, N 5.53%, found: C 61.46%, H 6.77%, N 5.55%.

NMR Spectra

K[(HCDippN)2BO] [2]

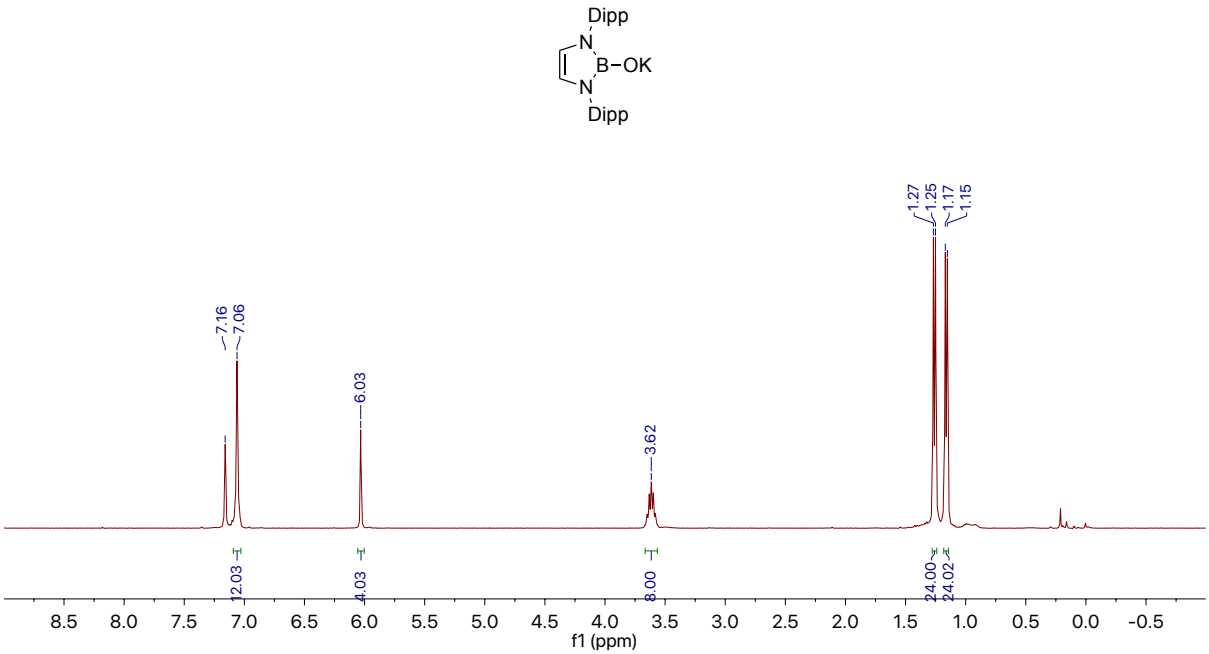


Figure 7. ^{1}H NMR spectrum of **2**.

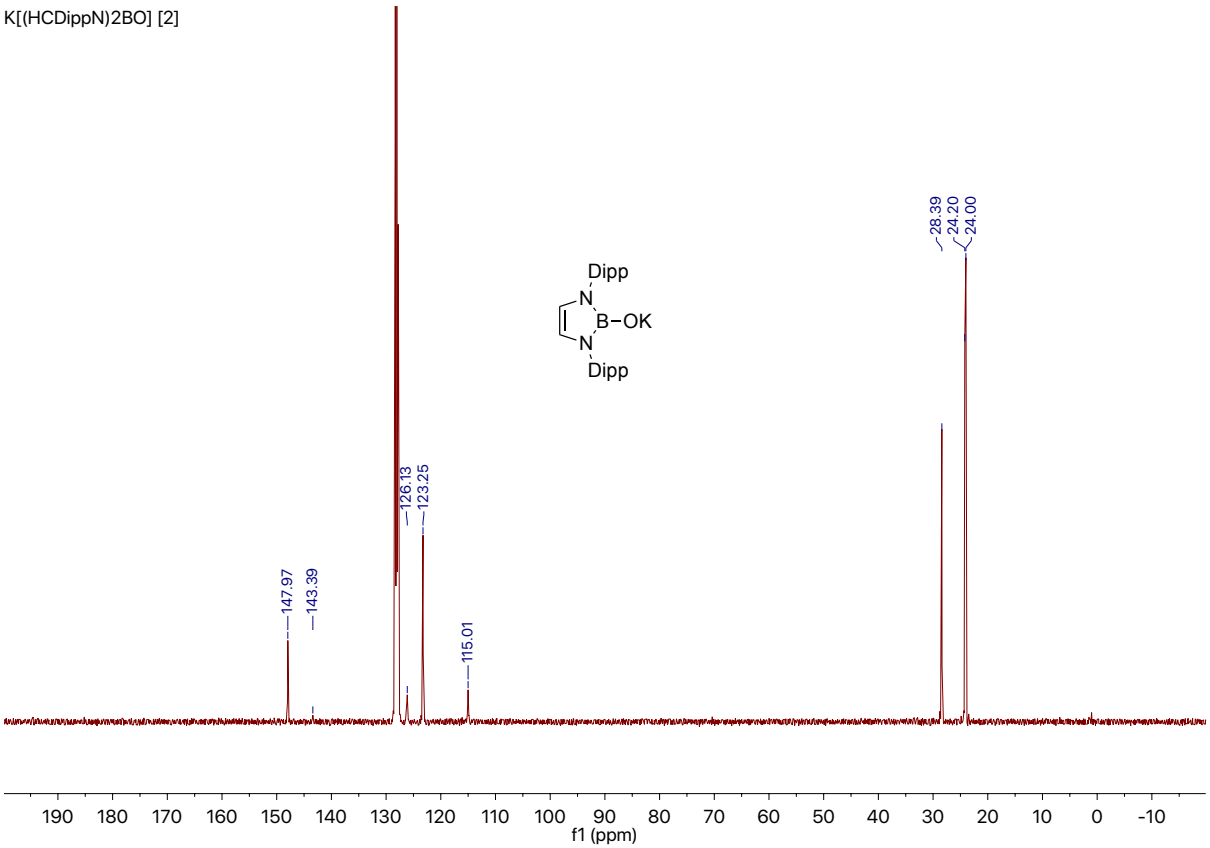


Figure 8. $^{13}C\{^{1}H\}$ NMR spectrum of **2**.

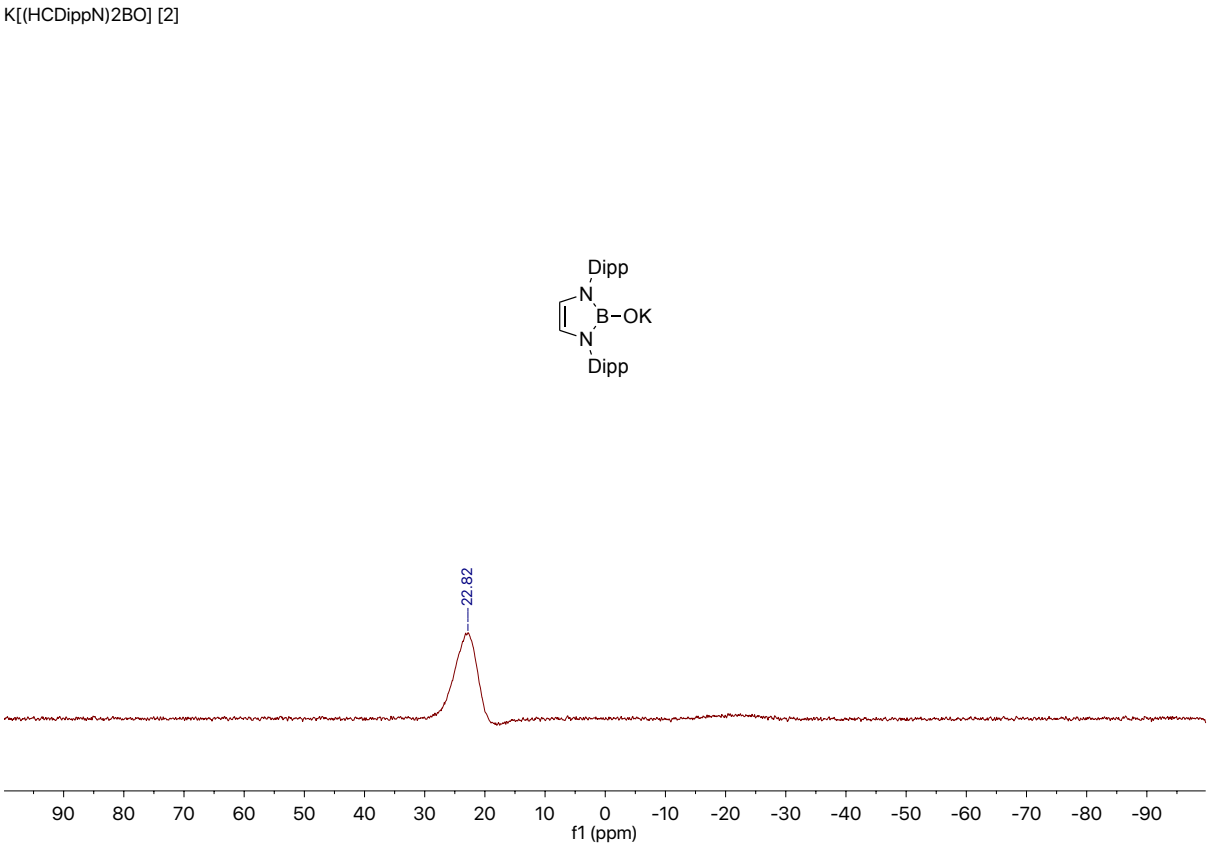


Figure 9. $^{11}B\{^{1}H\}$ NMR spectrum of **2**.

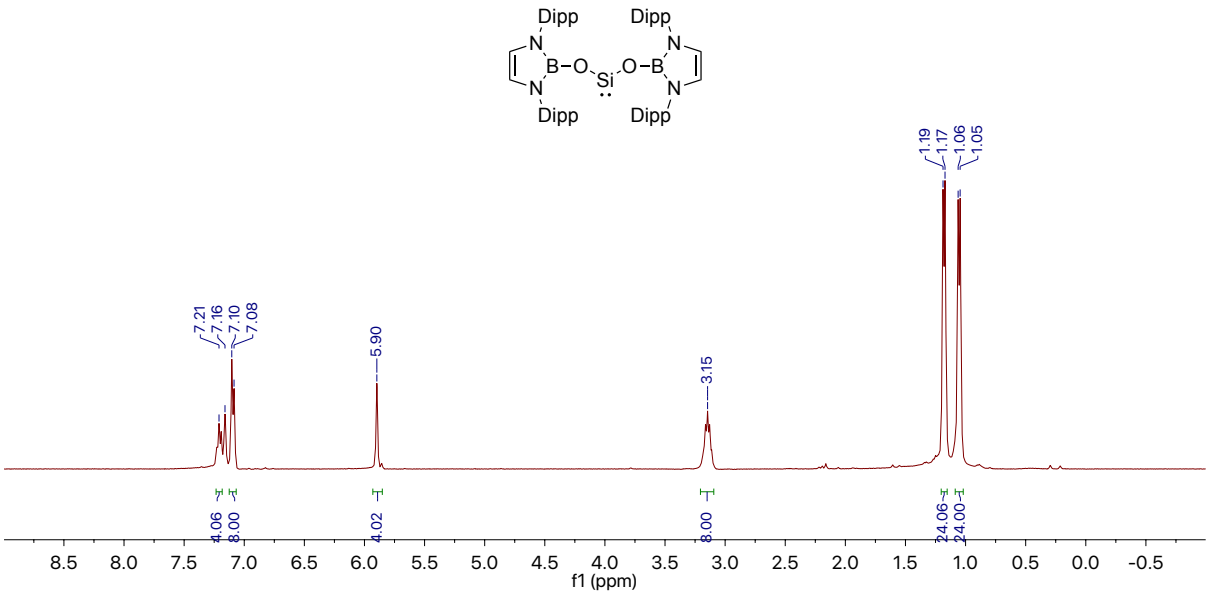


Figure 10. ^{1}H NMR spectrum of **3**.

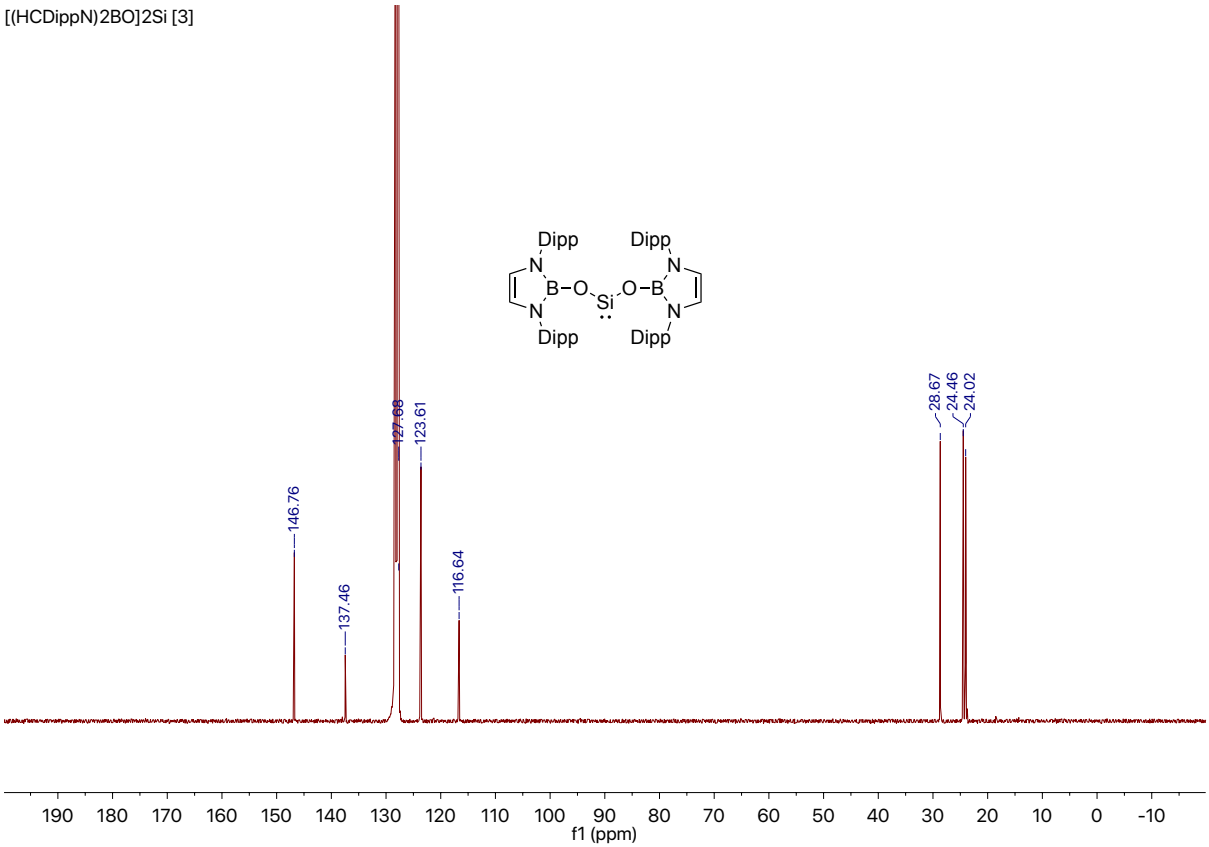


Figure 11. ^{13}C{^{1}H} NMR spectrum of **3**.

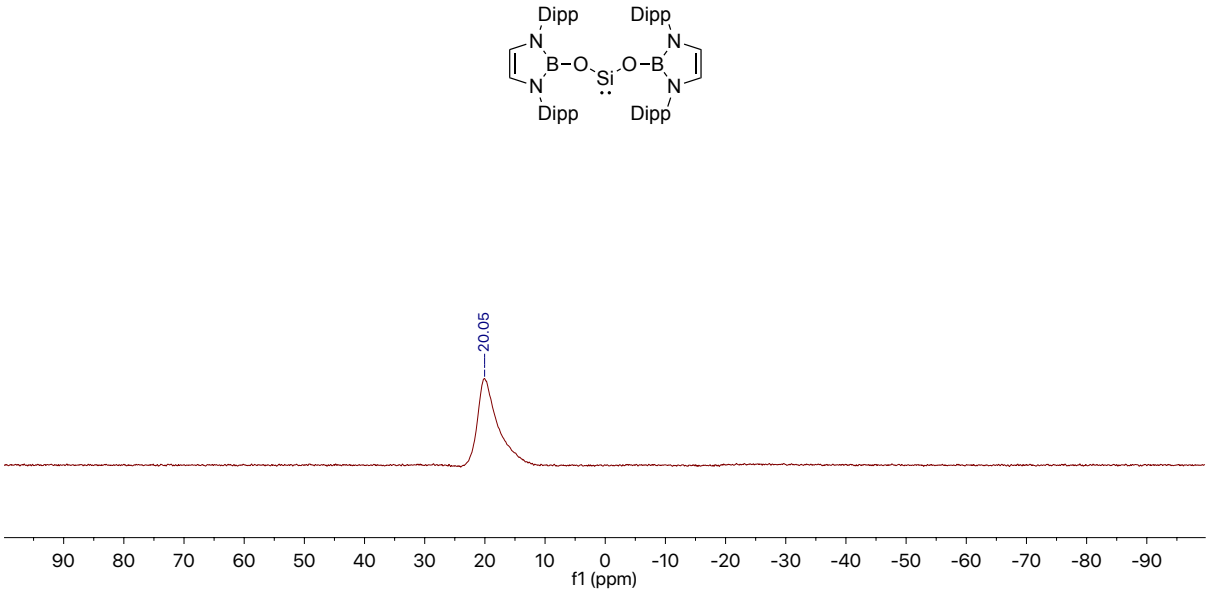


Figure 12. $^{11}B\{^{1}H\}$ NMR spectrum of **3**.

[(HCDippN)2BO]2Si [3]

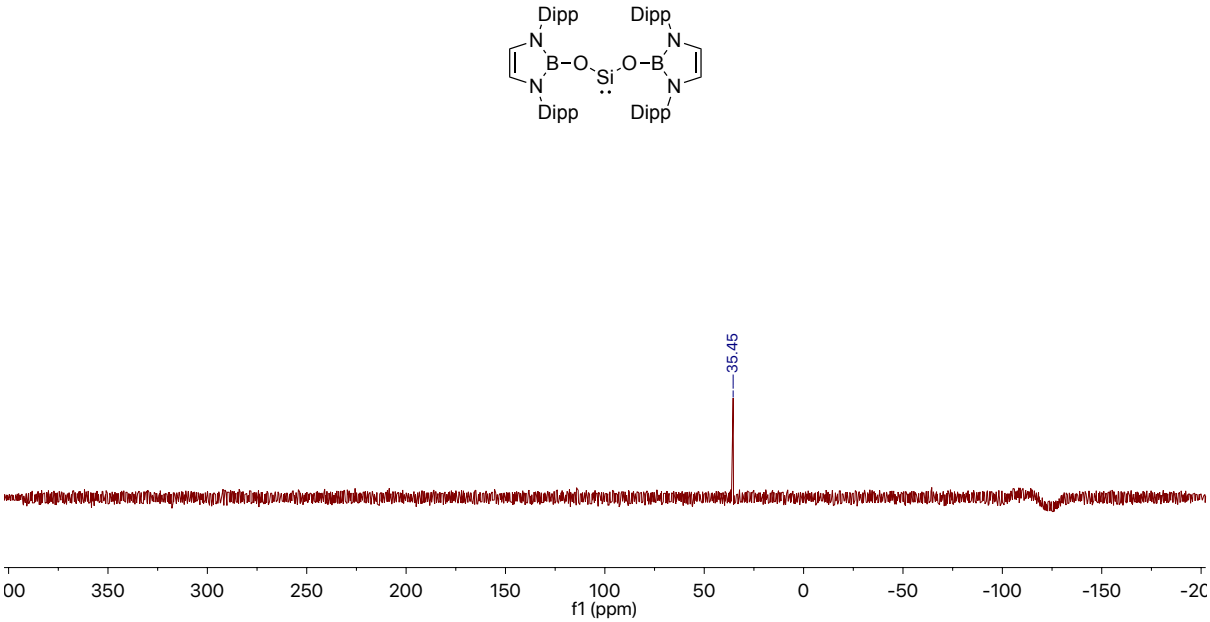


Figure 13. $^{29}Si\{^{1}H\}$ NMR spectrum of **3**.

[(HCDippN)2BO]2Ge [4]

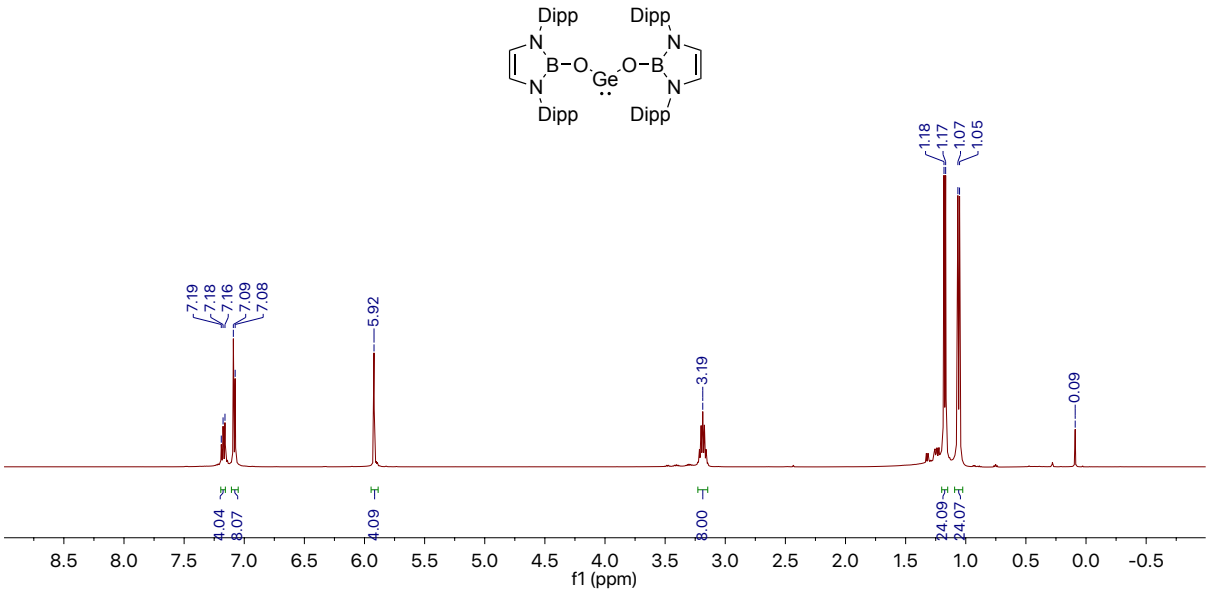


Figure 14. ^{1}H NMR spectrum of **4**.

[(HCDippN)2BO]2Ge [4]

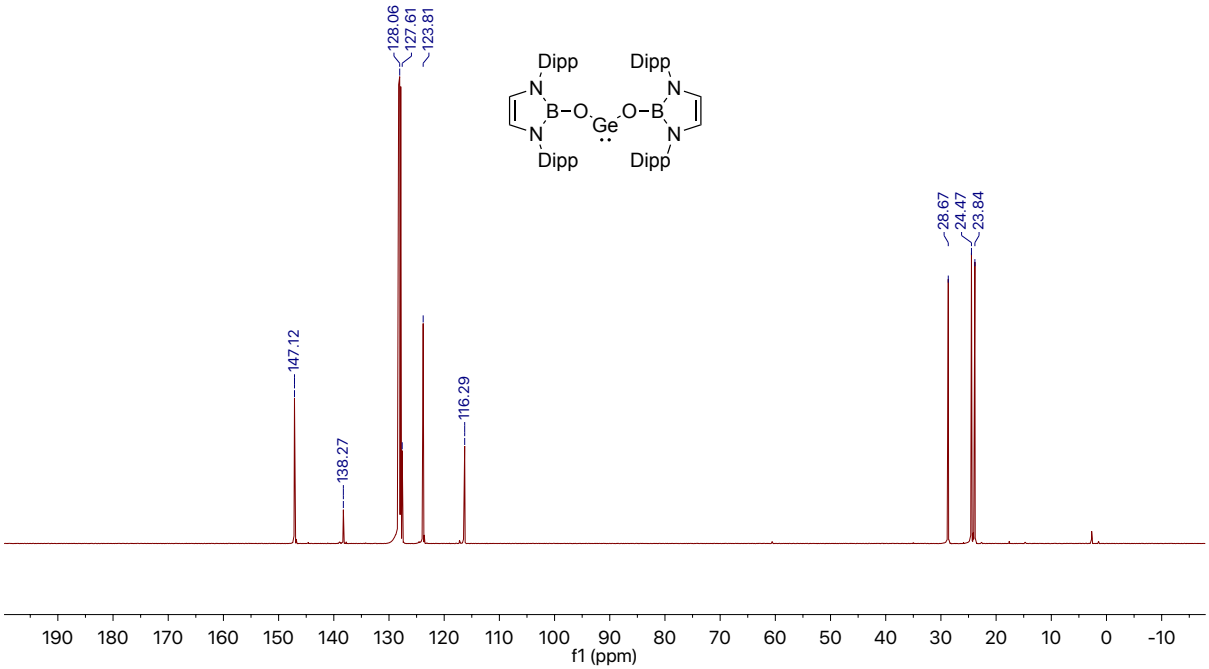


Figure 15. ^{13}C{^{1}H} NMR spectrum of **4**.

[(HCDippN)2BO]2Ge [4]

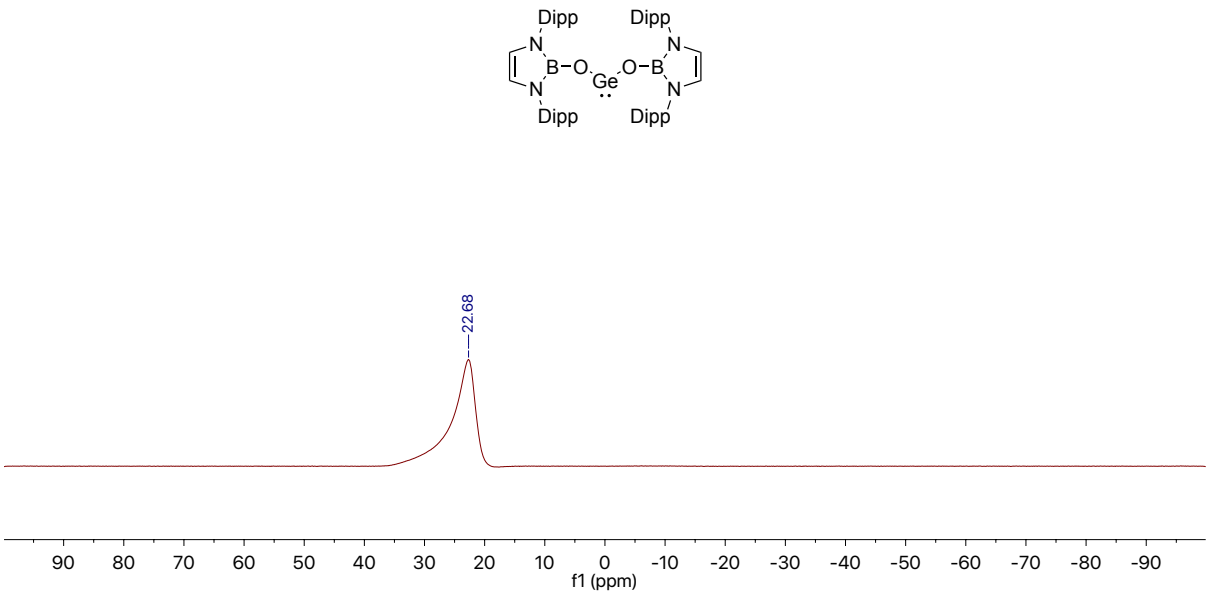


Figure 16. $^{11}B\{^{1}H\}$ NMR spectrum of **4**.

[(HCDippN)2BO]2Sn [5]

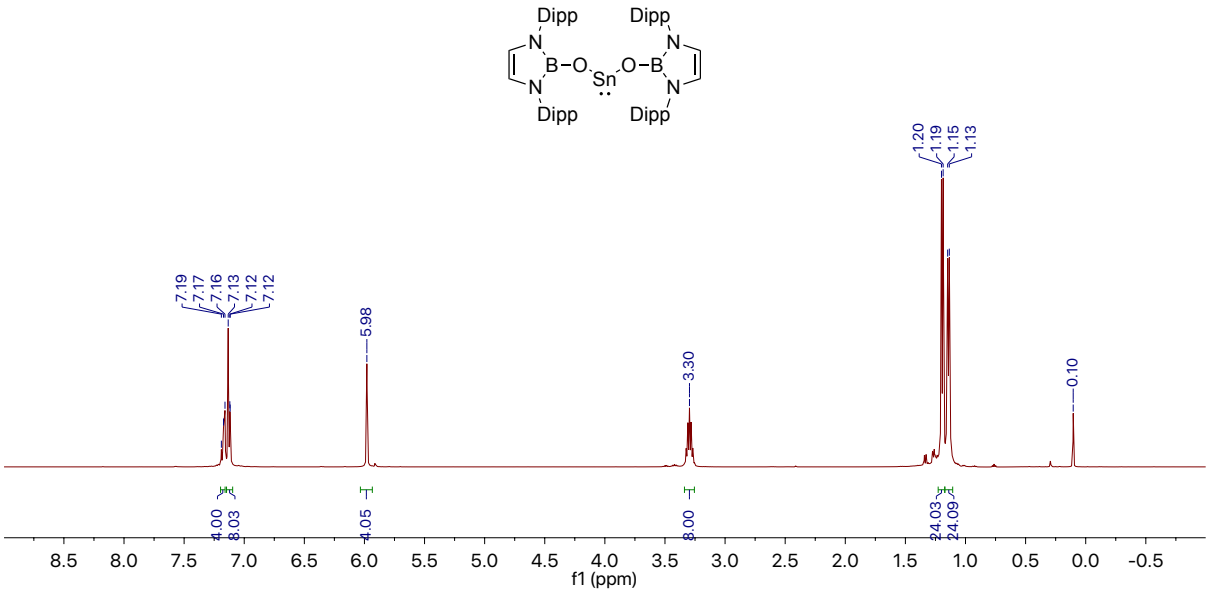


Figure 17. ^{1}H NMR spectrum of **5**.

[(HCDippN)2BO]2Sn [5]

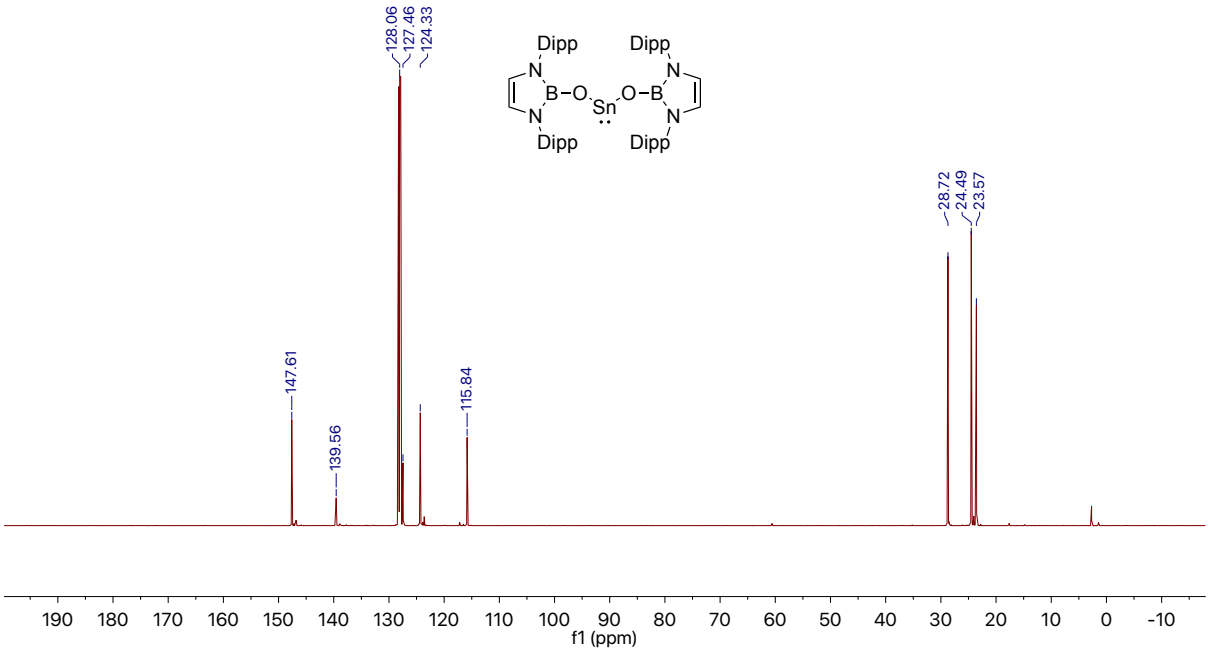


Figure 18. ^{13}C{^{1}H} NMR spectrum of **5**.

[(HCDippN)2BO]2Sn [5]

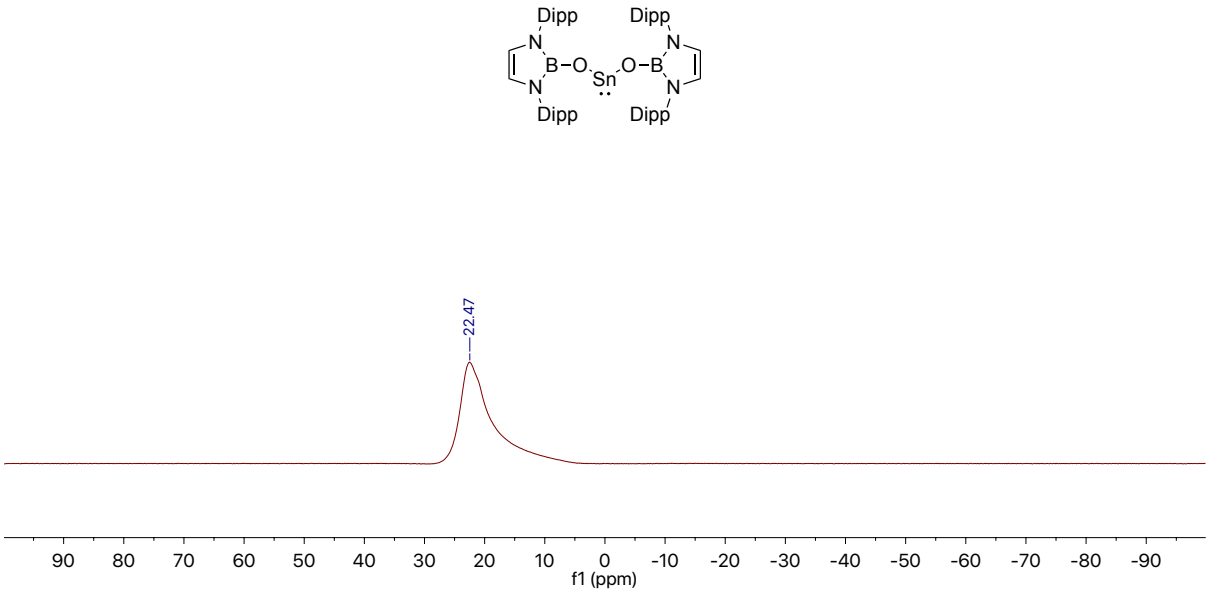


Figure 19. $^{11}B\{^{1}H\}$ NMR spectrum of **5**.

[(HCDippN)2BO]2Sn [5]

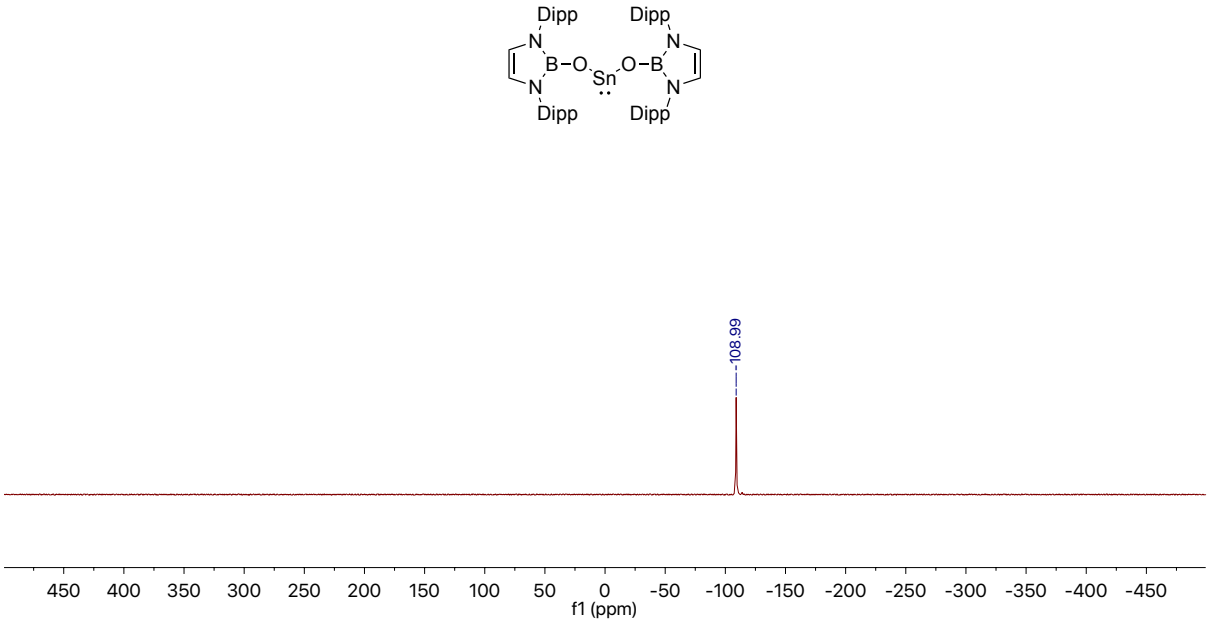


Figure 20. $^{119}Sn\{^{1}H\}$ NMR spectrum of **5**.

[(HCDippN)2BO]2Pb [6]

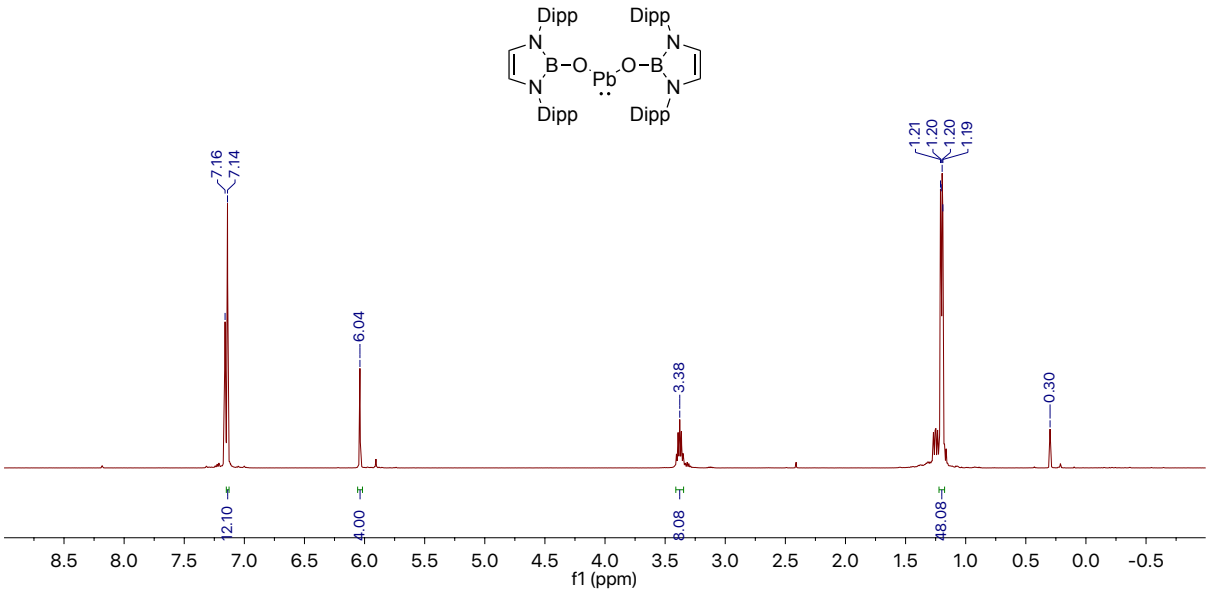


Figure 21. ^{1}H NMR spectrum of **6**.

[(HCDippN)2BO]2Pb [6]

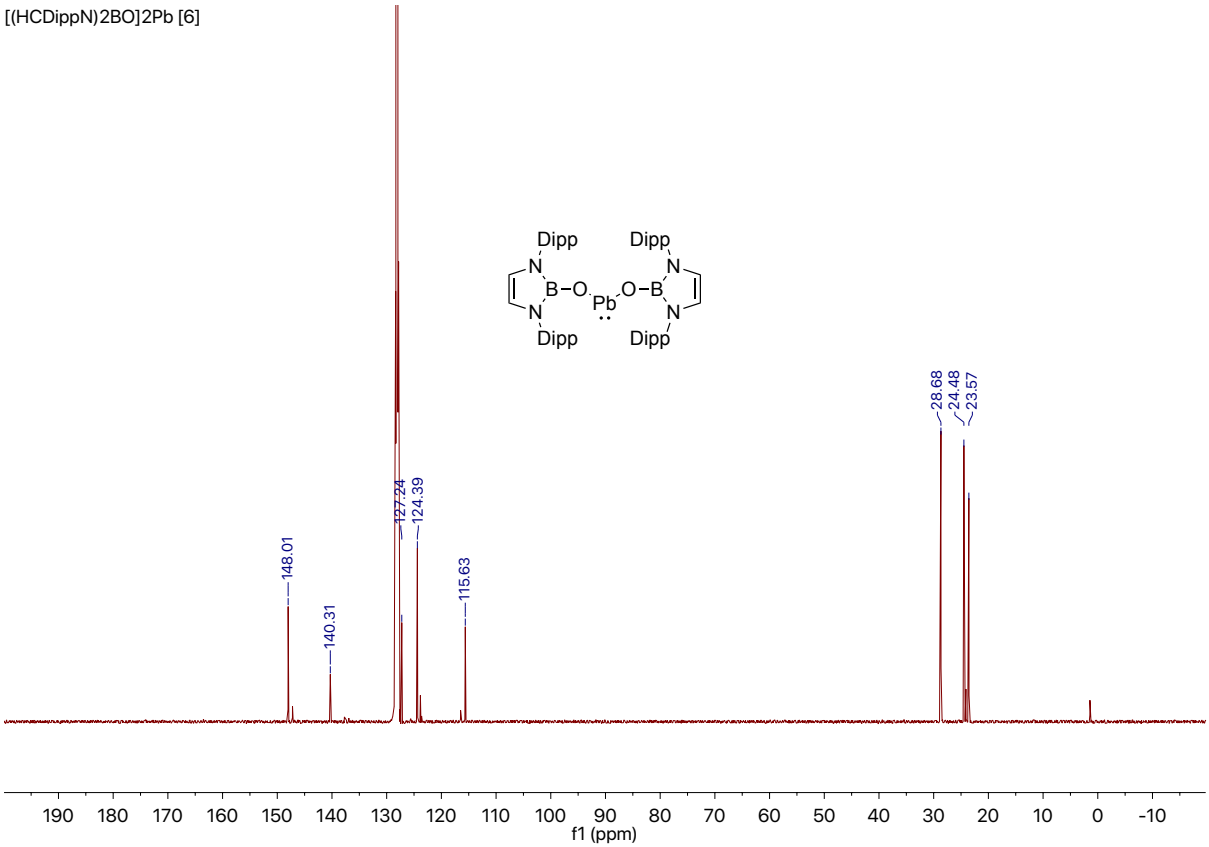


Figure 22. ^{13}C{^{1}H} NMR spectrum of **6**.

[(HCDippN)2BO]2Pb [6]

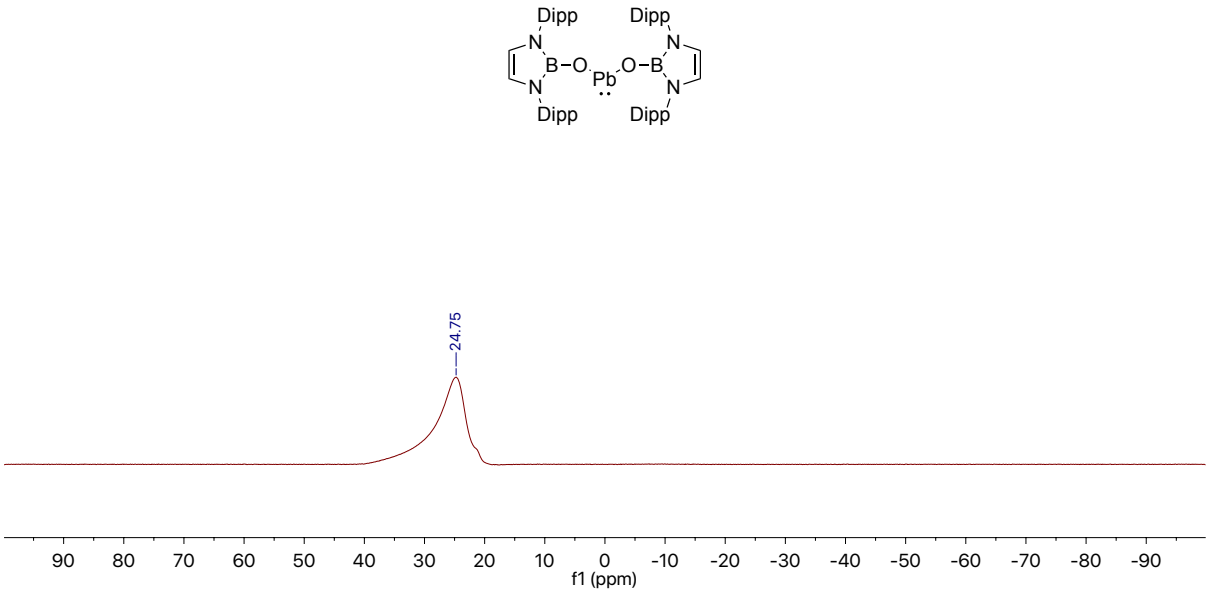


Figure 23. $^{11}B\{^{1}H\}$ NMR spectrum of **6**.

[(HCDippN)2BO]2Pb [6]

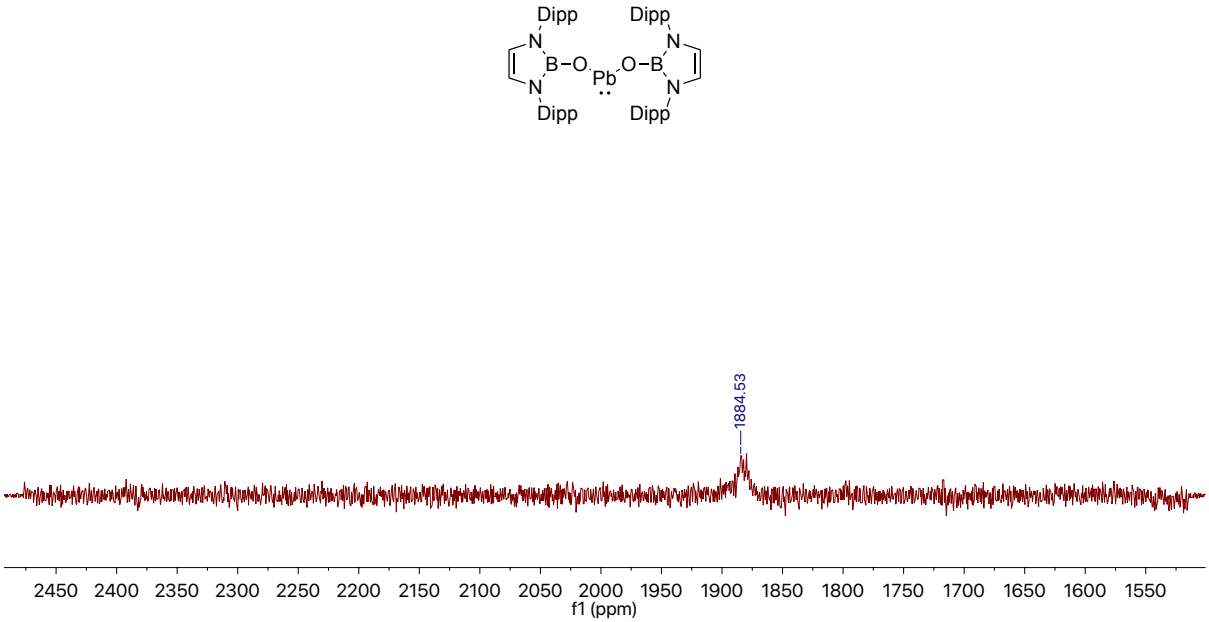


Figure 24. $^{207}Pb\{^{1}H\}$ NMR spectrum of **6**.

X-Ray Crystallographic Studies

Single-crystal X-ray diffraction data for **2–6** were collected at 150 K on Oxford Diffraction/Agilent SuperNova diffractometers with Cu-$K\alpha$ (λ = 1.54184 Å) radiation equipped with nitrogen gas Oxford Cryosystems Cryostream unit.[17] Raw frame data were reduced using CrysAlisPro.[18] The structures were solved using SHELXT[19] and refined to convergence on F^2 and against all independent reflections by full-matrix least-squares using SHELXL[20] in combination with the SHELXLE[21] program. Distances and angles were calculated using the full covariance matrix. Restraints were used to maintain sensible geometries for the disordered groups and approximate the displacement parameters to typical values. The structure of compound **2** is highly disorder which prevent discussion of the metrics in detail; however, its atom connectivity can be established. For **3**, **4**, and **6**, several isopropyl groups were modelled as disordered over two sites. Selected crystallographic data are summarized in Table 2 and full details are given in the supplementary deposited CIF files (CCDC 1873893-97). These data can be obtained free of charge from the Cambridge Crystallographic Data Centre via http://www.ccdc.cam.ac.uk/data_request/cif.

Table 2. Selected crystallographic and refinement data for **2**–**6**.

	2	**3**	**4**	**5**	**6**
Formula	$C_{52}H_{72}B_2K_2N_4O_2$	$C_{52}H_{72}B_2N_4O_2Si$	$C_{52}H_{72}B_2GeN_4O_2$	$C_{52}H_{72}B_2N_4O_2Sn$	$C_{52}H_{72}B_2N_4O_2Pb$
Fw	884.95	834.84	879.34	925.44	1013.94
Cryst. System	Monoclinic	Monoclinic	Monoclinic	Monoclinic	Monoclinic
Space Group	P 2/c	P 21/c	P 21/c	P 21/c	P 21/c
Wavelength/Å	1.54184	1.54184	1.54184	1.54184	1.54184
a/Å	22.6308(2)	30.5570(5)	30.9446(6)	15.9058(3)	15.8154(2)
b/Å	10.71260(10)	12.6386(2)	12.9840(2)	15.7758(3)	15.79820(10)
c/Å	44.2670(4)	30.7014(6)	29.2783(5)	20.9246(3)	20.9983(2)
α/°	90	90	90	90	90
β/°	99.7670(10)	117.926(2)	118.072(2)	100.418(2)	100.8170(10)
γ/°	90	90	90	90	90
Volume/Å^3	10576.31(17)	10476.1(4)	10379.7(4)	5163.98(16)	5153.30(9)
Z	8	8	8	4	4
Temp./K	150(2)	150(2)	150(2)	150(2)	150(2)
Refls. Collect.	89364	52306	47648	23032	40134
$2\theta_{max}$	152.64	149.00	149.00	149.00	152.93
R_{int}	0.0315	0.0250	0.0267	0.0389	0.0296
Goodness of fit	1.030	1.044	1.014	1.020	1.037
$R[F^2>2\sigma]$, F	0.0687	0.0591	0.0511	0.0390	0.0228
R_w (all data), F^2	0.1957	0.1792	0.1547	0.1029	0.0605

Computational Studies

The reported computational work was performed at the DFT level, using Gaussian09 (Revision D.01) program package.[22] Geometry optimizations of the monoanionic ligand systems were performed with the PBE1PBE hybrid exchange-correlation functional[23] using the SVP basis sets.[24] Geometry optimizations of the tetrelene complexes were performed with the same functional, employing the TZVP basis sets for light elements (H, B, C, N, O),[25] and the Def2-TZVP basis sets[26] with relativistic large core ECP[27] for heavy nuclei (Sn, Pb). Grimme's empirical dispersion correction (DFT-D3) was included in all geometry optimizations.[28] Unless otherwise stated, geometry optimizations were carried out for the full ligand systems, and were reported as Gibbs free energies in the gas phase. Full frequency calculations were performed to confirm the nature of the stationary points found (minimum). The natural bond orbital (NBO) analyses were performed using NBO 3.1 as implemented in Gaussian09.[29]

References

(1) For alkoxy or aryloxy ligands: (a) Bradley, D. C.; Mehrotra, R. C.; Gaur, D. P. *Metal Alkoxides*; Academic Press: New York, 1978. (b) Goel, S. C.; Chiang, Y.; Buhro, W. E. Preparation of six lead(II) dialkoxides, X-ray crystal structures of $[Pb(\mu,\eta^1\text{-}OCH_2CH_2OMe)_2]_\infty$ and $[Pb_3(\mu\text{-}O\text{-}t\text{-}Bu)_6]$, and hydrolysis studies. *Inorg. Chem.* **1990**, *29*, 4640-4646. (c) Cetinkaya, B.; Gümrükcü, L.; Lappert, M. F.; Atwood, J. L.; Rogers, R. D.; Zaworotko, M. J. Bivalent germanium, tin, and lead 2,6-di-*tert*-butylphenoxides and the crystal and molecular structures of $M(OC_6H_2Me\text{-}4\text{-}Bu^t_2\text{-}2,6)_2$ (M = Ge or Sn). *J. Am. Chem. Soc.* **1980**, *102*, 2088-2089. (d) Stanciu, C.; Richards, A. F.; Stender, M.; Olmstead, M. M.; Power, P. P. New terphenylphenoxides of group 13 or 14 elements. *Polyhedron* **2006**, *25*, 477-483. (e) Rekken, B. D.; Brown, T. M.; Olmstead, M. M.; Fettinger, J. C.; Power, P. P. Stable plumbylene dichalcogenolate monomers with large differences in their interligand angles and the synthesis and characterization of a monothiolato Pb(II) bromide and lithium trithiolato plumbate. *Inorg. Chem.* **2013**, *52*, 3054-3062. (f) Yao, S.; Block, S.; Brym, M.; Driess, M. A new type of heteroleptic complex of divalent lead and synthesis of the *P*-plumbyleniophosphasilene, $R_2Si{=}P{-}Pb(L)$: (L = β-diketiminate). *Chem. Commun.* **2007**, 3844-3846.

(2) For reviews on heavier main group elements and small molecule activation: (a) Power, P. P. π-Bonding and the lone pair effect in multiple bonds between heavier main group elements. *Chem. Rev.* **1999**, *99*, 3463-3503. (b) Power, P. P. Main-group elements as transition metals. *Nature* **2010**, *463*, 171-177.

(3) For boryloxy ligands: (a) Coles, M. P. Metal compounds of boron-substituted alkoxide ('boroxide') ligands. *Coord. Chem. Rev.* **2016**, *323*, 52-59. (b) Weese, K. J.; Bartlett, R. A.; Murray, B. D.; Olmstead, M. M.; Power, P. P. Synthesis and spectroscopic and structural characterization of derivatives of the quasi-alkoxide ligand $[OBMes_2]^-$ (Mes= 2, 4, 6-$Me_3C_6H_2$). *Inorg. Chem.* **1987**, *26*, 2409-2413. (c) Beck, G.; Hitchcock, P. B.; Lappert, M. F.; MacKinnon, I. A. Lipophilic lithium alkoxides or dialkylboroxides; X-ray structures of $[Li(\mu\text{-}OR')]_2$ and $Li(OBR_2)(tmeda)$, [tmeda=$(Me_2NCH_2)_2$, R= $CH(SiMe_3)_2$, R′= CBu^t_3 or BR_2]. *J. Chem. Soc., Chem. Commun.* **1989**, 1312-1314. (d) Anulewicz-Ostrowska, R.; Luliński, S.; Serwatowski, J.; Suwińska, K. Diverse

Reactivity of Dialkylaluminum Dimesitylboryloxides [(μ-Mes_2BO)AlR_2]$_2$. Synthetic and Structural Study. *Inorg. Chem.* **2000**, *39*, 5763-5767. (e) Someşan, A.; Coz, E. L.; Roisnel, T.; Silvestru, C.; Sarazin, Y. Stable lead(II) boroxides. *Chem. Commun.* **2018**, *54*, 5299-5302. (f) Coz, E. L.; Dorcet, V.; Roisnel, T.; Tobisch, S.; Carpentier, J.; Sarazin, Y. Low-Coordinate Barium Boryloxides: Synthesis and Dehydrocoupling Catalysis for the Production of Borasiloxanes. *Angew. Chem., Int. Ed.* **2018**, *57*, 11747-11751.

(4) For reviews on NHI: (a) Ochiai, T.; Franz, D.; Inoue, S. Applications of N-heterocyclic imines in main group chemistry. *Chem. Soc. Rev.* **2016**, *45*, 6327-6344. (b) Wu, X.; Tamm, M. Transition metal complexes supported by highly basic imidazolin-2-iminato and imidazolin-2-imine N-donor ligands. *Coord. Chem. Rev.* **2014**, *260*, 116-138.

(5) For NHI-stabilized main group systems: for B: (a) Franz, D.; Irran, E.; Inoue, S. Isolation of a three-coordinate boron cation with a boron−sulfur double bond. *Angew. Chem., Int. Ed.* **2014**, *53*, 14264-14268. (b) Lui, M. W.; Paisley, N. R.; McDonald, R.; Ferguson, M. J.; Rivard, E. Metal-free dehydrogenation of amine-boranes by tunable N-heterocyclic iminoboranes. *Chem. Eur. J.* **2016**, *22*, 2134-2145. for Al: (c) Franz, D.; Inoue, S. Activation of elemental sulfur by aluminum dihydride: Isolation of mono- and bis(hydrogensulfide) complexes of aluminum. *Chem. Eur. J.* **2014**, *20*, 10645-10649. (d) Franz, D.; Szilvási, T.; Irran, E.; Inoue, S. A monotopic aluminum telluride with an Al=Te double bond stabilized by *N*-heterocyclic carbenes. *Nat. Commun.* **2015**, *6*, 10037. for C: (e) Loh, Y. K.; Fuentes, M. A.; Vasko, P.; Aldridge, S. Succsessive protonation of an N-heterocyclic imine derived carbonyl: superelectrophilic dication versus masked acylium ion. *Angew. Chem., Int. Ed.* **2018**, *57*, 16559-16563. for Ge: (f) Lui, M. W.; Merten, C.; Ferguson, M. J.; McDonald, R.; Xu, Y.; Rivard, E. Contrasting reactivities of silicon and germanium complexes supported by an *N*-heterocyclic guanidine ligand. *Inorg. Chem.* **2015**, *54*, 2040-2049. (g) Ochiai, T.; Franz, D.; Wu, X.; Inoue, S. Isolation of germanium(II) cation and a germylene iron carbonyl complex utilizing an imidazolin-2-iminato ligand. *Dalton Trans.* **2015**, *44*, 10952-10956. (h) Ochiai, T.; Szilvási, T.; Franz, D.; Irran, E.; Inoue, S. Isolation and structure of germylene-germyliumylidenes stabilized by N-heterocyclic imines. *Angew. Chem. Int. Ed.* **2016**, *55*, 11619-11624. for Sn: (i) Ochiai, T.; Franz, D.; Irran, E.; Inoue, S. Formation of an imino-stabilized cyclic tin(II) cation from an amino(imino)stannylene. *Chem. Eur. J.* **2015**, *21*, 6704-6707. (j) Ochiai, T.; Franz, D.; Wu, X.; Irran,

E.; Inoue, S. A tin analogue of carbenoid: isolation and reactivity of a lithium bis(imidazolin-2-imino)stannylenoid. *Angew. Chem. Int. Ed.* **2016**, *55*, 6983-6987. for P: (k) Dielmann, F.; Back, O.; Henry-Ellinger, M.; Jerabek, P.; Frenking, G.; Bertrand, G. A crystalline singlet phosphinonitrene: a nitrogen atom-transfer agent. *Science* **2012**, *337*, 1526-1528. (l) Loh, Y. K.; Gurnani, C.; Ganguly, R.; Vidovic, D. A dicationic iminophosphane. *Inorg. Chem.* **2015**, *54*, 3087-3089.

(6) For NHI-stabilized Si species: (a) Inoue, S.; Leszczyńska, K. An acyclic imino-substituted silylene: synthesis, isolation and its facile conversion into a zwitterionic silaimine. *Angew. Chem., Int. Ed.* **2012**, *51*, 8589-8593. (b) Wendel, T. D.; Porzelt, A.; Herz, F. A. D.; Sarkar, D.; Jandl, C.; Inoue, S.; Rieger, B. From Si(II) to Si(IV) and back: reversible intramolecular carbon−carbon bond activation by an acyclic iminosilylene. *J. Am. Chem. Soc.* **2017**, *139*, 8134-8137. (c) Wendel, D.; Reiter, D.; Porzelt, A.; Altmann, J.; Inoue, S.; Rieger, B. Silicon and oxygen's bond of affection: an acyclic three-coordinate silanone and its transformation to an iminosiloxysilylene. *J. Am. Chem. Soc.* **2017**, *139*, 17193-17198. (d) Wendel, D.; Szilvási, T.; Henschel, D.; Altmann, P. J.; Jandl, C.; Inoue, S.; Rieger, B. Twist of a silicon−silicon double bond: selective *anti*-addition of hydrogen to an iminodisilene. *J. Am. Chem. Soc.* **2017**, *139*, 9156-9159. (e) Wendel, D.; Szilvási, T.; Henschel, D.; Altmann, P. J.; Jandl, C.; Inoue, S.; Rieger, B. Precise activation of ammonia and carbon dioxide by an iminodisilene. *Angew. Chem., Int. Ed.* **2018**, *57*, 14575-14579.

(7) For NHB: (a) Segawa, Y.; Yamashita, M.; Nozaki, K. Boryllithium: isolation, characterization, and reactivity as a boryl anion. *Science* **2006**, *314*, 113-115. (b) Segawa, Y.; Suzuki, Y.; Yamashita, M.; Nozaki, K. Chemistry of boryllithium: synthesis, structure, and reactivity. *J. Am. Chem. Soc.* **2008**, *130*, 16069-16079.

(8) For recent reviews on NHB: (a) Weber, L. Modern 1,3,2-diazaborole chemistry - metamorphosis from electrophilic to nucleophilic boron. *Eur. J. Inorg. Chem.* **2012**, *21*, 5595-5609. (b) Weber, L. 1,3,2-diazaborolyl anions - from lab curiosities to versatile reagents in synthesis. *Eur. J. Inorg. Chem.* **2017**, *21*, 3461-3488.

(9) For NHB as ligand for transition-metal complexes: Segawa, Y.; Yamashita, M.; Nozaki, K. Syntheses of PBP pincer iridium complexes: a supporting boryl ligand. *J. Am. Chem. Soc.* **2009**, *131*, 9201-9203.

(10) For stable cyclic and acyclic two-coordinate silylenes: (a) Denk, M.; Lennon, R.; Hayashi, R.; West, R.; Belyakov, A. V.; Verne, H. P.; Haaland, A.; Wagner, M.; Metzler, N. Synthesis and structure of a

stable silylene. *J. Am. Chem. Soc.* **1994**, *116*, 2691-2692. (b) Protchenko, A. V.; Birjkumar, K. H.; Dange, D.; Schwarz, A. D.; Vidovic, D.; Jones, C.; Kaltsoyannis, N.; Mountford, P.; Aldridge, S. A stable two-coordinate acyclic silylene. *J. Am. Chem. Soc.* **2012**, *134*, 6500-6503. (c) Rekken, B. D.; Brown, T. M.; Fettinger, J. C.; Tuononen, H. M.; Power, P. P. Isolation of a stable, acyclic, two-coordinate silylene. *J. Am. Chem. Soc.* **2012**, *134*, 6504-6507. (c) Protchenko, A. V.; Schwarz, A. D.; Blake, M. P.; Jones, C.; Kaltsoyannis, N.; Mountford, P.; Aldridge, S. A generic one-pot route to two-coordinate silylenes from silicon(IV) precursors: synthesis and structural characterization of a silylsilylene. *Angew. Chem., Int. Ed.* **2013**, *52*, 568-571. (d) Rekken, B. D.; Brown, T. M.; Fettinger, J. C.; Lips, F.; Tuononen, H. M.; Herber, R. H.; Power, P. P. Dispersion forces and counterintuitive steric effects in main group molecules: heavier group 14 (Si-Pb) dichalcogenolate carbene analogues with sub-90° interligand bond angles. *J. Am. Chem. Soc.* **2013**, *135*, 10134-10148. (e) Hadlington, T.; Abdalla, J. A. B.; Tirfoin, R.; Aldridge, S.; Jones, C. Stabilization of a two-coordinate, acyclic diaminosilylene (ADASi): completion of the series of isolable diaminotetrylenes, :E(NR_2)$_2$ (E = group 14 element). *Chem. Commun.* **2016**, *52*, 1717-1720.

(11) For recent review of NHO: Roy, M. M. D.; Rivard, E. Pushing chemical boundaries with *N*-heterocyclic olefins (NHOs): from catalysis to main group element chemistry. *Acc. Chem. Res.* **2017**, *50*, 2017-2025.

(12) For B–O multiple bonding: (a) Franz, D.; Inoue, S. Advances in the development of complexes that contain a group 13 element chalcogen multiple bond. *Dalton Trans.* **2016**, *45*, 9385-9397. (b) Vidovic, D.; Moore, J. A.; Jones, J. N.; Cowley, A. H. Synthesis and characterization of a coordinated oxoborane: Lewis acid stabilization of a boron−oxygen double bond. *J. Am. Chem. Soc.* **2005**, *127*, 4566-4567. (c) Wang, Y.; Hu, H.; Zhang, J.; Cui, C. Comparison of anionic and Lewis acid stabilized N-heterocyclic oxoboranes: their facile synthesis from a borinic acid. *Angew. Chem., Int. Ed.* **2011**, *50*, 2816-2819. (d) Loh, Y. K.; Chong, C. C.; Ganguly, R.; Li, Y.; Vidovic, D.; Kinjo, R. 1,2,4,3-Triazaborole-based neutral oxoborane stabilized by a Lewis acid. *Chem. Commun.* **2014**, *50*, 8561-8564. (e) Swarnarkar, A. K.; Hering-Junghans, C.; Ferguson, M. J.; Mcdonald, R.; Rivard, E. Oxoborane (RBO) complexation and concomitant electrophilic bond activation processes. *Chem. Eur. J.* **2017**, *23*, 8628-8631. (f) Zheng, Y.; Wang, X.; Bai, Y.; Wang, X.; Ru, C.; Chen, W.; Lv, X.; Pan, X.;

Wu, J. Diradical anion of potassium aggregate: reduction of dimer boroxide complex. *Inorg. Chem.* **2018**, *57*, 13544-13551.

(13)For arene donor interactions in heavier main group elements: Jones, C. Bulky guanidinates for the stabilization of oxidation state metallacycles. *Coord. Chem. Rev.* **2010**, *254*, 1273-1289.

(14)Herrmanndörfer, D.; Kaaz, M.; Puntigam, O.; Bender, J.; Nieger, M.; Gudat, D. The reaction between diazadienes and tribromides EBr_3 (E = P, B) revisited: metal-free synthesis of halogenated N-heterocyclic phosphanes and boranes. *Eur. J. Inorg. Chem.* **2015**, 4819-4828.

(15)Bonyhady, S. J.; Jones, C.; Nembenna, S.; Stasch, A.; Edwards, A. J.; McIntyre, G. J. β-diketiminate-stabilized magnesium(I) dimers and magnesium(II) hydride complexes: synthesis, characterization, adduct formation, and reactivity studies. *Chem. Eur. J.* **2010**, *16*, 938-955.

(16)Heidemann, T.; Mathur, S. Air-stable and volatile bis(pyridylalkenolato)germanium(II), -tin(II), and -lead(II) complexes. *Eur. J. Inorg. Chem.* **2014**, 506-510.

*(17)*Cosier, J.; Glazer, A. M. A nitrogen-gas-stream cryostat for general X-ray diffrcaction studies. *J. Appl. Cryst.* **1986**, *19*, 105-107.

(18)CrysAlisPro, Agilent Technologies, Version 1.171.35.8.

(19)Sheldrick, G. M. SHELXT - Integrated space-group and crystal structure determination. *Acta Cryst. Sect. A* **2015**, *71*, 3-8.

(20)Sheldrick, G. M. *Acta Cryst. Sect. A* **2008**, *64*, 112-122.

(21)Hübschle, C. B.; Sheldrick, G. M.; Dittrich, B. ShelXle: a Qt graphical user interface for SHELXL. *J. Appl. Cryst.* **2011**, *44*, 1281-1284.

(22)Frisch, M. J.; Trucks, G. W.; Schlegel, H. B.; Scuseria, G. E.; Robb, M. A.; Cheeseman, J. R.; Scalmani, G.; Barone, V.; Mennucci, B.; Petersson, G. A.; Nakatsuji, H.; Li, X.; Caricato, M.; Li, X.; Hratchian, H. P.; Izmaylov, A. F.; Bloino, J.; Zheng, G.; Sonnenberg, J. L.; Hada, M.; Ehara, M.; Toyota, K.; Fukuda, R.; Hasegawa, J.; Ishida, M.; Nakajima, T.; Honda, Y.; Kitao, O.; Nakai, H.; Vreven, T.; Montgomery, J. A., Jr.; Peralta, J. E.; Ogliaro, F.; Bearpark, M. J.; Heyd, J. J.; Brothers, E. N.; Kudin, K. N.; Staroverov, V. N.; Kobayashi, R.; Normand, J.; Raghavachari, K.; Rendell, A. P.; Burant, J. C.; Iyengar, S. S.; Tomasi, J.; Cossi, M.; Rega, N.; Millam, J. M.; Klene, M.; Adamo, C.; Jaramillo, J.; Gomperts, R.; Stratmannm R. E.; Yazyev, O; Austin, A.J.; Cammi, R.; Pomelli, C.; Ochterski, J. W.; Martin, R. L.; Morokuma, K.; Zakrzewski, V. G.; Voth, G. A.; Salvador, P;

Dannenberg, J. J.; Dapprich, S.; Daniels, A. D.; Farkas, O.; Foresman, J. B.; Ortiz, J. V.; Cioslowski, J.; Fox, D. J. *Gaussian 09*, *Revision D.01*, Gaussian, Inc., Wallingford, CT **2009**.

(23)(a) Ernzerhof, M.; Scuseria, G. E. *J. Chem. Phys.* **1999**, *110*, 5029-5036. (b) Adamo, C.; Barone, V. *J. Chem. Phys.* **1999**, *110*, 6158-6170. (c) Perdew, J. P.; Burke, K.; Ernzerhof, M. *Phys. Rev. Lett.* **1997**, *78*, 1396. (d) Perdew, J. P.; Burke, K.; Ernzerhof, M. *Phys. Rev. Lett.* **1996**, *77*, 3865-3868. (e) Perdew, J. P.; Ernzerhof, M.; Burke, K. *J. Chem. Phys.* **1996**, *105*, 9982-9985.

(24)Schäfer, A.; Horn, H.; Ahlrichs, R. *J. Chem. Phys.* **1992**, *97*, 2571-2577.

(25)Schäfer, A.; Huber, C.; Ahlrichs, R. *J. Chem. Phys.* **1994**, *100*, 5829-5835.

(26)Weigend, F.; Ahlrichs, R. *Phys. Chem. Chem. Phys.* **2005**, *7*, 3297-3305.

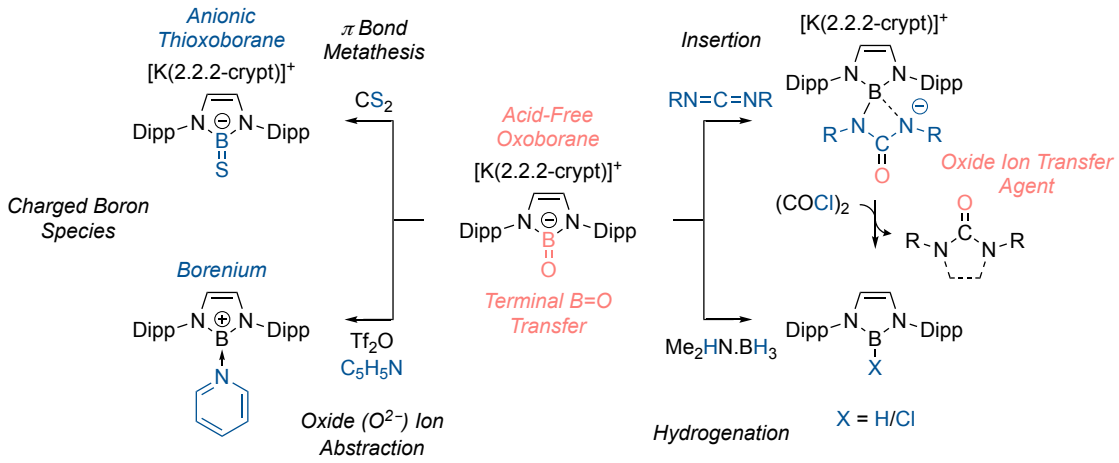
(27)Bergner, A.; Dolg, M.; Küchle, W.; Stoll, H.; Preuß, H. *Mol. Phys.* **1993**, *80*, 1431-1441.

(28)(a) Grimme, S.; Antony, J.; Ehrlich, S.; Krieg, H. *J. Chem. Phys.* **2010**, *132*, 154104-154119. (b) Grimme, S.; Ehrlich, S.; Goerigk, L. *J. Comput. Chem.* **2011**, *32*, 1456-1465.

(29)Glendening, E. D.; Reed, A. E.; Carpenter, J. E.; Weinhold,F. NBO Version 3.1.

Chapter 4

An Acid-Free Anionic Oxoborane Isoelectronic with Carbonyl: Access and Transfer of a Terminal B=O Double Bond



Loh, Y. K.; Porteous, K.; Fuentes, M. A.; Do, D. C. H.; Hicks, J.; Aldridge, S.

J. Am. Chem. Soc. **2019**, *141*, 8073-8077.

CONTENTS

Introduction 1

The Affinity of Boron for Oxygen 1

Oxoboranes 2

Acid- and Base-Free Main Group E=O Doubly Bonded Species 3

Results and Discussion 5

Synthesis of an Acid-Free Anionic Oxoborane 5

Synthesis of an Anionic Thioxoborane via Thionation of the Oxoborane Anion 7

Carbonyl-like Reactions of the Anionic Oxoborane 10

The Anionic Oxoborane as an Oxide Ion Transfer Agent 12

Conclusions 15

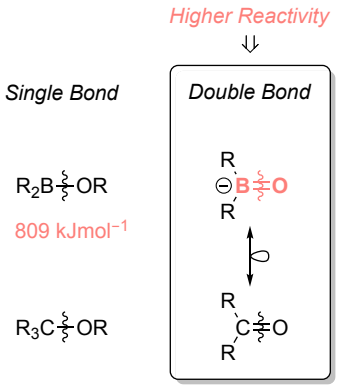
Experimental 16

References 34

Introduction

The Affinity of Boron for Oxygen

Boron has great affinity for oxygen, forming thermodynamically strong B−O bonds (809 kJ mol^{-1}) (Scheme 1).[1] As such, naturally occurring boron is typically locked in the form of borate minerals.[2] In synthetic chemistry, the highly oxophilic nature of boron is often exploited to drive important transformations such as Suzuki coupling and carbonyl hydroboration.[3] While these processes are increasingly being adopted by pharmaceutical production, chemical recycling of the resultant B−O bonds typically requires harsh conditions and reagents (e.g. production of BCl_3 from carbon and Cl_2 at 500°C). Hence, our approach was to induce new modes of reactivity for the BO fragment which might enable it to be (re)converted in more facile fashion to chemically useful entities. Given the higher reactivity typically associated with multiply bonded systems (as illustrated by the relatively

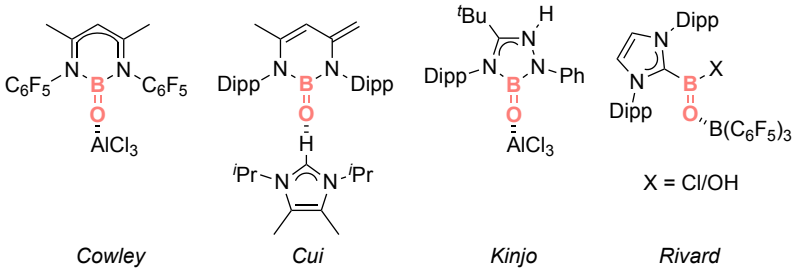


Scheme 1. Exploiting the hypothesized higher reactivity of a B=O double bond to induce B−O bond cleavage, by analogy with the known behaviour of C−O and C=O bonds (i.e. ether versus carbonyl functionalities).

inert nature of the C−O single bonds in ethers compared to the C=O double bonds in carbonyls), we wondered whether a B=O double bond which is isoelectronic with classical carbonyl compounds would be more amenable to facile B−O bond cleavage (Scheme 1).

Oxoboranes

Oxoboranes (R−B=O) are a class of transient organoboron species that contain a B=O double bond.[4] The quest for isolable oxoboranes has been hampered by the high polarity of the BO fragment and the unsaturated nature of the central boron atom, making them prone to head-to-tail oligomerization. Thus, monomeric species are highly elusive and only observable in the gas phase, or in a low-temperature matrix, or isolable via chemical trapping.[5] In 2005, seminal work by Cowley and co-workers described a monomeric Lewis acid stabilized oxoborane containing a short B=O double bond distance of 1.304(2) Å (Scheme 2).[6a] Subsequently, the concept of Lewis/Brønsted acid stabilization has been successfully employed by several groups to furnish a series of oxoboranes featuring similar B=O distances.[6] These include a report from the Cui group of a Brønsted acid stabilized anionic oxoborane, featuring strong hydrogen-bonding interaction between the [BO] and imidazolium fragments.[6b] More recently, Kinjo and co-workers documented a Lewis acid induced intramolecular proton migration of the parent borinic acid to access an oxoborane based on a five-membered 1,2,4,3-triazaborole framework.[6c] Additionally, the Rivard group have demonstrated that an ayclic oxoborane can be stabilized by simultaneous N-heterocyclic carbene (NHC) and borane coordination at the BO fragment.[6d] Another strategy is to introduce the BO motif into the coordination sphere of a transition metal, as shown by the groups of Braunschweig and Yamashita.[7]

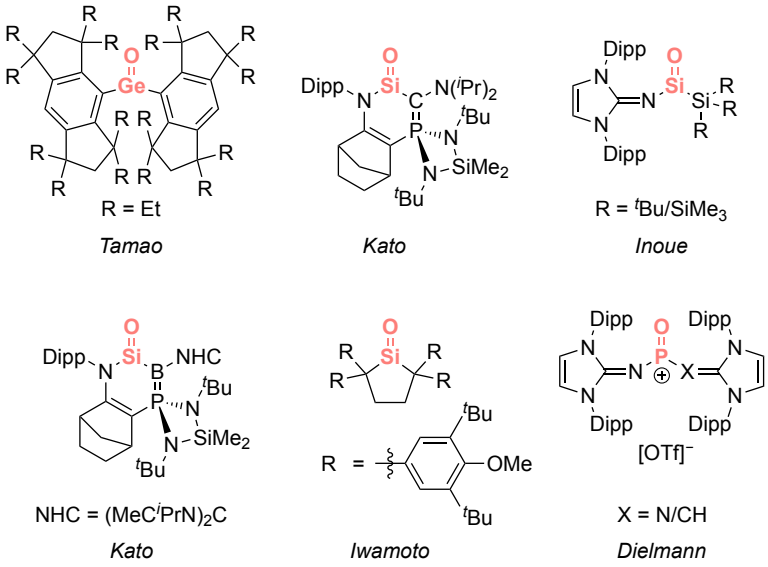


Scheme 2. Examples of acid-stabilized oxoboranes.

While implementing these stabilization strategies has enabled chemists to isolate compounds containing discrete BO fragments, evidence for carbonyl-like reactivity patterns appears to be uncharted, possibly due to the electronic perturbation and steric protection of the BO fragment by the capping group at the O-terminus. Hence, it was believed that access to an acid-free oxoborane is highly desirable.

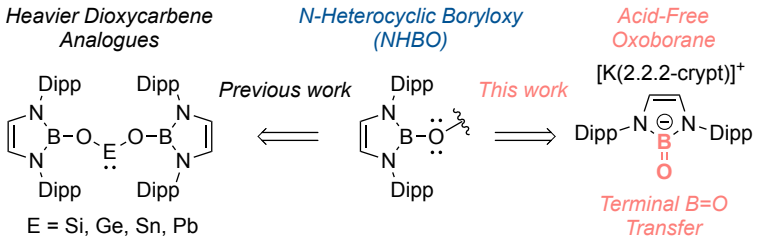
Acid- and Base-Free Main Group E=O Doubly Bonded Species

Aside from boron, tremendous progress has been made recently in the isolation of compounds featuring acid- and base- free main group element E=O double bonds, which are isoelectronic with the C=O double bonds of classical carbonyl compounds. In 2012, Tamao and co-workers document the breakthrough discovery of a stable monomeric germanone, $R_2Ge=O$, a heavier ketone analogue possessing a Ge=O double bond (Scheme 3).[8a] Another landmark achievement was the fulfillment of "Kipping's dream" by the groups of Kato, Inoue and Iwamoto describing isolable silanones with Si=O double bonds.[8b-e] Furthermore, in a seminal report by Dielmann and co-workers, a novel synthetic route to access a Lewis base free oxophosphonium ion $[R_2P=O]^+$ containing a P=O double bond has been described.[8f]



Scheme 3. Examples of acid- and base-free main group E=O doubly bonded species isoelectronic with the carbonyl functional group.

Inspired by these reports, we wondered whether an acid-free oxoborane anion $[R_2B{=}O]^-$ could be accessed (Scheme 4). Exploiting its isoelectronic relationship with the carbonyl functional group, we believed that such a species might exhibit carbonyl-like reactivity, and therefore targeted an exploration of new B−O bond cleaving reactivity patterns.

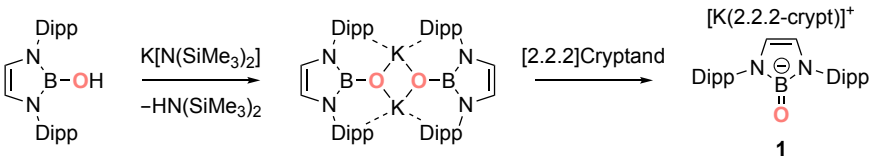


Scheme 4. Previous work with the NHBO ligand and present work.

Results and Discussion

Synthesis of an Acid-Free Anionic Oxoborane

Very recently, we introduced a new class of N-heterocyclic boryloxy (NHBO) ligand, $(HCDippN)_2BO-$, and demonstrated its ability to stabilize a complete homoleptic series of heavier group 14 dioxycarbene analogues (Scheme 4; Chapter 3).[9] We believed that the NHBO framework, possessing a 6π diazaborolyl functionality flanked by sterically demanding Dipp groups would have the capabilities to enable the isolation of an acid-free oxoborane. In view of this, we targeted the potassiated ligand $\{K[(HCDippN)_2BO]\}_2$, which is dimeric in the solid-state, as the starting point of our investigation. To sequester the potassium ions from this dimer, two equivalents of [2.2.2]cryptand were employed, resulting in an immediate colour change from yellow to red (Scheme 5). The $^{11}B\{^1H\}$ NMR spectrum displays a broad singlet at 20.7 ppm, which is slightly upfield shifted by ~2 ppm, suggesting (if anything) a slight increase electron density at the boron centre.



Scheme 5. Deprotonation/sequestration to give acid-free anionic oxoborane (**1**).

Single crystals obtained by slow evaporation from a benzene solution were subjected to X-ray diffraction analysis. Gratifyingly, the solid-state structure reveals the successful sequestration of the potassium ion to generate a monomeric anionic oxoborane **1** (as the $K(2.2.2\text{-crypt})]^+$ salt) (Figure 1). The oxygen atom assumes a terminal position, with the

closest contacts being an O1···K1 distance of 5.919(6) Å and O···H interactions involving the C−H bonds of the flanking ^{i}Pr groups or the cryptand methylene units (~2.5 Å). Hence, **1** represents the first example of an acid-free anionic oxoborane. The central boron atom adoptsa trigonal planar geometry. Perhaps the most striking feature is the very short B−O bond distance of 1.273(8) Å, when compared with other Lewis/Brønsted acid stabilized B=O double bond distances reported to date in the literature (1.287(4)−1.329(6) Å),[6] presumably reflecting the effect of acid liberation. In comparison with the parent borinic acid $(HCDippN)_2BOH$ (1.373(3) Å), complete removal of the proton results in a remarkable shortening of the B−O distance by 0.10 Å (~8%),[10] suggesting enhanced B=O π bond character. Consistently, the adjacent B−N bonds within the heterocycle lengthen significantly from $(HCDippN)_2BOH$ (mean: 1.429(3) Å) to **1** (mean: 1.487(7) Å).

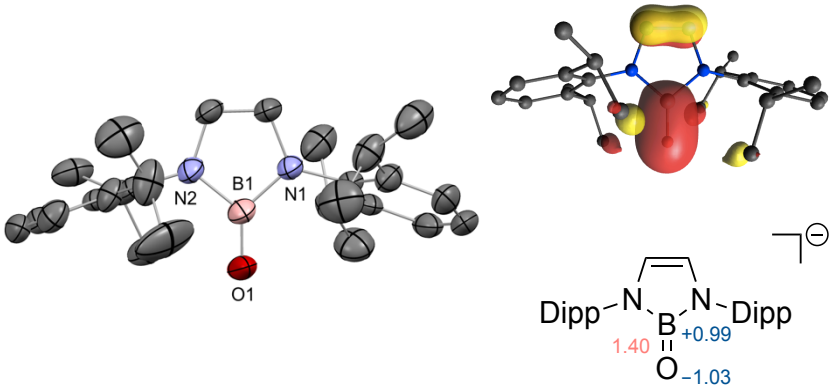


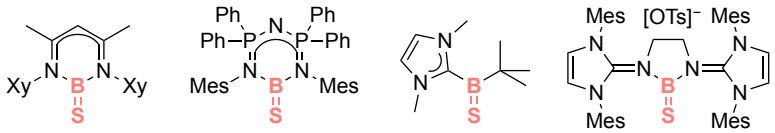
Figure 1. Solid-state structure of **1**, Kohn-Sham HOMO−2, WBI bond order (red) and NPA charges (blue). For clarity, $[K(2.2.2\text{-crypt})]^+$ and hydrogen atoms are omitted. Thermal ellipsoids set at 50% probability. Key bond lengths (Å) and angles (°): B1−O1 1.273(8), B1−N1 1.484(7), B1−N2 1.489(7), N1−B1−N2 100.6(4).

To gain further insight into the nature of the BO fragment in oxoborane **1**, we turned our attention to DFT calculations using PBE1PBE hybrid exchange-correlation functional and TZVP basis sets. The B=O π bond can be located in the HOMO−2 (Figure 1). The

Wiberg bond index (WBI) of 1.40 and NPA charges on B (+0.99) and O (−1.03) are consistent with the formulation as a B=O double bond that is strongly polarized towards oxygen. For comparison, the isoelectronic carbonyl compound $(HCDippN)_2CO$ was calculated to have a WBI bond order of 1.61 and NPA charges on C (+0.72) and O (−0.64), hinting at the resemblance of oxoborane **1** to classical carbonyl compounds.

Synthesis of an Anionic Thioxoborane via Thionation of the Oxoborane Anion

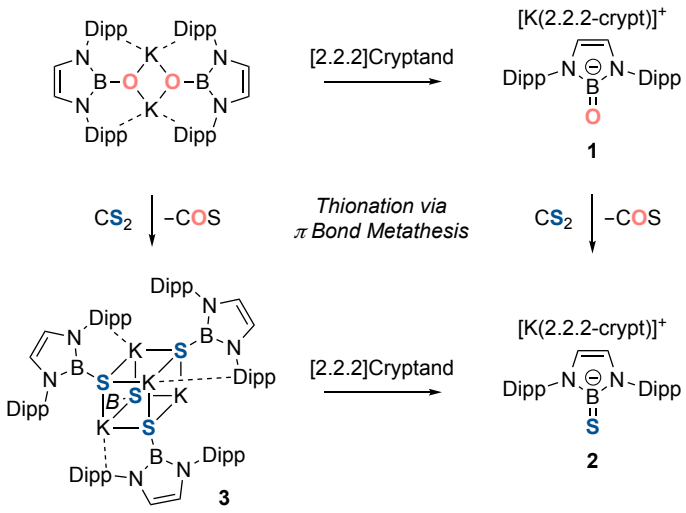
In stark contrast with its lighter congener, monomeric thioxoboranes (R−B=S) have been isolated in the absence of acid protection, as demonstrated in reports from the groups of Cui, Singh and Braunschweig, featuring short B=S double bonds (Scheme 6).[11a-c] However, while Inoue and co-workers have reported a cationic thioxoborane,[11d] an anionic analogue $[R_2B{=}S]^-$, which is isoelectronic with the thiocarbonyl functional group, remains conspicuously absent.



Scheme 6. Examples of neutral and cationic thioxoboranes.

With this in mind, the isolated acid-free B=O motif in oxoborane **1** seemed to be an ideal candidate to explore carbonyl-like metathesis of the terminal oxygen. Treatment of oxoborane **1** with carbon disulfide, CS_2 at room temperature leads to an upfield shift of the $^{11}B\{^1H\}$ NMR signal by ~12 ppm to 33.1 ppm, which is close to that of Inoue's cationic thioxoborane (33.9 ppm)[11d] (Scheme 7). Furthermore, a signal at 153.4 ppm was detected in

the $^{13}C\{^{1}H\}$ NMR spectrum which can be assigned to carbonyl sulfide, COS, hinting at successful B=O / B=S metathesis. Slow evaporation of a concentrated solution of **2** in benzene at room temperature afforded single crystals. X-ray diffraction analysis unambiguously revealed the identity of **2** as an anionic thioxoborane isostructural with oxoborane **1**, with sulfur in the terminal position (Figure 2), representing the first monomeric B=S containing anion isoelectronic with thiocarbonyl. As in the case of oxoborane **1**, the central boron atom of thioxoborane **2** adopts a trigonal planar geometry. Closer inspection reveals the B−S bond distance to be 1.774(1) Å, i.e. significantly lengthened compared to previously reported cationic (1.710(5) Å)[11d] and neutral (1.739(2)−1.752(5) Å)[11a-c] systems, indicating a stepwise decrease in bond order with accumulation of negative charge on the BS fragment.



Scheme 7. Thionation to give anionic thioxoborane (**2**). Alternative route to (**2**) via thionation/sequestration sequence.

As with oxoborane **1**, we turned to DFT calculations for further insight into the bonding situation in thioxoborane **2**. The B=S π bond can be located in the HOMO−2 (Figure 2). Moreover, the WBI bond order of 1.56 and NPA charges on B (+0.61) and S (−0.71) for the BS fragment are consistent with a formulation as a B=S double bond that is

polarized towards sulfur, although to a lesser extent than towards the oxygen centre in oxoborane **1**.

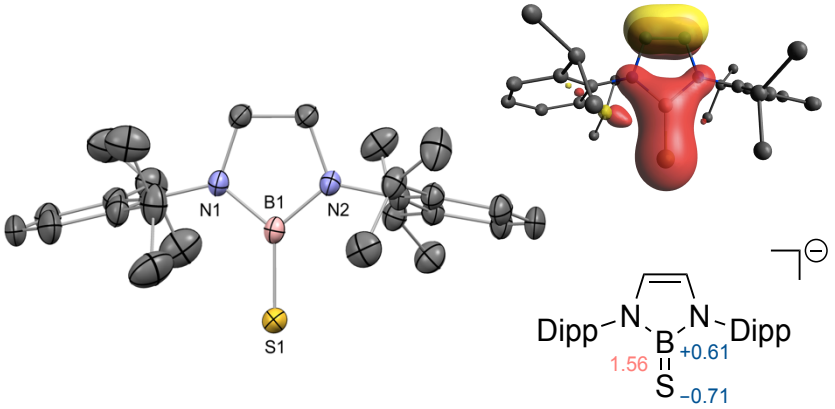


Figure 2. Solid-state structure of **2**, Kohn-Sham HOMO−2, WBI bond order (red) and NPA charges (blue). For clarity, $[K(2.2.2\text{-crypt})]^+$ and hydrogen atoms are omitted. Thermal ellipsoids set at 50% probability. Key bond lengths (Å) and angles (°): B1−S1 1.774(1), B1−N1 1.457(2), B1−N2 1.461(2), N1−B1−N2 101.4(9).

As $\{K[(HCDippN)_2BO]\}_2$ is a convenient precursor to the N-heterocyclic boryloxy (NHBO) ligand, we were curious whether a heavier NHBS ligand could be similarly accessed. In view of this, treatment of $\{K[(HCDippN)_2BO]\}_2$ with CS_2 in benzene resulted in precipitation of a white solid (Scheme 7). Single crystals were obtained by slow evaporation of a concentrated solution of **3** in benzene at room temperature. X-ray diffraction analysis revealed **3** to exist as a tetrameric cluster formed by the aggregation of four $K[(HCDippN)_2BS]$ units, forming a near perfect K_4−S_4 cube with sides of 3.143(1) Å length on average (Figure 3). Within this structural motif, the NHBS ligand displays arene π interactions from the Dipp groups to the potassium ions, screening it from possible further aggregation.[9] Moreover, treatment of tetrameric **3** with [2.2.2]cryptand (4 equiv.) sequesters the potassium ions and breaks apart the cube to furnish the monomeric thioxoborane **2**.

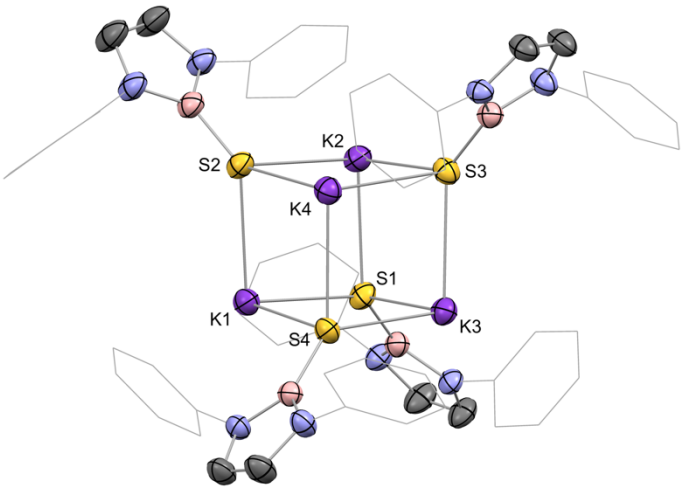
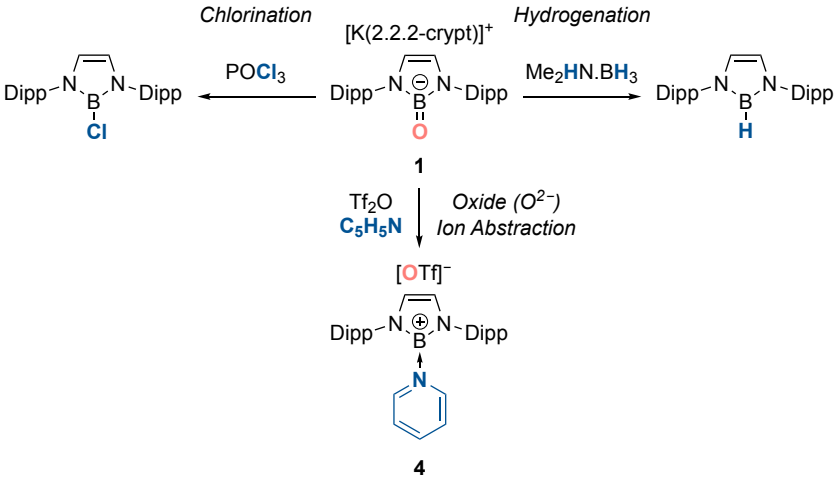


Figure 3. Solid-state structure of **3**. For clarity, hydrogen atoms and ^{i}Pr groups are omitted, Dipp groups are simplified as wireframes. Thermal ellipsoids set at 50% probability. Key bond lengths (Å) and angles (°): B1−S1 1.789(4), S1−K1 3.112(1), S1−K2 3.084(1), S1−K3 3.185(1).

Carbonyl-like Reactions of the Anionic Oxoborane

The facile access of a heavier B=S via π bond metathesis from its lighter congener resembles the thionation of carbonyl to thiocarbonyl compounds. Motivated by this, we turned our attention to other classical carbonyl transformations. One such fundamentally important reaction is hydrogenation, typically accomplished with highly reactive metal hydride reagents. In our case, treating oxoborane **1** with dimethylamineborane, $Me_2HN{\cdot}BH_3$ affords the hydrogenated product $(HCDippN)_2BH$ (Scheme 8).[10] It is noteworthy that an analogous hydrogenation of the cationic thioxoborane $[R_2B{=}S]^+$ by hydrogen transfer from $H_3N{\cdot}BH_3$ was reported by Inoue and co-workers.[11d] While both cases involve a net H_2 transfer to the B=E functionality, hydrogenation of the anionic oxoborane $[R_2B{=}O]^-$ is likely initiated by H^+ transfer followed by H^-, in contrast to the H^- / H^+ sequence proposed by Inoue for the cationic thioxoborane $[R_2B{=}S]^+$, reflecting the contrasting charges inherent in these two species.



Scheme 8. Carbonyl-like reactions of oxoborane **1**.

While B−H bond containing compounds are valuable reagents for hydroboration reactions, we wondered whether other R_2BX species could be accessed. A conventional protocol to activate the carbonyl group towards nucleophilic attack is by chlorination. To probe this analogy, we subjected oxoborane **1** to phosphoryl chloride, $POCl_3$ at room temperature, leading to an immediate colour change from red to yellow (Scheme 8). The signal in the $^{11}B\{^1H\}$ NMR shifts to 22.5 ppm, hinting at the generation of a new boron containing species. A single set of resonances in the ^1H NMR spectrum matches that of a previous report and confirms its identity as the chlorinated product $(HCDippN)_2BCl$.[10] Due to its labile nature, B−Cl bond containing compounds are versatile building blocks to access key organoboron species, such as boronic acids for Suzuki coupling, or even boryl anions, containing a nucleophilic boron for umpolung B−C bond formations.

Carbonyl compounds are also known to undergo rearrangements in the presence of trifluoromethanesulfonic anhydride, Tf_2O, and transient carbocations are often proposed as reactive intermediates.[12] We wondered whether an analogous boron cation could be directly accessed and trapped in the process. With this in mind, we subjected oxoborane **1** to Tf_2O in the presence of pyridine (Scheme 8). To our delight, X-ray diffraction analysis

unambiguously confirmed the complete oxide ion (O^{2-}) abstraction from **1** to yield the borenium cation **4** trapped by a molecule of pyridine (Figure 4).[13] Closer inspection of the structural parameters revealed a remarkable contraction of the endocyclic B−N bond distances from anionic oxoborane **1** (mean: 1.487(7) Å) to cationic borenium **4** (mean: 1.409(7) Å) hinting at significant loss of π electron density at boron upon oxide ion transfer − which is compensated by simultaneous π electron donation from the adjacent nitrogen atoms.

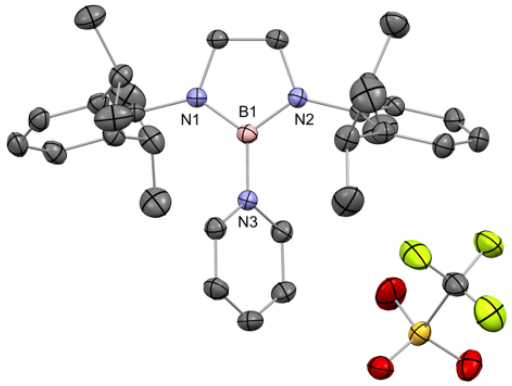
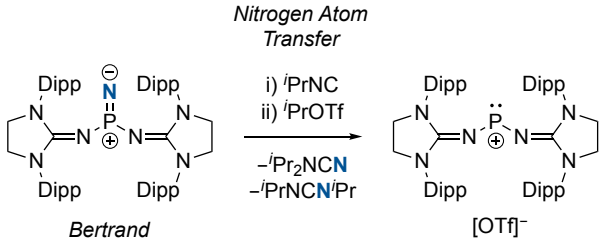


Figure 4. Solid-state structure of **4**. For clarity, hydrogen atoms are omitted. Thermal ellipsoids set at 50% probability. Key bond lengths (Å) and angles (°): B1−N3 1.5087(19), B1−N1 1.4100(19), B1−N2 1.4071(19), N1−B1−N2 108.24(12).

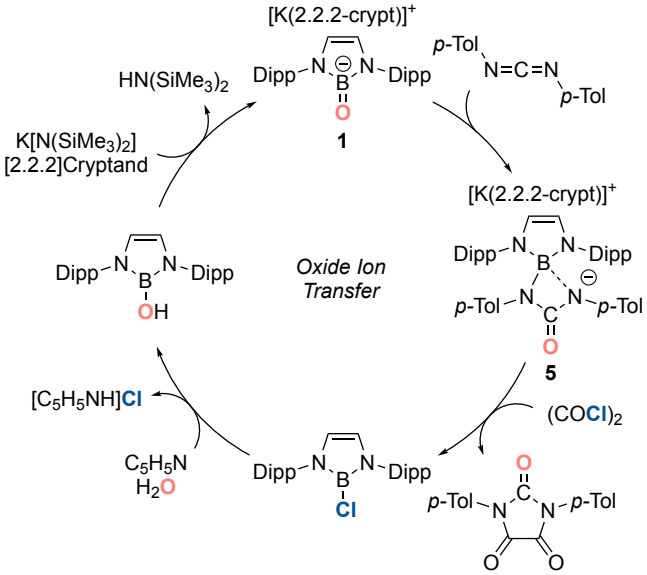
The Anionic Oxoborane as an Oxide Ion Transfer Agent

In a recent report, Bertrand and co-workers demonstrated that a main group species can act as a nitrogen atom transfer agent, a mode of reactivity more familiar to transition metal systems (Scheme 9).[14] In this process a phosphinonitrene initially forms an adduct with isocyanide, and subsequent alkylation releases the substrate to afford a mixture of cyanamide and carbodiimide, with accompanying regeneration of the phosphenium ion.[14a-b]



Scheme 9. Bertrand's phosphinonitrene as a nitrogen atom transfer agent.

The isoelectronic analogy between oxoborane **1** and Bertrand's phosphinonitrene inspired us to investigate the possibility of using **1** as an oxide ion transfer agent, a task typically also accomplished by transition-metal systems.[15] As a proof of concept, we treated oxoborane **1** with 1,3-di-*p*-tolylcarbodiimide (Scheme 10). To our surprise, X-ray diffraction analysis revealed not simple adduct formation, but the 1,2-addition of the B−O bond across the C=N double bond to afford complex **5** (Figure 5). Although unsymmetrical coordination of the substrate to boron (B1−N3 1.4611(17) Å versus B1−N4 2.6204(18) Å) is implied from the solid-state structure, interestingly, the ^{1}H NMR spectrum of **5** shows a single *p*-Tol



Scheme 10. Synthetic cycle with oxoborane **1** acting as an oxide ion transfer agent.

group environment in solution, hinting at the facile exchange between the nitrogen atoms in the NC(O)N fragment. Formally, this can be considered an insertion of a carbodiimide into the B=O double bond.

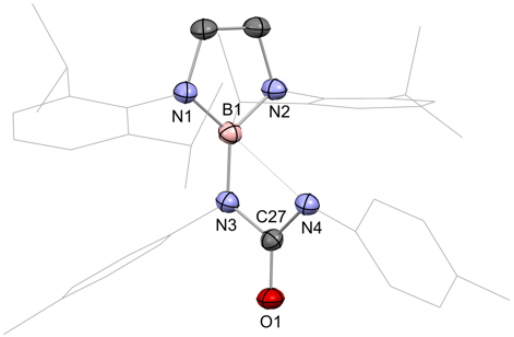


Figure 5. Solid-state structure of **5**. For clarity, hydrogen atoms are omitted. Thermal ellipsoids set at 50% probability. Key bond lengths (Å) and angles (°): B1−N3 1.4611(17), B1−N4 2.6204(18), B1−N1 1.4418(17), B1−N2 1.4441(18), N3−C27 1.4322(16), N4−C27 1.3290(17), C27−O1 1.2476(16), N1−B1−N2 103.96(11).

To release the functionalized substrate, oxalyl chloride was employed, which ties up the nitrogen atoms to release a cyclic urea derivative (OC(*p*-Tol)N)$_2$CO and regenerates (HCDippN)$_2$BCl (Scheme 10).[10] While this stepwise procedure closely resembles the N-transfer methodology reported by Bertrand,[14a-b] we could also achieve this transformation in a one-pot sequence without intermediate isolation of **5**. To close the oxide ion transfer cycle, (HCDippN)$_2$BCl could be converted to its corresponding borinic acid (HCDippN)$_2$BOH with water in the presence of pyridine, and subsequently back to oxoborane **1** via a simple deprotonation/sequestration sequence.[9]

Conclusions

In conclusion, the synthesis of first acid-free anionic oxoborane **1** is reported, this system being isoelectronic with classical carbonyl compounds. Oxoborane **1** can be readily accessed from parent borinic acid by a simple deprotonation/sequestration sequence. DFT analysis supports the presence of a highly polarized terminal B=O double bond. We also disclose an unprecedented π bond metathesis which converts the terminal B=O moiety to a heavier B=S double bond, thereby accessing the first anionic thioxoborane **2**. This facile B−O bond cleavage can also be applied to access synthetically versatile B−H and B−Cl containing organoboron species. Furthermore, we could demonstrate a complete oxide ion (O^{2-}) abstraction to generate a borenium cation **4**. Finally, we were able to show that oxoborane **1** can even act as an oxide ion transfer agent to an organic substrate, a task which is typically found in the realm of transition-metal reagents. Hence, our work demonstrates that B−O bonds which were once considered thermodynamic sinks, can now be activated towards facile bond cleavage and transfer by exploiting the higher reactivity inherent in the B=O double bond.

Experimental

General Considerations and Starting Material Preparations

All manipulations were carried out using standard Schlenk line or dry-box techniques under an atmosphere of argon or dinitrogen. Solvents were degassed by sparging with argon and dried by passing through a column of the appropriate drying agent. NMR spectra were measured in benzene-d_6 (which was dried over potassium), with the solvent then being distilled under reduced pressure and stored under argon in Teflon valve ampoules. NMR samples were prepared under argon in 5 mm Wilmad 507-PP tubes fitted with J. Young Teflon valves. ^{1}H, ^{13}C{^{1}H}, ^{11}B{^{1}H} and ^{19}F{^{1}H} NMR spectra were recorded on Bruker Avance III HD nanobay 400 MHz or Bruker Avance 500 MHz spectrometer at ambient temperature and referenced internally to residual protio-solvent (^{1}H) or solvent (^{13}C) resonances and are reported relative to tetramethylsilane (δ = 0 ppm). ^{19}F resonances are referenced externally to $CFCl_3$. Assignments were confirmed using two-dimensional ^{1}H-^{1}H and ^{13}C-^{1}H NMR correlation experiments. Chemical shifts are quoted in δ (ppm) and coupling constants in Hz. Elemental analyses were carried out by London Metropolitan University. $\{K[(HCDippN)_2BO]\}_2$ was prepared by literature method.[9] All other reagents were used as received.

Synthetic, Spectroscopic and Analytical Data

Preparation of [K(2.2.2-crypt)][(HCDippN)$_2$BO] (1). To a mixture of $\{K[(HCDippN)_2BO]\}_2$ (200 mg, 0.23 mmol) and [2.2.2]cryptand (170 mg, 0.45 mmol) was added toluene (5 mL) and the reaction mixture stirred for 5 min at room temperature to form a red solution.

Volatiles were removed under vacuum to yield [K(2.2.2-crypt)][(HCDippN)$_2$BO] (**1**) (342 mg, 93% yield) as a red powder. Single crystals suitable for X-ray crystallography were obtained by slow evaporation of a concentrated solution of **1** in benzene at room temperature. ^{1}H NMR (500 MHz, C_6D_6, 297 K): δ = 1.48 (d, $^3J_{HH}$ = 6.0 Hz, 12H, CH(C*H*$_3$)$_2$), 1.50 (d, $^3J_{HH}$ = 6.9 Hz, 12H, CH(C*H*$_3$)$_2$), 2.28 (t, $^3J_{HH}$ = 4.8 Hz, 12H, crypt-C*H*$_2$), 3.11 (t, $^3J_{HH}$ = 4.8 Hz, 12H, crypt-C*H*$_2$), 3.16 (s, 12H, crypt-C*H*$_2$), 4.09 (sept, $^3J_{HH}$ = 6.7 Hz, 4H, C*H*(CH$_3$)$_2$), 6.26 (s, 2H, NC*H*), 7.21-7.28 (m, 6H, Dipp-C*H*); ^{13}C{^{1}H} NMR (126 MHz, C_6D_6): δ = 24.3 (CH(*C*H$_3$)$_2$), 25.1 (CH(*C*H$_3$)$_2$), 28.7 (*C*H(CH$_3$)$_2$), 56.1 (crypt-*C*H$_2$), 68.6 (crypt-*C*H$_2$), 70.2 (crypt-*C*H$_2$), 115.7 (N*C*H), 122.6 (Dipp-*m*-*C*H), 124.4 (Dipp-*p*-*C*H), 146.2 (Dipp-*i*-*C*), 148.2 (Dipp-*o*-*C*); ^{11}B{^{1}H} NMR (128 MHz, C_6D_6): δ = 20.7; anal. calc. for $C_{44}H_{72}BKN_4O_7$: C 64.53%, H 8.86%, N 6.84%, found: C 64.64%, H 9.02%, N 6.72%.

Preparation of [K(2.2.2-crypt)][(HCDippN)$_2$BS] (2). To a solution of **1** (50 mg, 0.06 mmol) in benzene (0.3 mL) was added CS_2 (0.05 mL, 0.83 mmol) at room temperature. Volatiles were removed under vacuum to yield [K(2.2.2-crypt)][(HCDippN)$_2$BS] (**2**) (51 mg, 100% yield) as a red powder. Single crystals suitable for X-ray crystallography were obtained by slow evaporation of a concentrated solution of **2** in benzene at room temperature. ^{1}H NMR (500 MHz, C_6D_6, 297 K): δ = 1.50 (d, $^3J_{HH}$ = 7.0 Hz, 12H, CH(C*H*$_3$)$_2$), 1.60 (d, $^3J_{HH}$ = 6.9 Hz, 12H, CH(C*H*$_3$)$_2$), 2.23 (t, $^3J_{HH}$ = 4.6 Hz, 12H, crypt-C*H*$_2$), 3.24 (t, $^3J_{HH}$ = 4.6 Hz, 12H, crypt-C*H*$_2$), 3.28 (s, 12H, crypt-C*H*$_2$), 4.00 (sept, $^3J_{HH}$ = 6.9 Hz, 4H, C*H*(CH$_3$)$_2$), 6.47 (s, 2H, NC*H*), 7.27-7.32 (m, 6H, Dipp-C*H*); ^{13}C{^{1}H} NMR (126 MHz, C_6D_6): δ = 24.6 (CH(*C*H$_3$)$_2$), 24.8 (CH(*C*H$_3$)$_2$), 28.8 (*C*H(CH$_3$)$_2$), 54.9 (crypt-*C*H$_2$), 68.1 (crypt-*C*H$_2$), 70.6 (crypt-*C*H$_2$), 117.4 (N*C*H), 122.5 (Dipp-*m*-*C*H), 125.3 (Dipp-*p*-*C*H), 145.1 (Dipp-*i*-*C*), 148.0 (Dipp-*o*-*C*); ^{11}B{^{1}H} NMR (128 MHz, C_6D_6): δ = 33.1; anal. calc. for $C_{44}H_{72}BKN_4O_6S$: C 63.29%, H 8.69%, N 6.71%, found: C 63.43%, H 8.84%, N 6.67%.

Preparation of {K[(HCDippN)$_2$BS]}$_4$ (3). To a solution of {K[(HCDippN)$_2$BO]}$_2$ (200 mg, 0.23 mmol) in toluene (2 mL) was added CS_2 (0.1 mL, 1.66 mmol) at room temperature. The solution was concentrated until the precipitation of solid, and subsequently washed with additional toluene (1 mL). Volatiles were removed under vacuum to yield {K[(HCDippN)$_2$BS]}$_4$ (**3**) (104 mg, 51% yield) as a pale yellow powder. Single crystals suitable for X-ray crystallography were obtained by slow evaporation of a concentrated solution of **3** in benzene at room temperature. ^{1}H NMR (500 MHz, C_6D_6, 297 K): δ = 1.28 (d, $^3J_{HH}$ = 6.9 Hz, 24H, CH(C*H*$_3$)$_2$), 3.46 (bs, 4H, C*H*(CH$_3$)$_2$), 6.13 (s, 2H, NC*H*), 7.13 (s, 6H, Dipp-C*H*); ^{13}C{^{1}H} NMR (126 MHz, C_6D_6): δ = 24.4 (CH(*C*H$_3$)$_2$), 28.5 (*C*H(CH$_3$)$_2$), 118.0 (N*C*H), 123.6 (Dipp-*m*-*C*H), 127.0 (Dipp-*p*-*C*H), 143.0 (Dipp-*i*-*C*), 148.1 (Dipp-*o*-*C*); ^{11}B{^{1}H} NMR (128 MHz, C_6D_6): δ = 32.1; anal. calc. for $C_{104}H_{144}B4K4N_8S_4$: C 68.10%, H 7.91%, N 6.11%, found: C 67.97%, H 7.86%, N 6.01%.

Preparation of [(HCDippN)$_2$B(NC$_5$H$_5$)][OTf] (4). To a solution of **1** (50 mg, 0.06 mmol) in benzene (5 mL) was added Tf_2O (0.3 mL of a 0.02 M solution in benzene, 0.06 mmol) and pyridine (1 mL) at room temperature. Volatiles were removed under vacuum. To the residue was added diethyl ether (5 mL) and the mixture filtered. The filtrate was dried under vacuum to yield [(HCDippN)$_2$B(NC$_5$H$_5$)][OTf] (**4**) (19 mg, 51% yield) as a bright yellow powder. Single crystals suitable for X-ray crystallography were obtained by slow evaporation of a concentrated solution of **4** in 1,2-difluorobenzene at room temperature. ^{1}H NMR (500 MHz, CD_2Cl_2, 297 K): δ = 1.01 (d, $^3J_{HH}$ = 7.0 Hz, 12H, CH(C*H*$_3$)$_2$), 1.25 (d, $^3J_{HH}$ = 6.8 Hz, 12H, CH(C*H*$_3$)$_2$), 2.85 (sept, $^3J_{HH}$ = 6.9 Hz, 4H, C*H*(CH$_3$)$_2$), 6.56 (s, 2H, NC*H*), 7.36 (d, $^3J_{HH}$ = 7.8 Hz, 4H, Dipp-*m*-C*H*), 7.50 (t, $^3J_{HH}$ = 7.8 Hz, 2H, Dipp-*p*-C*H*), 7.94-7.97 (m, 2H, Py-*m*-C*H*), 8.03-8.04 (m, 2H, Py-*o*-C*H*), 8.70-8.73 (m, 1H, Py-*p*-C*H*); ^{13}C{^{1}H} NMR (126 MHz, CD_2Cl_2): δ = 23.4 (CH(*C*H$_3$)$_2$), 25.1 (CH(*C*H$_3$)$_2$), 29.2 (*C*H(CH$_3$)$_2$), 121.5 (N*C*H), 125.6

(Dipp-*m*-*C*H), 129.7 (Py-*m*-C*H*), 130.3 (Dipp-*p*-*C*H), 134.2 (Dipp-*i*-*C*), 143.8 (Py-*o*-C*H*), 145.4 (Dipp-*o*-*C*), 149.6 (Py-*p*-C*H*); $^{11}B\{^1H\}$ NMR (128 MHz, CD_2Cl_2): δ = 20.4; $^{19}F\{^1H\}$ NMR (377 MHz, CD_2Cl_2): δ = −79.0; anal. calc. for $C_{32}H_{40}BF_3N_3O_3S$: C 62.54%, H 6.56%, N 6.84%, found: C 62.35%, H 6.71%, N 6.75%.

Preparation of [K(2.2.2-crypt)][(HCDippN)$_2$B(p-Tol)NCON(p-Tol)] (5). To a mixture of **1** (100 mg, 0.12 mmol) and (*p*-Tol)NCN(*p*-Tol) (27 mg, 0.12 mmol) was added benzene (0.5 mL) and the reaction mixture agitated at room temperature to form a red solution. Single crystals of [K(2.2.2-crypt)][(HCDippN)$_2$B(*p*-Tol)NCON(*p*-Tol)] (**5**) (21 mg, 17% yield) suitable for X-ray crystallography were obtained from a concentrated solution in tetrahydrofuran at room temperature. ^1H NMR (400 MHz, C_6D_6, 297 K): δ = 1.31 (d, $^3J_{HH}$ = 6.8 Hz, 12H, CH(CH_3)$_2$), 1.45 (d, $^3J_{HH}$ = 6.8 Hz, 12H, CH(CH_3)$_2$), 2.00 (t, $^3J_{HH}$ = 4.6 Hz, 12H, crypt-CH_2), 2.32 (s, 6H, *p*-Tol-CH_3), 2.98 (t, $^3J_{HH}$ = 4.6 Hz, 12H, crypt-CH_2), 3.06 (s, 12H, crypt-CH_2), 4.32-4.38 (m, 4H, CH(CH$_3$)$_2$), 6.39 (s, 2H, NCH), 7.04 (d, $^3J_{HH}$ = 8.2 Hz, 4H, *p*-Tol-CH), 7.18-7.25 (m, 6H, Dipp-CH), 7.64 (d, $^3J_{HH}$ = 7.9 Hz, 4H, *p*-Tol-CH); $^{13}C\{^1H\}$ NMR (126 MHz, C_6D_6): δ = 21.4 (*p*-Tol-*C*H$_3$), 23.9 (CH(*C*H$_3$)$_2$), 27.4 (CH(*C*H$_3$)$_2$), 28.4 (*C*H(CH$_3$)$_2$), 54.1 (crypt-*C*H$_2$), 67.6 (crypt-*C*H$_2$), 70.4 (crypt-*C*H$_2$), 118.7 (N*C*H), 123.3 (Dipp-*m*-*C*H), 124.0 (*p*-Tol-*C*H), 125.1 (*p*-Tol-*C*), 125.7 (Dipp-*p*-*C*H), 143.0 (*p*-Tol-*C*), 147.8 (Dipp-*i*-*C*), 149.0 (Dipp-*o*-*C*), 162.4 (N*C*(O)N); $^{11}B\{^1H\}$ NMR (128 MHz, C_6D_6): δ = 17.6; anal. calc. for $C_{59}H_{86}BKN_6O_7$: C 68.06%, H 8.33%, N 8.07%, found: C 67.76%, H 8.24%, N 7.97%.

Preparation of (HCDippN)$_2$BH. To a mixture of **1** (100 mg, 0.12 mmol) and $Me_2HN{\cdot}BH_3$ (15 mg, 0.25 mmol) was added toluene (5 mL) and stirred at 80 °C overnight to form a red solution. Volatiles were removed under vacuum. To the residue was added *n*-hexane (10 mL)

and the mixture filtered. The filtrate was dried under vacuum to yield $(HCDippN)_2BH$ (12 mg, 26% yield) as a white powder. ^{1}H and ^{11}B NMR data matches previously reported literature values.[10]

Preparation of $(HCDippN)_2BCl$. To a solution of **1** (100 mg, 0.12 mmol) in benzene (5 mL) was added $POCl_3$ (0.60 mL of a 0.02 M solution in benzene, 0.12 mmol) to form a yellow solution. Volatiles were removed under vacuum. To the residue was added *n*-hexane (5 mL) and the mixture filtered. The filtrate was dried under vacuum to yield $(HCDippN)_2BCl$ (39 mg, 76% yield) as a yellow powder. ^{1}H and ^{11}B NMR data matches previously reported literature values.[10]

Preparation of $(OC(p\text{-}Tol)N)_2CO$ and $(HCDippN)_2BCl$. To a mixture of **1** (100 mg, 0.12 mmol) and (*p*-Tol)NCN(*p*-Tol) (27 mg, 0.12 mmol) was added benzene (10 mL) and the reaction mixture agitated for 5 min at room temperature to form a red solution. Oxalyl chloride (0.10 mL, 1.16 mmol) was added and volatiles were removed under vacuum. The solid was redissolved in benzene (10 mL) and stirred at 80 °C for 1 h to form a brown solution. Volatiles were again removed under vacuum. To the residue was added *n*-hexane (10 mL) and the mixture filtered. The filtrate was dried under vacuum to yield $(HCDippN)_2BCl$ (49 mg, 95% yield) as a red powder. To the residue was added diethyl ether (10 mL) and the mixture filtered. The filtrate was dried under vacuum to yield $(OC(p\text{-}Tol)N)_2CO$ (17 mg, 48% yield) as a red powder. ^{1}H NMR data matches previously reported literature values.[10]

NMR Spectra

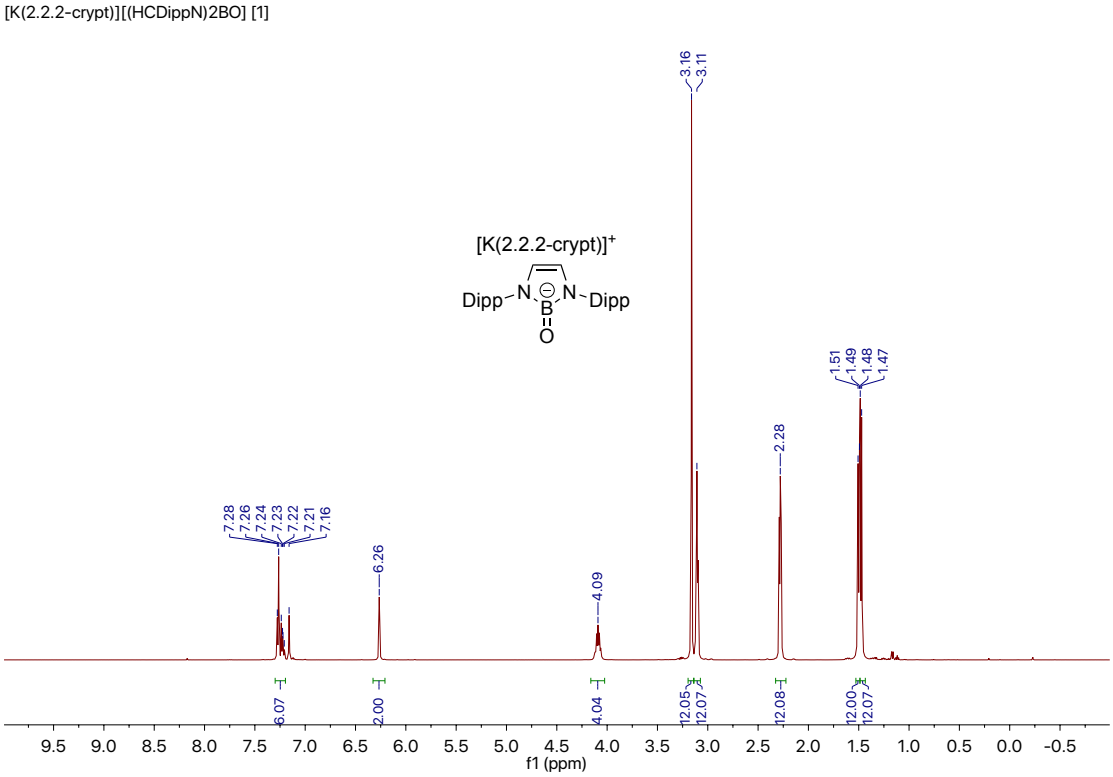


Figure 6. ^{1}H NMR spectrum of **1**.

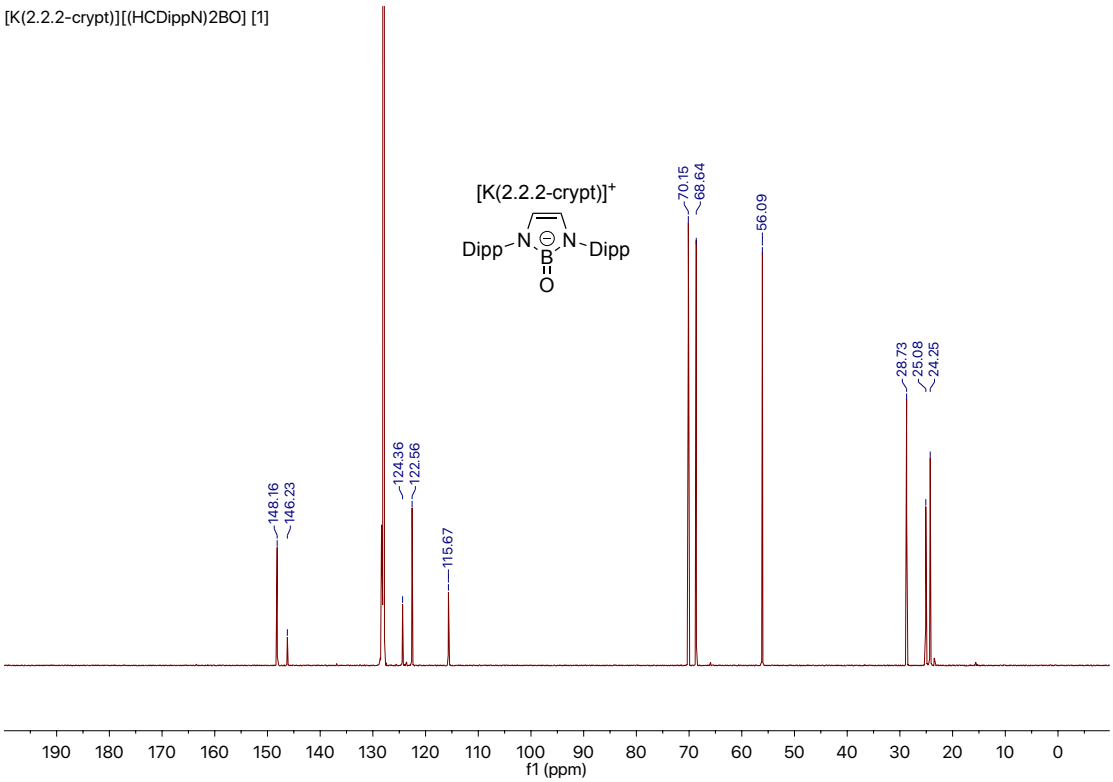


Figure 7. $^{13}C\{^{1}H\}$ NMR spectrum of **1**.

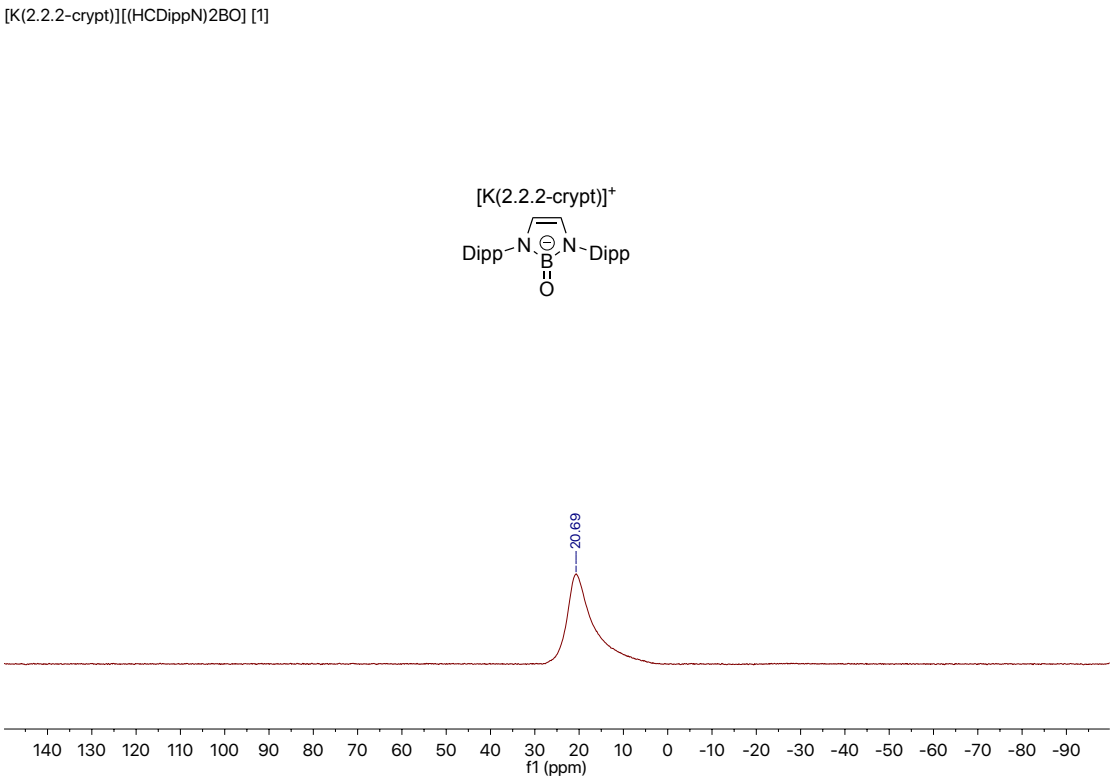


Figure 8. $^{11}B\{^{1}H\}$ NMR spectrum of **1**.

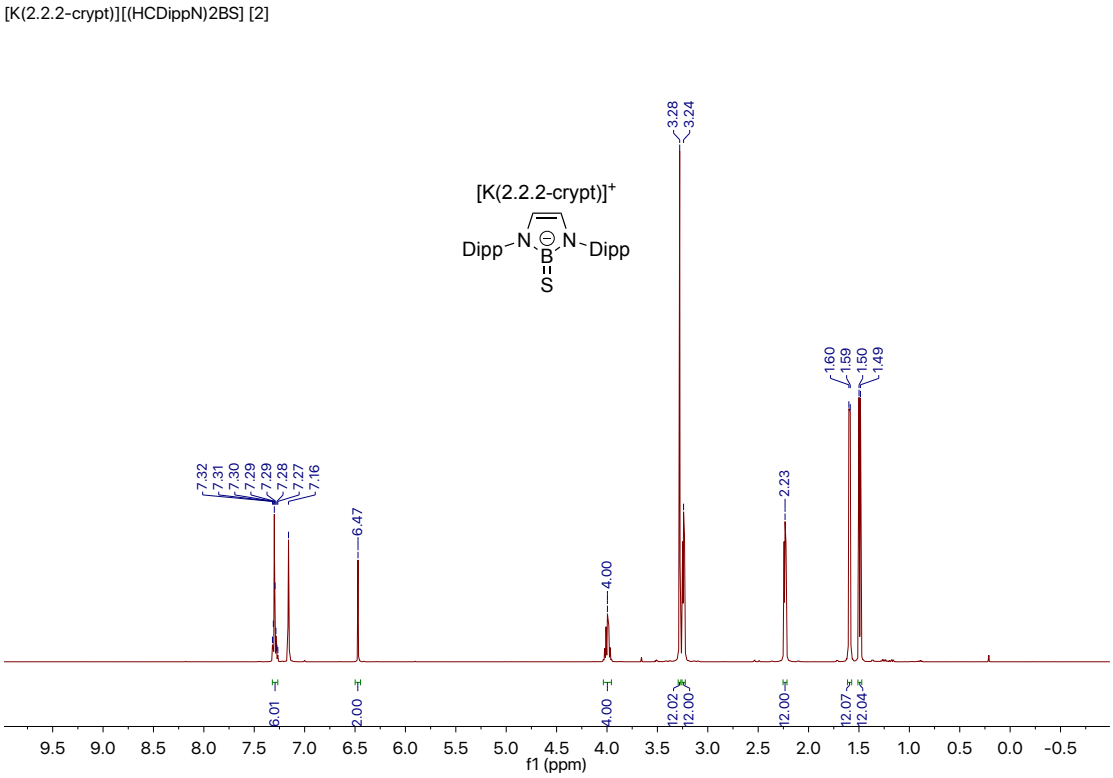


Figure 9. ^{1}H NMR spectrum of **2**.

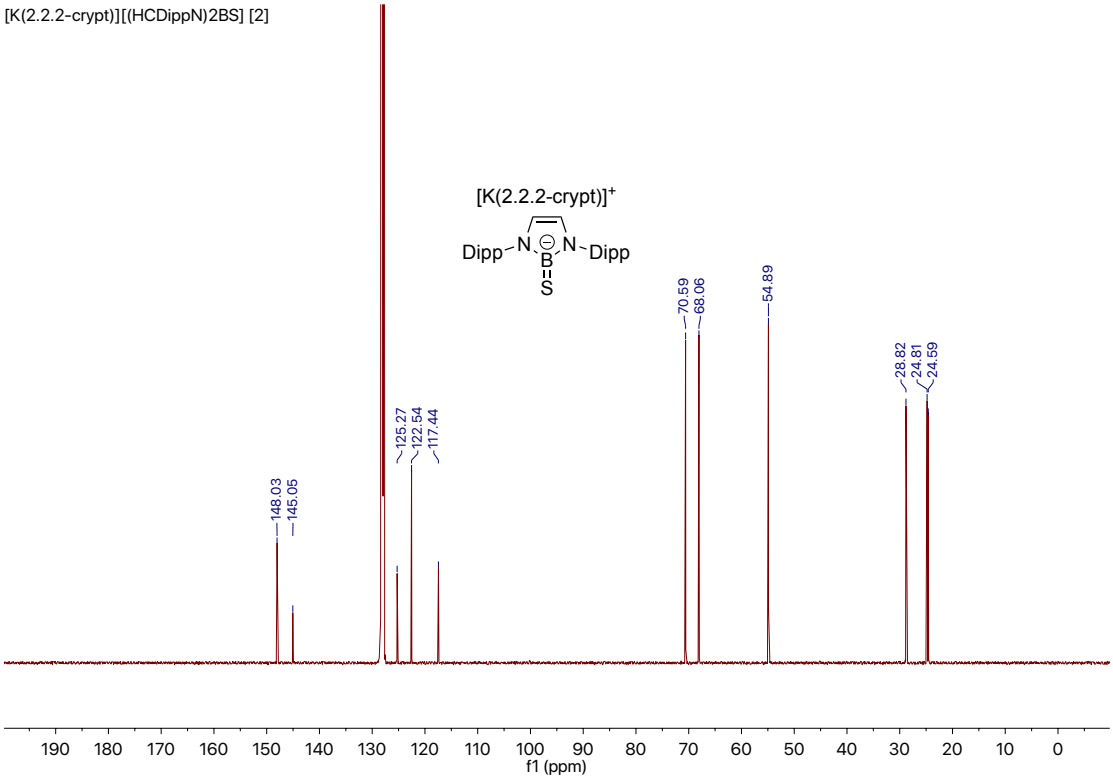


Figure 10. ^{13}C{^{1}H} NMR spectrum of **2**.

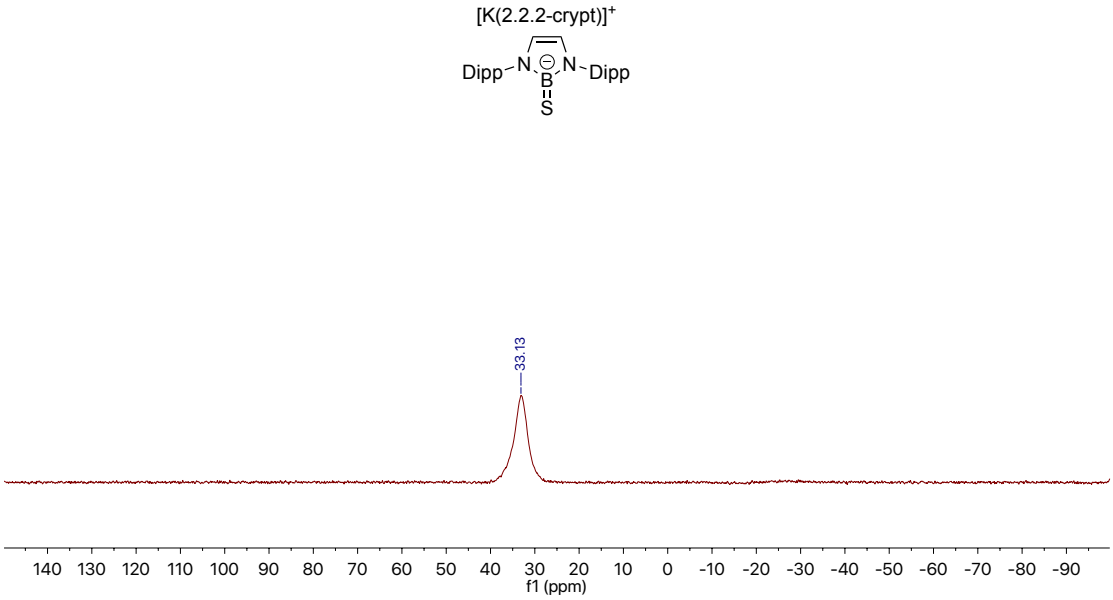


Figure 11. $^{11}B\{^{1}H\}$ NMR spectrum of **2**.

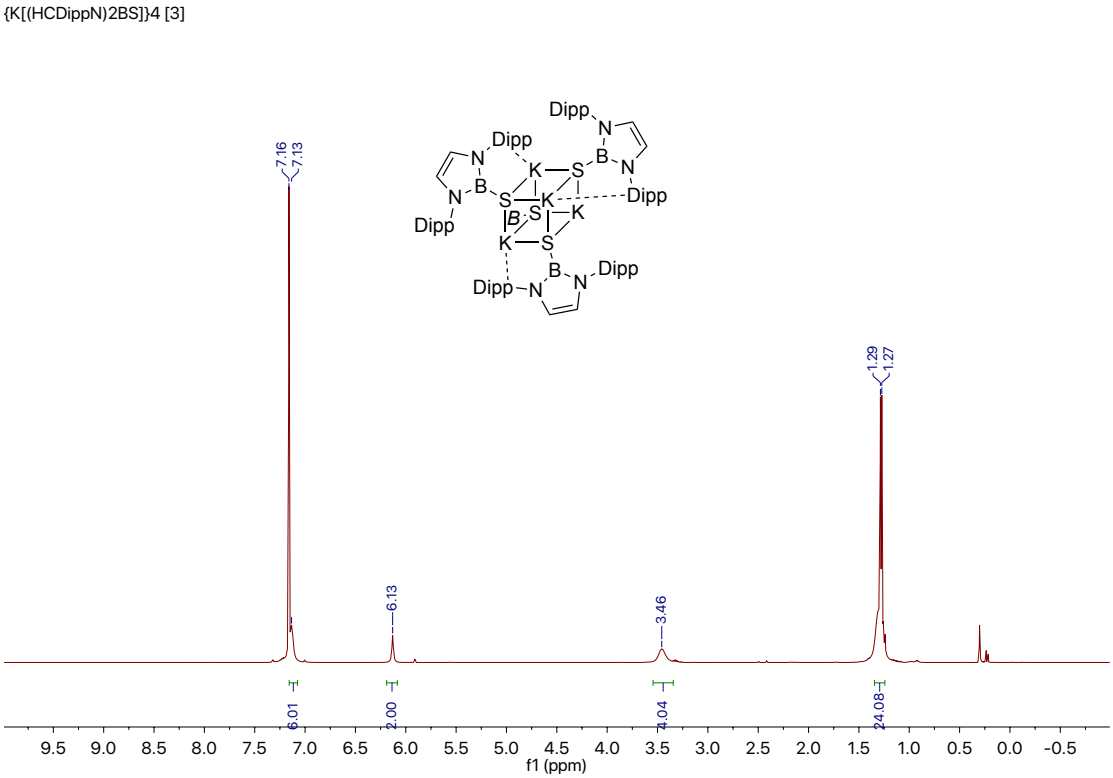


Figure 12. ^{1}H NMR spectrum of **3**.

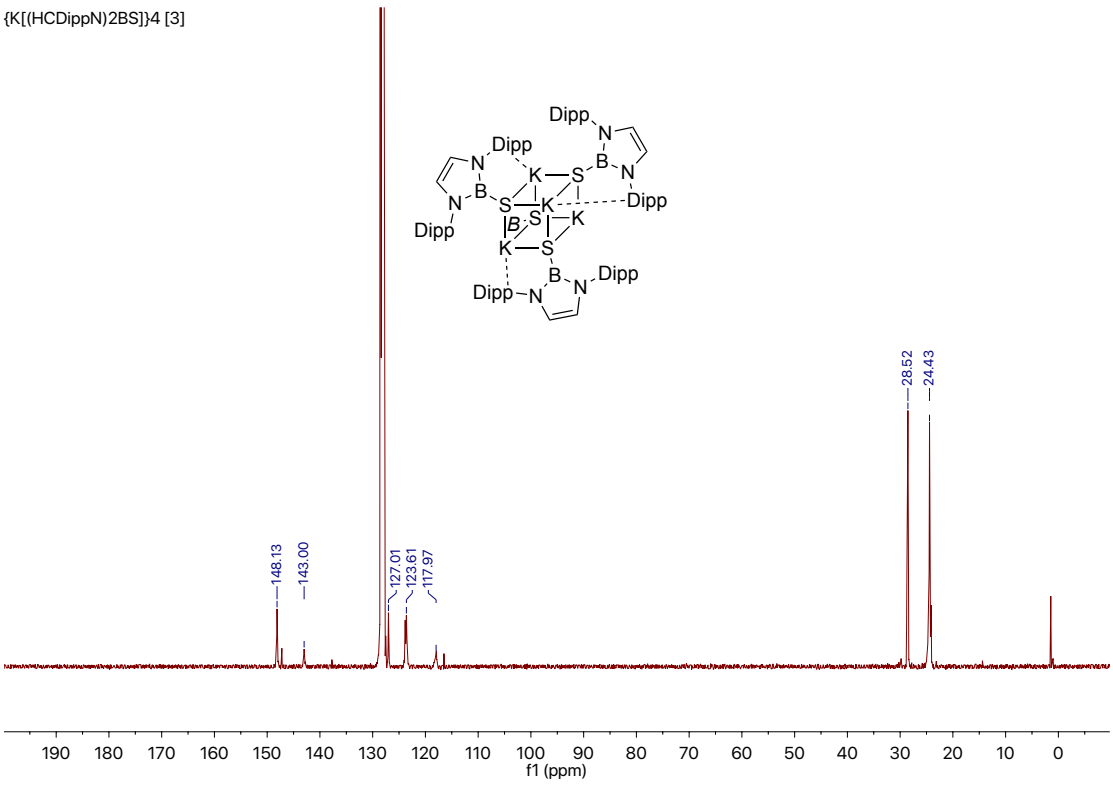


Figure 13. ^{13}C{ ^{1}H} NMR spectrum of **3**.

{K[(HCDippN)2BS]}4 [3]

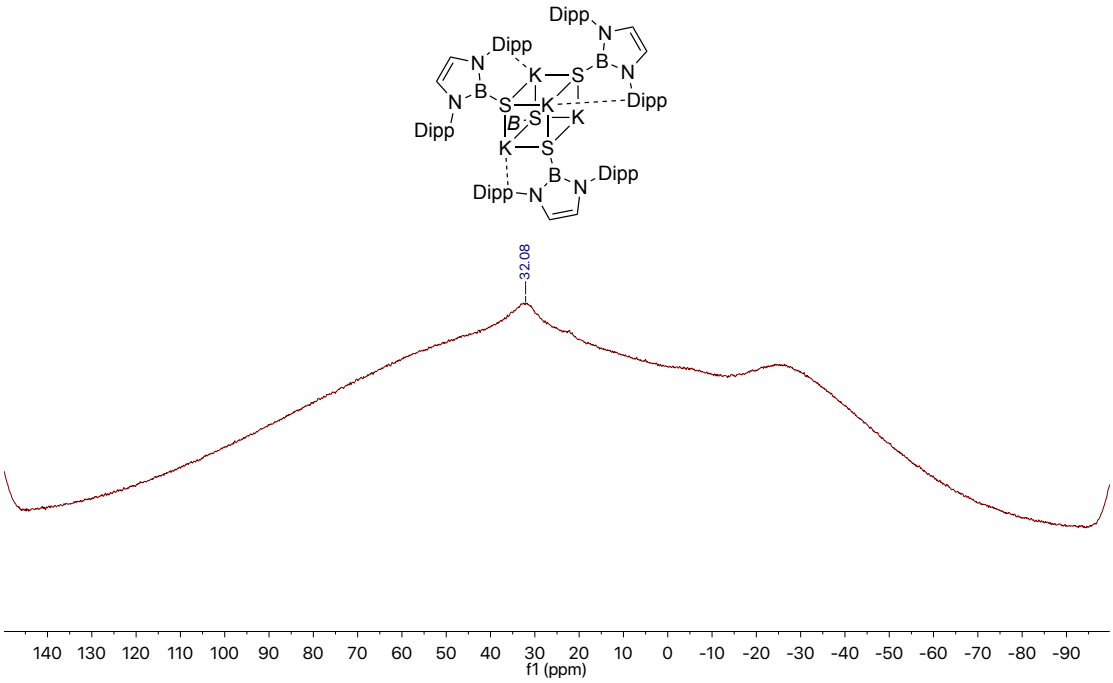


Figure 14. $^{11}B\{^{1}H\}$ NMR spectrum of **3**.

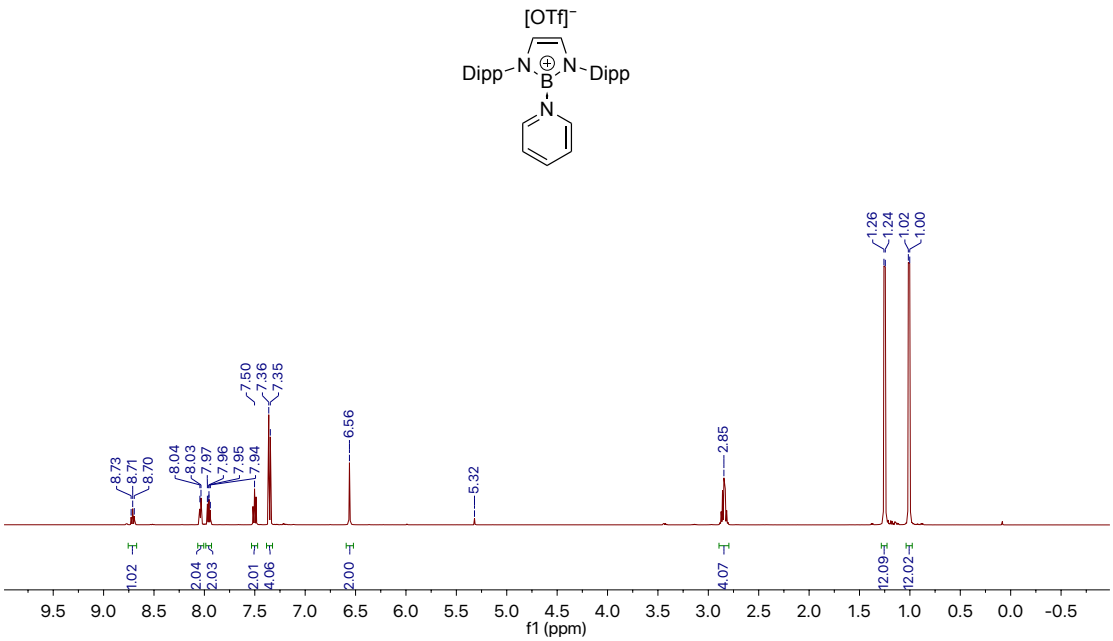


Figure 15. ^{1}H NMR spectrum of **4**.

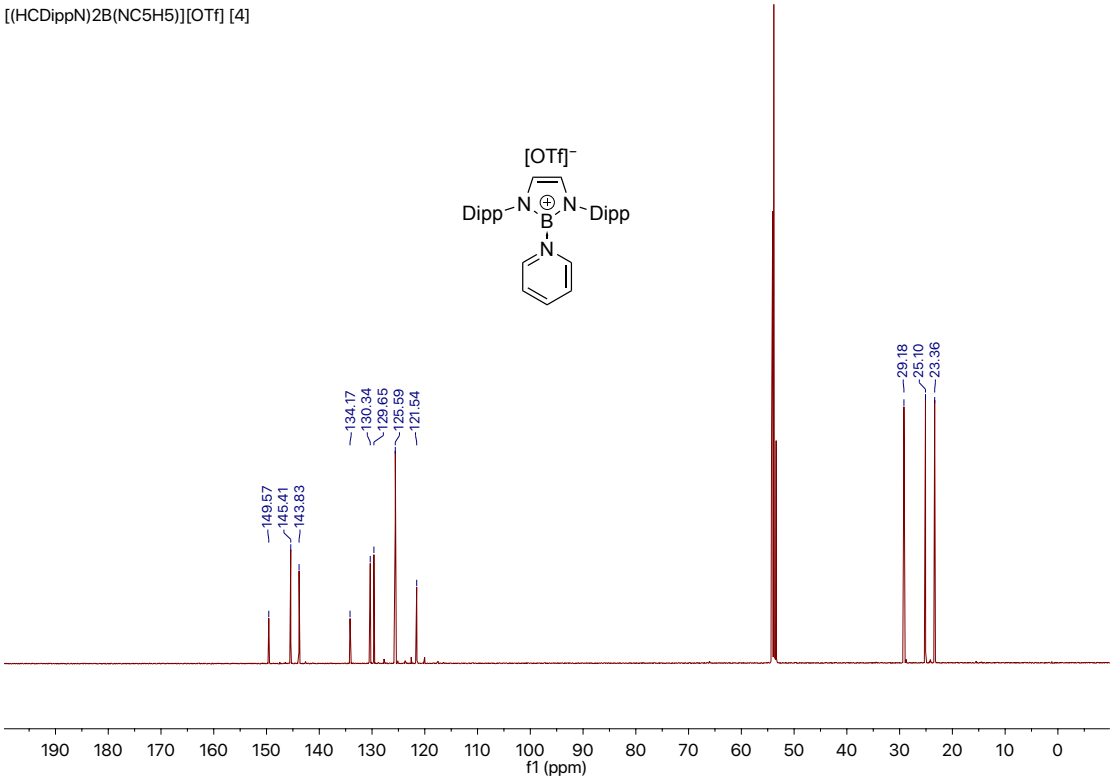


Figure 16. ^{13}C{ ^{1}H} NMR spectrum of **4**.

[(HCDippN)2B(NC5H5)][OTf] [4]

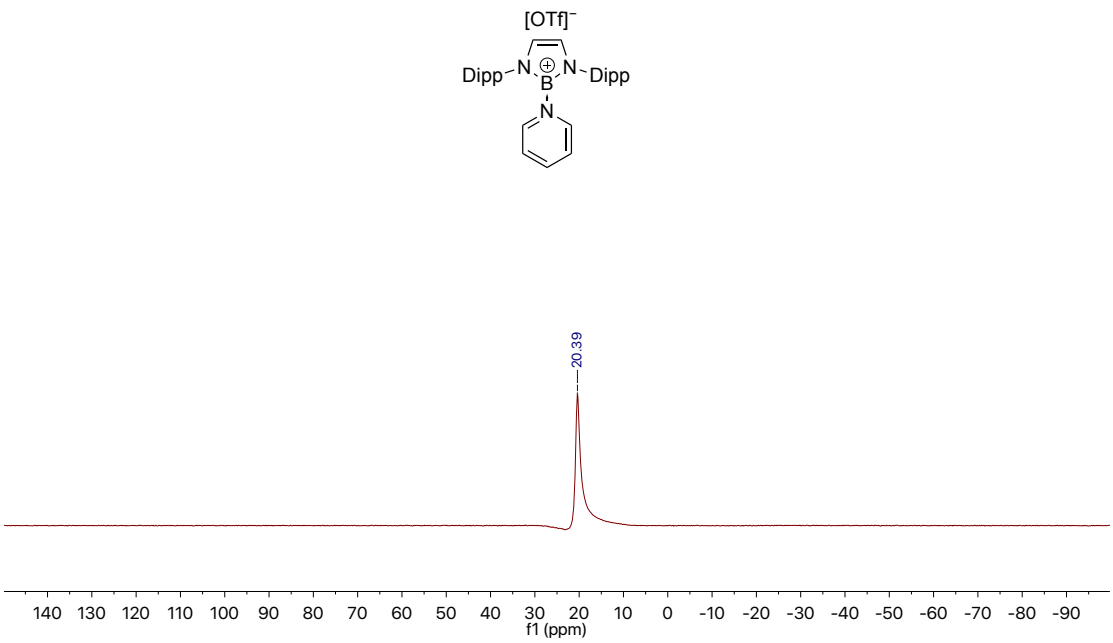


Figure 17. $^{11}B\{^{1}H\}$ NMR spectrum of **4**.

[(HCDippN)2B(NC5H5)][OTf] [4]

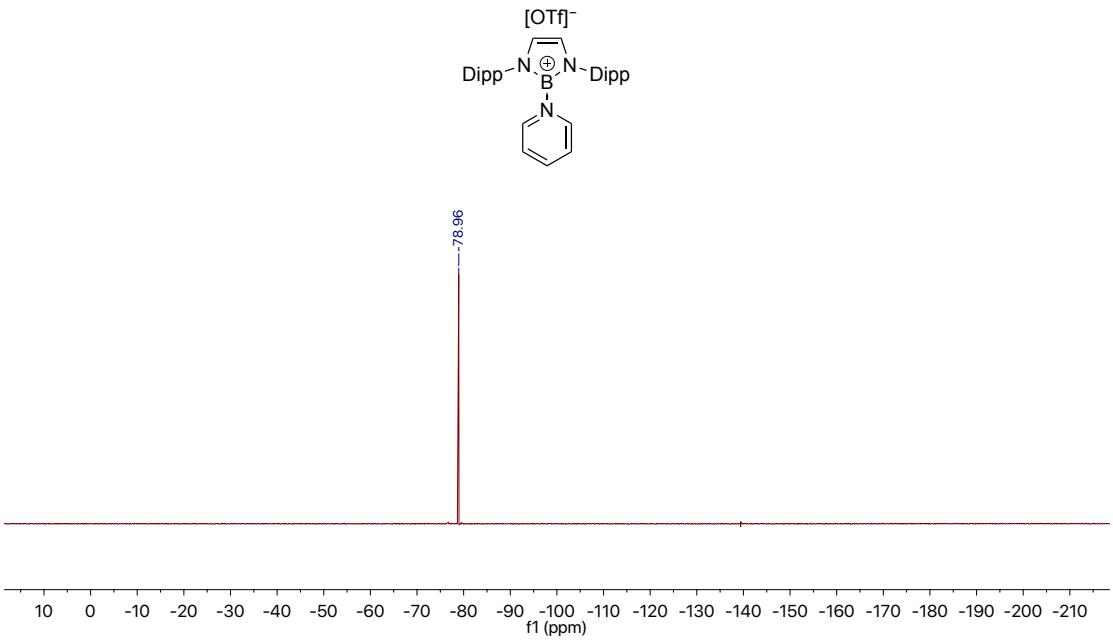


Figure 18. $^{19}F\{^{1}H\}$ NMR spectrum of **4**.

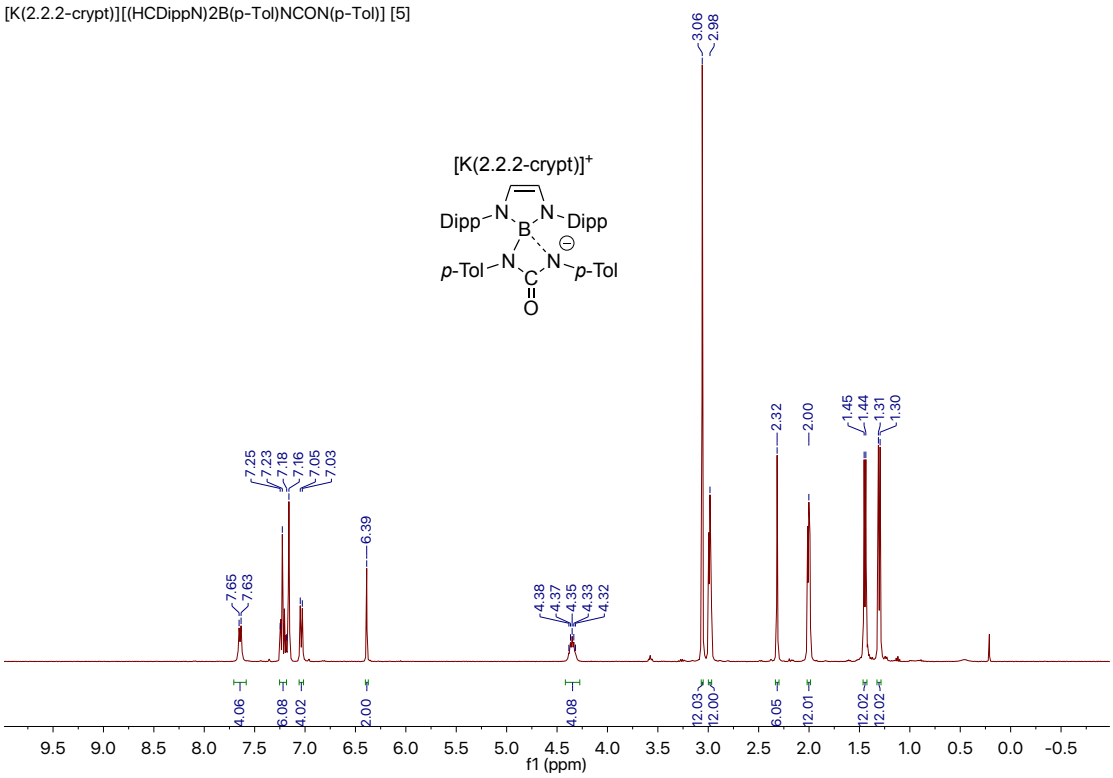


Figure 19. ^{1}H NMR spectrum of **5**.

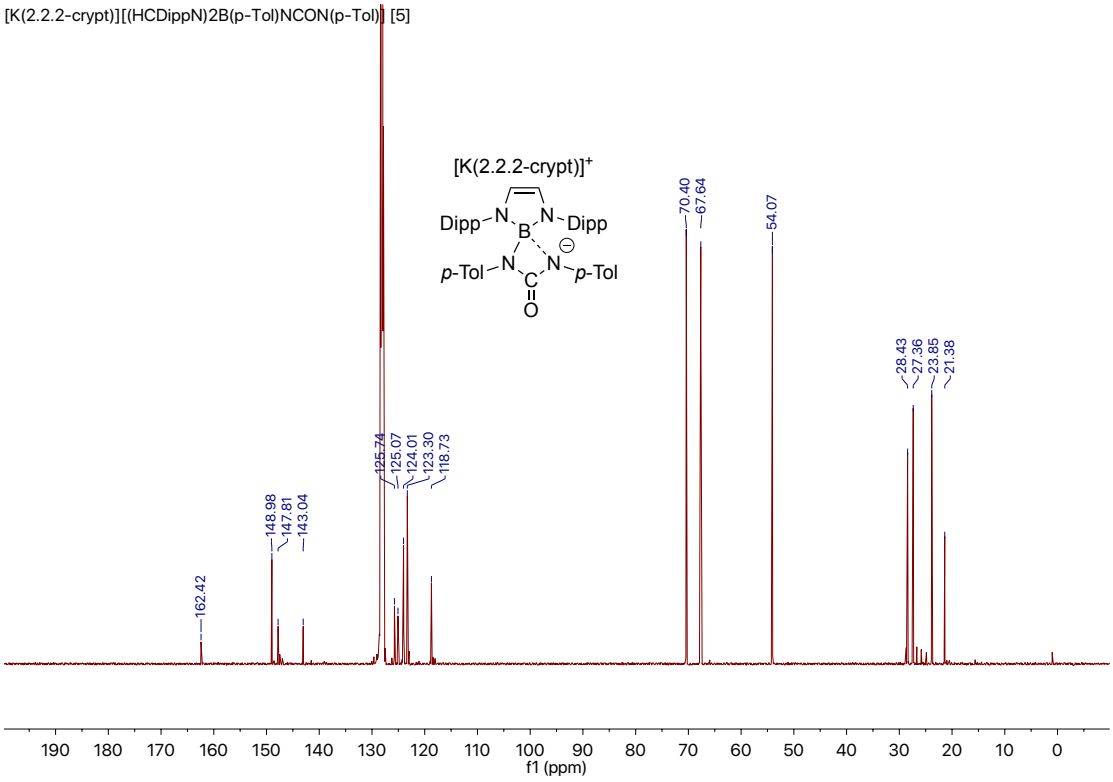


Figure 20. ^{13}C{^{1}H} NMR spectrum of **5**.

[K(2.2.2-crypt)][(HCDippN)2B(p-Tol)NCON(p-Tol)] [5]

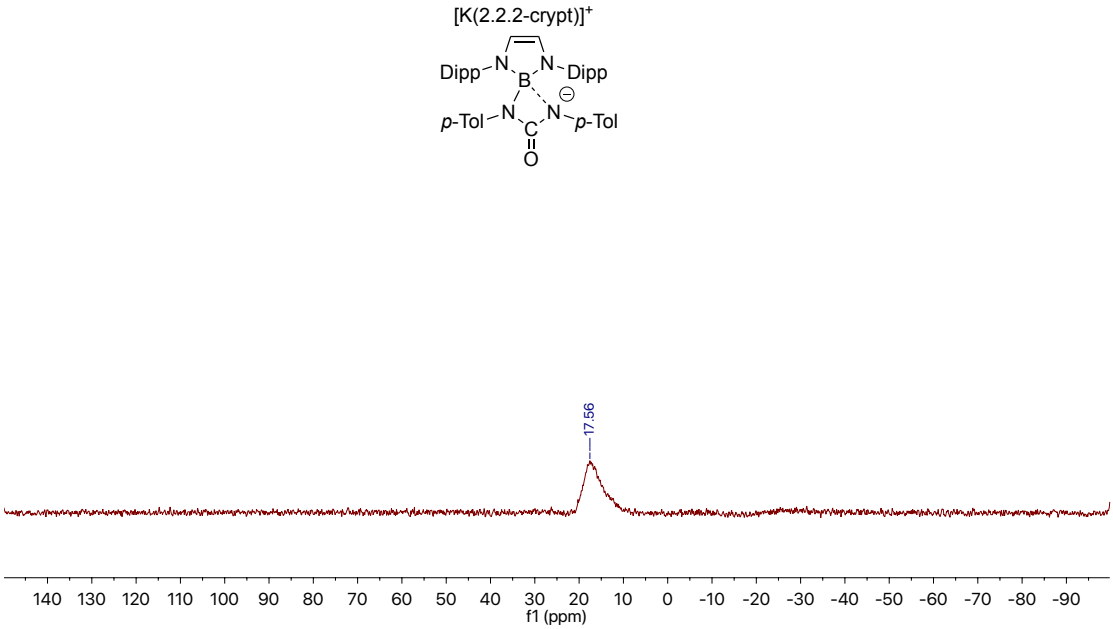


Figure 21. $^{11}B\{^{1}H\}$ NMR spectrum of **5**.

X-Ray Crystallographic Studies

Single-crystal X-ray diffraction data for **1–5** were collected at 150 K on Oxford Diffraction/Agilent SuperNova diffractometers with Cu-$K\alpha$ (λ = 1.54184 Å) radiation equipped with nitrogen gas Oxford Cryosystems Cryostream unit.[16] Raw frame data were reduced using CrysAlisPro.[17] The structures were solved using SHELXT[18] and refined to convergence on F^2 and against all independent reflections by full-matrix least-squares using SHELXL[19] in combination with the SHELXLE[20] program. Distances and angles were calculated using the full covariance matrix. Restraints were used to maintain sensible geometries for the disordered groups and approximate the displacement parameters to typical values. Selected crystallographic data are summarized in Table 1.

Table 1. Selected crystallographic and refinement data for **1–5**.

	1	**2**	**3**	**4**	**5**
Formula	C_{94} H_{150} B_2 K_2 N_8 O_{14}	C_{68} H_{96} B K N_4 O_6 S	C_{125} H_{165} B_4 K_4 N_8 S_4	C_{32} H_{41} B F_3 N_3 O_3 S	C_{59} H_{86} B K N_6 O_7
Fw	1716.03	1147.45	2107.52	615.55	1041.24
Cryst. System	Triclinic	Triclinic	Triclinic	Monoclinic	Monoclinic
Space Group	P 1	P -1	P -1	P 21/c	P 21/c
Wavelength/Å	1.54184	1.54184	1.54184	1.54184	1.54184
a/Å	13.8502(2)	13.0099(3)	15.5333(3)	11.8476(2)	12.24440(10)
b/Å	16.6927(3)	15.9376(4)	16.3399(3)	13.6268(2)	15.9465(2)
c/Å	23.0193(3)	16.4118(4)	27.9110(7)	19.9995(3)	30.3954(3)
α/°	90.2510(10)	80.367(2)	85.492(2)	90	90
β/°	90.3870(10)	86.833(2)	89.509(2)	94.4960(10)	92.7400(10)
γ/°	112.097(2)	86.675(2)	61.864(2)	90	90
Volume/Å^3	4930.84(15)	3345.71(14)	6224.4(3)	3218.88(9)	5928.08(11)
Z	2	2	2	4	4
Temp./K	150(2)	150(2)	150(2)	150(2)	150(2)
Refls. Collect.	135248	47664	58648	18302	28293
$2\theta_{max}$	152.50	152.45	140.14	152.93	153.26
R_{int}	0.0478	0.0336	0.0411	0.0352	0.0263
Goodness of fit	1.041	1.029	1.016	1.029	1.030
$R[F^2>2\sigma]$, F	0.0551	0.0386	0.0680	0.0395	0.0422
R_w (all data), F^2	0.1516	0.1051	0.2101	0.1065	0.1156

Computational Studies

All reported computational work was carried out using DFT, employing the Gaussian09 (Revision D.01) program package.[21] Geometry optimizations were performed in the gas phase, with PBE1PBE exchange-correlation functional[22] and def-TZVP basis set.[23] Grimme's empirical dispersion correction (DFT-D3) was also used.[24] The nature of stationary points found (minima) was confirmed by full frequency calculations. Natural bond orbital (NBO) analyses were performed using NBO 3.1 as implemented in Gaussian09.[25]

References

(1) For bond dissociation energies: Haynes, W. M. *CRC Handbook of Chemistry and Physics, Vol. 96*; CRC Press: Boca Raton, 2015.

(2) For minerals: Klein, C.; Hurlbut, C. S. *Manual of Mineralogy*; Wiley: New York, 1985.

(3) (a) Miyaura, N.; Suzuki, A. Palladium-catalyzed cross-coupling reactions of organoboron compounds. *Chem. Rev.* **1995**, *95*, 2457-2483. (b) Brown, H. C. Hydroboration – a powerful synthetic tool. *Tetrahedron* **1961**, *12*, 117-138.

(4) See for example: (a) Franz, D.; Inoue, S. Advances in the development of complexes that contain a group 13 element chalcogen multiple bond. *Dalton Trans.* **2016**, *45*, 9385-9397. (b) Fischer, R. C.; Power, P. P. π-Bonding and the lone pair effect in multiple bonds involving heavier main group elements: developments in the new millennium. *Chem. Rev.* **2010**, *110*, 3877-3923.

(5) For gas phase studies: (a) Hildenbrand, D. L.; Theard, L. P.; Saul, A. M. Transpiration and mass spectrometric studies of equilibria involving BOF(g) and $(BOF)_3$(g). *J. Chem. Phys.* **1963**, *39*, 1973-1978. (b) Bock, H.; Cederbaum, L.; Niessen, W. v.; Paetzold, P.; Rosmus, R.; Solouki, B. Methylboron oxide, H_3CBO. *Angew. Chem., Int. Ed.* **1989**, *28*, 88-90. For matrix isolation: (c) Burkholder, T. R.; Andrews, L. Reactions of boron atoms with molecular oxygen. Infrared spectra of BO, BO_2, B_2O_2, B_2O_3, and BO^-_2 in solid argon. *J. Chem. Phys.* **1991**, *95*, 8697-8709. (d) Lanzisera, D. V.; Andrews, L. Reactions of laser-ablated boron atoms with methanol. Infrared spectra and *ab initio* calculations of CH_3BO, CH_2BOH, and CH_2BO in solid argon. *J. Phys. Chem. A.* **1997**, *101*, 1482-1487. (e) Bettinger, H. F. Reversible formation of organyl(oxo)boranes (RBO) (R = C_6H_5 or CH_3) from boroxins ($(RBO)_3$): a matrix isolation study. *Organometallics* **2007**, *26*, 6263-6267. For chemical trapping: (f) Ito, M.; Tokitoh, N.; Okazaki, R. A novel approach to an oxoborane and its Lewis base complex *Tetrahedron Lett.* **1997**, *38*, 4451-4454. (g) Ito, M.; Tokitoh, N.; Okazaki, R. Formation of oxoborane and thioxoborane from a dithiastannaboretane derivative. *Phosphorus, Sulfur Silicon Relat. Elem.* **1997**, *124*, 533-536. (h) Paetzold, P.; Neyses. S.; Geret. L. Oxo(trisyl)boran $(Me_3Si)_3CBO$ als zwischenstufe. *Z. Anorg. Allg. Chem.* **1995**, *621*, 732-736. (i) Groteklaes, M.; Paetzold, P. Oxo(tri-*tert*-butylphenyl)boran ArBO als zwischenstufe. *Chem. Ber.* **1988**, *121*, 809-810. (j) Pachchaly, B.; West,

R. Synthesis of a 1,3-dioxa-2,4-diboretane, an oxoborane precursor. *J. Am. Chem. Soc.* **1985**, *107*, 2987-2988. (k) Hanecker, R.; Noth, H.; Wietelmann, U. Beiträge zur chemie des bors, 171. Kristall- und molekülstruktur von 2,4-bis(2,2,6,6-tetramethylpiperidino)-1,3,2,4-dichalcogendiboretanen. *Chem. Ber.* **1986**, *119*, 1904-1910.

(6) For acid-stabilized monomeric oxoboranes: (a) Vidovic, D.; Moore, J. A.; Jones, J. N.; Cowley, A. H. Synthesis and characterization of a coordinated oxoborane: Lewis acid stabilization of a boron−oxygen double bond. *J. Am. Chem. Soc.* **2005**, *127*, 4566-4567. (b) Wang, Y.; Hu, H.; Zhang, J.; Cui, C. Comparison of anionic and Lewis acid stabilized N-heterocyclic oxoboranes: their facile synthesis from a borinic acid. *Angew. Chem., Int. Ed.* **2011**, *50*, 2816-2819. (c) Loh, Y. K.; Chong, C. C.; Ganguly, R.; Li, Y.; Vidovic, D.; Kinjo, R. 1,2,4,3-Triazaborole-based neutral oxoborane stabilized by a Lewis acid. *Chem. Commun.* **2014**, *50*, 8561-8564. (d) Swarnarkar, A. K.; Hering-Junghans, C.; Ferguson, M. J.; Mcdonald, R.; Rivard, E. Oxoborane (RBO) complexation and concomitant electrophilic bond activation processes. *Chem. Eur. J.* **2017**, *23*, 8628-8631.

(7) For transition metal oxoboranes: (a) Braunschweig, H.; Radacki, K.; Schneider, A. Oxoboryl complexes: boron-oxygen triple bonds stabilized in the coordination sphere of platinum. *Science* **2010**, *328*, 345-347. (b) Westcott S. A. BO chemistry comes full circle. *Angew. Chem., Int. Ed.* **2010**, *49*, 9045-9046. (c) Braunschweig, H.; Radacki, K.; Schneider, A. Reactivity of an oxoboryl complex toward fluorinated aryl boron reagents. *Chem. Commun.* **2010**, *46*, 6473-6475. (d) Bertsch, S.; Brand, J.; Braunschweig, H.; Hupp, F.; Radacki, K. Platinum oxoboryl complexes as substrates for the formation of 1:1, 1:2, and 2:1 Lewis acid–base adducts and 1,2-dipolar additions. *Chem. Eur. J.* **2015**, *21*, 6278-6285. (e) Miyada, T.; Yamashita, M. Oxygenation of a ruthenium complex bearing a PBP-pincer ligand inducing the formation of a boronato ligand with a weak Ru–O bond. *Organometallics* **2013**, *32*, 5281-5284.

(8) For acid/base free main group E=O bonds: (a) Li, L.; Fukawa, T.; Matsuo, T.; Hashizume, D.; Fueno, H.; Tanaka, K.; Tamao, K. A stable germanone as the first isolated heavy ketone with a terminal oxygen atom. *Nat. Chem.* **2012**, *4*, 361-365. (b) Alvarado-Beltran, I.; Rosas-Sanchez, A.; Baceiredo, A.; Saffon-Merceron, N.; Branchadell, V.; Kato, T. A fairly stable crystalline silanone. *Angew. Chem., Int. Ed.* **2017**, *56*, 10481-10485. (c) Wendel, D.; Reiter, D.; Porzelt, A.; Altmann, J.; Inoue, S.; Rieger, B. Silicon and oxygen's bond of affection: an acyclic three-coordinate silanone and its transformation

to an iminosiloxysilylene. *J. Am. Chem. Soc.* **2017**, *139*, 17193-17198. (d) Rosas-Sanchez, A.; Alvarado-Beltran, I.; Baceiredo, A.; Saffon-Merceron, N.; Massou, S.; Hashizume, D.; Branchadell, V.; Kato, T. Cyclic (amino)(phosphonium bora-ylide)silanone: a remarkable room-temperature-persistent silanone. *Angew. Chem., Int. Ed.* **2017**, *56*, 15916-15920. (e) Kobayashi, R.; Ishida, S.; Iwamoto, T. An isolable analogue of a ketone that contains an unperturbed Si=O double bond. *Angew. Chem., Int. Ed.* **2019**, *58*, 9425-9428. (f) Wünsche, M. A.; Witteler, T.; Dielmann, F. Lewis base free oxophosphonium ions: tunable, trigonal-planar Lewis acids. *Angew. Chem., Int. Ed.* **2018**, *57*, 7234-7239.

(9) Loh, Y. K.; Ying, L.; Fuentes, M. A.; Do, D. C. H.; Aldridge, S. An N-heterocyclic boryloxy ligand isoelectronic with N-heterocyclic imines: access to an acyclic dioxysilylene and its heavier congeners. *Angew. Chem., Int. Ed.* **2019**, *58*, 4847-4851.

(10) Segawa, Y.; Suzuki, Y.; Yamashita, M.; Nozaki, N. Chemistry of boryllithium: synthesis, structure and reactivity. *J. Am. Chem. Soc.* **2008**, *130*, 16069-16079.

(11) For monomeric thioxoboranes: (a) Wang. H.; Zhang, J.; Hu, H.; Cui, C. Access to B═S and B═Se double bonds via sulfur and selenium insertion into a B−H bond and hydrogen migration. *J. Am. Chem. Soc.* **2010**, *132*, 10998-10999. (b) Jaiswal, K.; Prashanth, B.; Ravi, S.; Shasundar, K. R.; Singh, S. Reactivity of a dihydroboron species: synthesis of a hydroborenium complex and an expedient entry into stable thioxo- and selenoxo-boranes. *Dalton Trans.* **2015**, *44*, 15779-15785. (c) Liu, S.; Legare, M.; Hofmann, A.; Braunschweig, H. A boradiselenirane and a boraditellurirane: isolable heavy analogs of dioxiranes and dithiiranes. *J. Am. Chem. Soc.* **2018**, *140*, 11223-11226. (d) Franz, D.; Irran, E.; Inoue, S. Isolation of a three-coordinate boron cation with a boron–sulfur double bond. *Angew. Chem., Int. Ed.* **2014**, *53*, 14264-14268.

(12) Baraznenok, I. L.; Nenajdenko, V. G.; Balenkova, E. S. Chemical transformations induced by triflic anhydride. *Tetrahedron* **2000**, *56*, 3077-3119.

(13) See for example: Franz, D.; Inoue, S. Cationic complexes of boron and aluminum: an early 21st century viewpoint. *Chem. Eur. J.* **2019**, *25*, 2898-2926.

(14) (a) Dielmann, F.; Back, O.; Henry-Ellinger, M.; Jerabek, P.; Frenking, G.; Bertrand, G. A crystalline singlet phosphinonitrene: a nitrogen atom–transfer agent. *Science* **2012**, *337*, 1526-1528. (b) Schulz, A.; Villinger, A. Stabilized transient R_2PN species. *Angew. Chem., Int. Ed.* **2013**, *52*, 3068-3070. (c)

Dielmann, F.; Moore, C. E.; Rheingold, A. L.; Bertrand, G. Crystalline, Lewis base-free, cationic phosphoranimines (iminophosphonium salts). *J. Am. Chem. Soc.* **2013**, *135*, 14071-14073. (d) Dielmann, F.; Andrada, D. M.; Frenking, G.; Bertrand, G. Isolation of bridging and terminal coinage metal-nitrene complexes. *J. Am. Chem. Soc.* **2014**, *136*, 3800-3802. (e) Dielmann, F.; Bertrand, G. Reactivity of a stable phosphinonitrene towards small molecules. *Chem. Eur. J.* **2015**, *21*, 191-198.

(15) For oxide ion transfer by transition metals, see for example: Lee, G. R.; Cooper, N. J. Transfer of an oxide ion from an anionic carbon dioxide complex to a cationic carbonyl complex. *Organometallics* **1985**, *4*, 1467-1468.

(16) Cosier, J.; Glazer, A. M. A nitrogen-gas-stream cryostat for general X-ray diffrcaction studies. *J. Appl. Cryst.* **1986**, *19*, 105-107.

(17) CrysAlisPro, Agilent Technologies, Version 1.171.35.8.

(18) Sheldrick, G. M. SHELXT - Integrated space-group and crystal structure determination. *Acta Cryst. Sect. A* **2015**, *71*, 3-8.

(19) Sheldrick, G. M. *Acta Cryst. Sect. A* **2008**, *64*, 112-122.

(20) Hübschle, C. B.; Sheldrick, G. M.; Dittrich, B. ShelXle: a Qt graphical user interface for SHELXL. *J. Appl. Cryst.* **2011**, *44*, 1281-1284.

(21) Frisch, M. J.; Trucks, G. W.; Schlegel, H. B.; Scuseria, G. E.; Robb, M. A.; Cheeseman, J. R.; Scalmani, G.; Barone, V.; Mennucci, B.; Petersson, G. A.; Nakatsuji, H.; Li, X.; Caricato, M.; Li, X.; Hratchian, H. P.; Izmaylov, A. F.; Bloino, J.; Zheng, G.; Sonnenberg, J. L.; Hada, M.; Ehara, M.; Toyota, K.; Fukuda, R.; Hasegawa, J.; Ishida, M.; Nakajima, T.; Honda, Y.; Kitao, O.; Nakai, H.; Vreven, T.; Montgomery, J. A., Jr.; Peralta, J. E.; Ogliaro, F.; Bearpark, M. J.; Heyd, J. J.; Brothers, E. N.; Kudin, K. N.; Staroverov, V. N.; Kobayashi, R.; Normand, J.; Raghavachari, K.; Rendell, A. P.; Burant, J. C.; Iyengar, S. S.; Tomasi, J.; Cossi, M.; Rega, N.; Millam, J. M.; Klene, M.; Adamo, C.; Jaramillo, J.; Gomperts, R.; Stratmannm R. E.; Yazyev, O; Austin, A.J.; Cammi, R.; Pomelli, C.; Ochterski, J. W.; Martin, R. L.; Morokuma, K.; Zakrzewski, V. G.; Voth, G. A.; Salvador, P; Dannenberg, J. J.; Dapprich, S.; Daniels, A. D.; Farkas, O.; Foresman, J. B.; Ortiz, J. V.; Cioslowski, J.; Fox, D. J. *Gaussian 09*, *Revision D.01*, Gaussian, Inc., Wallingford, CT **2009**.

(22) (a) Ernzerhof, M.; Scuseria, G. E. *J. Chem. Phys.* **1999**, *110*, 5029-5036. (b) Adamo, C.; Barone, V. *J. Chem. Phys.* **1999**, *110*, 6158-6170. (c) Perdew, J. P.; Burke, K.; Ernzerhof, M. *Phys. Rev. Lett.* **1997**,

78, 1396. (d) Perdew, J. P.; Burke, K.; Ernzerhof, M. *Phys. Rev. Lett.* **1996**, *77*, 3865-3868. (e) Perdew, J. P.; Ernzerhof, M.; Burke, K. *J. Chem. Phys.* **1996**, *105*, 9982-9985.

(23) Schäfer, A.; Huber, C.; Ahlrichs, R. *J. Chem. Phys.* **1994**, *100*, 5829-5835.

(24) (a) Grimme, S.; Antony, J.; Ehrlich, S.; Krieg, H. *J. Chem. Phys.* **2010**, *132*, 154104-154119. (b) Grimme, S.; Ehrlich, S.; Goerigk, L. *J. Comput. Chem.* **2011**, *32*, 1456-1465.

(25) Glendening, E. D.; Reed, A. E.; Carpenter, J. E.; Weinhold,F. NBO Version 3.1.